Organic Electrosynthesis of Carboxylic Acids Facilitated by CO_2-eXpanded Electrolytes

Matt Stalcup

B.S. New Mexico Institute of Mining and Technology, 2018

Submitted to the graduate degree program in Chemical and Petroleum Engineering and the Graduate Faculty of the University of Kansas in partial fulfillment of the requirements for the degree of Doctor of Philosophy.

Committee members

Kevin Leonard, Chairperson

Bala Subramaniam

Alan Allgeier

Mark Shiflett

James Blakemore, External Reviewer

Date defended: December 2nd, 2022

The Dissertation Committee for Matt Stalcup certifies
that this is the approved version of the following dissertation :

Organic Electrosynthesis of Carboxylic Acids Facilitated by CO_2-eXpanded Electrolytes

Kevin Leonard, Chairperson

Date approved: December 14th, 2022

Abstract

This work focuses on forming carbon-carbon bonds between CO_2 and organic substrates utilizing electrochemistry alongside CO_2 eXpanded Electrolytes (CXEs) to enhance traditional synthesis techniques. Traditionally, electrochemical carboxylation reactions are plagued with low rates and selectivity due to the lack of CO_2 in the liquid phase resulting in the formation of pinacols and alcohols. Additionally, the effect of CO_2 concentration on the reaction rate can not be studied in traditional systems due to the low concentrations of CO_2. Using CXEs, our electrochemistry was able to overcome the CO_2 availability limitations and find that the selectivity of the acetophenone carboxylation toward atrolactic acid is highly dependent on the concentration of CO_2 in the liquid phase. As the CO_2 concentration increased, the selectivity shifted from producing 1-phenylethanol ($[CO_2] < 0.1$ M) to exclusively producing atrolactic acid ($[CO_2] > 1.7$ M).

The electrochemical reduction of acetophenone was further studied using multiphysics simulations to provide insights into the kinetics of the acetophenone carboxylation. Typically, kinetic information on irreversible systems is not easily attainable through traditional electrochemical techniques Simulations were developed to regress key kinetic parameters characteristic of the acetophenone reduction and helped identify that the electrochemical chemical, electrochemical reaction pathway is the most likely reaction pathway. Additionally, we identified the first electron transfer as the rate-determining step. These simulations provide insight into fundamental electrochemistry previously unavailable for acetophenone reduction.

The knowledge of the acetophenone system was extended to a study of a structure-property relationship specifically, the electron donating and withdrawing effects by adding and removing substituents. We found that adding a trifluoromethyl group to acetophenone shifted the reduction potential to less negative potentials decreasing the energy input required to reduce the molecule. Using styrene as a case study, we found that not having an electron-withdrawing group shifted the

reduction potential more negative, increasing the energy required to reduce the molecule. Understanding the complex interaction between the electronic effects and electrochemistry can inform the types of chemistry that are available to undergo electrochemical carboxylation.

In addition to the main body of work, several secondary projects were conducted. The first is developing a machine-learning model for extracting textual information from the literature. Roughly two-thirds of our time as researchers is spent on literature search and reading. Unfortunately, some of that time is wasted searching for relevant papers. Creating a searchable-subject material based database can free up a significant portion of a researcher's time. Our machine-learning model can annotate CO_2RR literature highlighting the critical parameters for electrochemical CO_2 reduction. This model was trained and tested on a dataset of 500 papers relating to CO_2 reduction. The result was a reasonably accurate model capable of tagging the features we wanted to be tagged. However, extraction and word vectoring are still in development to obtain the essential information.

Another secondary project was developing high-surface area gold electrodes. The aim of this project was to push the gold-CXE system that was previously studied to the limit using high surface area gold. To further enhance the system, larger electrodes were required to increase the rate of CO formation. We developed a method to electroplate gold onto nickel foams. This resulted in a high surface area gold-plated electrode with a unique surface structure. In addition to plating the gold, we also investigated how the nickel surface effected the deposition of the gold. Etching the surface reduced the roughness of the surface, producing a more uniform coating. Both the dendritic and uniform gold electrocatalysts offer significant enhancements to electrochemically active surface area enhancements over traditional planar electrodes, potentially providing a scaleable route to electrochemically generated CO.

Finally, the last project is Hypothesis-Based Career Planning. During this project, we developed a curriculum to help students better understand the roles available to them and lay the groundwork for their careers. Currently, many graduating students are unprepared to enter the workforce. Often, they lack the communication skills and network required to find a satisfactory position.

The aim of this project is to supply students with a guide toward approaching career planning like research while developing their communication skills and building their networks. The students created and tested assumptions and hypotheses about potential career options so that they could be better informed about their decisions by conducting interviews with professional researchers.

Acknowledgements

Without the encouragement from my family, I would not have pursued a degree of this level, without the support of my friends, I would not have been able to achieve it, and without my mentors, I would not have learned as much as I have. Truly, the cornerstone of success is the community you surround yourself with.

I want to thank my friends for making the good parts great and the bad parts tolerable. I will forever hold the daily crossword, Halloween parties, and late nights as some of my favorite memories and I look forward to all the memories we are yet to make.

Additionally, I was fortunate to have an incredibly diverse and collaborative research education. Bala, James, and Kevin have been instrumental in my education and development as a researcher. Each week I was pushed to communicate clearly, think critically, and research carefully. The passion and drive for research from this collaboration is the cornerstone of my education and the multi-faceted training from each of these mentors made me exceptionally well-rounded. Thank you for your patience and instruction over the last five years.

Finally, special thanks are reserved for my family. There are too many of you to name so I hope this will suffice. Without you, I would not be writing this document. A range of emotions from stress, frustration, and anger to excitement, joy, and anticipation was felt during this journey. Although some of these emotions are far more enjoyable than others, you were there, for better or worse, to share them with me. Thank you for teaching me how to work hard and pushing me to do my best. I can not wait to see what awaits us.

Contents

List of Figures

List of Tables

Chapter 1

Introduction

1.1 Climate Change & Sustainability

Over the last thirty years, the extent of the ability of the human race to negatively impact the environment has been realized.[2] Our contribution to global atmospheric CO_2 concentrations has continued to rise, prompting the escalation from a warning to a crisis. Fig. 1.1 is the famous Keeling curve measuring the concentration of atmospheric CO_2 in parts per million over the last 60 years. The continuous increase in greenhouse gases has led to our current climate situation.[3] The effects of climate change are widespread and devastating, and as atmospheric CO_2 concentrations rise will worsen. The ramifications of climate change have been more frequent extreme weather (heavy flooding, droughts, hurricanes), rising sea levels, and acidification of the oceans.[4] The immediate impact of climate change can be felt in many aspects of our life, from food security to transportation and water quality.

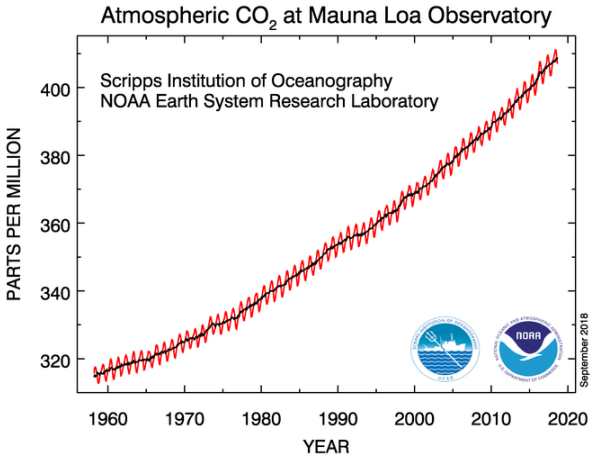

Figure 1.1: Chronological growth of atmospheric CO_2 concentration (red line) and seasonally corrected concentration of CO_2 (black line) measured at the Mauna Loa Observatory.[1]

With the current climate crisis, scientists and engineers must develop ways to reduce the impact our technologies have on the environment and develop new technologies to reverse the damage done. These technologies include carbon capture and sequestration alongside renewable energy sources like wind and solar.[5] One plan is to capture CO_2 from large point sources such as refineries and manufacturing facilities and store it underground in geological formations.[5] A major problem with this tactic is the unknown long-term viability, especially if the captured CO_2 can escape. A way to mitigate this problem is using CO_2 as a cheap, readily available carbon source to produce specialty chemicals and fuels. However, traditional thermochemical routes to CO_2 valorization are energy intensive and often offer poor energy efficiency.[6] One way to address issues with energy storage and the use of CO_2 as a carbon source is through the electrochemical conversion of CO_2

into high carbon content molecules. The CO_2 reduction reaction (CO_2RR) uses CO_2 as a feedstock and excess renewable electricity as a green reagent to reduce CO_2 and produce a wide range of carbon-containing molecules.

1.2 Utilizing Carbon Dioxide as a Carbon Source

The use of CO_2 as a feedstock has been a topic of interest for quite some time. It is a cheap, readily available carbon source; however, it is very thermodynamically stable and requires a large energy input to utilize it to produce valuable products effectively.[5,8,9] The general concept of CO_2 valorization is outlined in Fig. 1.2 where the CO_2 that is expelled from energy generation and transportation and, through an electrochemical process powered by renewable electricity, is converted to carbon monoxide (CO) or higher carbon-containing compounds (ethane, ethanol, propane, etc.).[7] The CO can be used with electrochemically generated hydrogen to produce syngas. Syngas is very commonly used in industrial processes, and the electrochemical generation of a product that does not require retrofitting of existing systems can make the employment of electrochemical methods more advantageous.

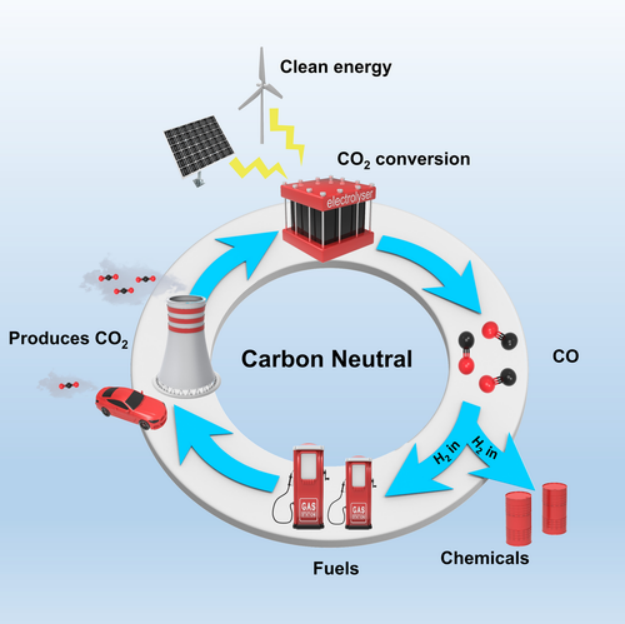

Figure 1.2: Carbon dioxide as a feedstock for carbon neutral production of furls and chemicals through the electrochemical reduction of CO_2[7]

Traditionally the energy to drive syngas production is supplied in the form of thermal energy, and the energy efficiency of the reaction is very low. One attempt to increase the sustainability of using CO_2 as a feedstock is by using electricity as an energy source. The electron is known as a green reagent and can reduce CO_2 at room temperature in a reaction called electrochemical CO_2 reduction or CO_2RR. Not only does the electrochemical approach allow the CO_2RR to be carried

out at room temperature, but the choice of electrode material dramatically influences the selectivity of the reaction.[10] There are a wide array of CO_2RR products ranging from producing CO on gold to forming multi-carbon-containing molecules like ethane and ethanol on copper.[11–14] However, there are a few grand challenges in the CO_2RR.

Firstly, CO_2 is a thermodynamically stable molecule. Electrochemical reduction of CO_2 is accompanied by slow electron transfer kinetics and often requires large overpotentials to achieve a reasonable current density.[15] However, these disadvantages can be mitigated through the development of electrocatalysts. In addition, the utilization of metal oxides and alloys can provide unique properties to tune CO_2RR selectivity.[16–18] This selectivity can be directly related to the binding energies of CO_2RR intermediates.[19] Metals that strongly bind CO_2 intermediates, such as gold, tend to form carbon monoxide exclusively; however, other metals, such as copper, exhibit moderate intermediate binding energy and produce various products.[20]

Secondly, at room temperature and pressure, the concentration of CO_2 in the liquid phase is governed by Henry's law and is quite low (34 mM in water at 25 °C).[21] This causes the reaction kinetics to be sluggish. Additionally, low concentrations of CO_2 in carboxylation reactions lead to side product formation.[22,23] These mass transfer limitations make it challenging to study the system's kinetics at the electrode since we rely on diffusion to replenish reactants to the electrode. However, developing unique electrochemical systems such as high-pressure electrochemistry and the clever design of specialized electrolytes like ionic liquids and CXEs have helped overcome the issues with CO_2 concentration.[24,25]

Finally, the number of electrochemical and chemical reaction steps required to form carbon-carbon bonds from CO_2RR is very high.[19] Generally, the mechanism is governed by a multi-step-based coordination chemistry comprising two, six, eight, ten, and twelve electrons for forming carbon monoxide, methanol, methane, acetaldehyde, and ethylene respectively (table 1.1). The most challenging step in the CO_2RR is the formation of C-C bonds due to the tendency of the reaction intermediates to desorb from the surface before they form these bonds.[26] Additionally, the high number of chemical and electrochemical steps give many opportunities to produce side

reactions. The binding energy of the intermediates has been shown to dramatically affect the selectivity of CO_2RR, with copper being the only metal that exhibits significant formation of C2 products.[10,19,26] Not only is it challenging to reduce CO_2, but controlling the selectivity of direct reduction of CO_2 to form C2+ products has proven exceedingly difficult.

Chemical Reaction	E^0/V vs. RHE	Product Name
$CO_2 + 2\,H^+ + 2\,e^- \longrightarrow CO + H_2O$	-0.11	Carbon Monoxide
$CO_2 + 2\,H^+ + 2\,e^- \longrightarrow HCOOH$	-0.12	Formic Acid
$CO_2 + 6\,H^+ + 6\,e^- \longrightarrow CH_3OH + H_2O$	0.03	Methanol
$CO_2 + 8\,H^+ + 8\,e^- \longrightarrow CH_4 + 2\,H_2O$	0.17	methane
$2\,CO_2 + 10\,H^+ + 10\,e^- \longrightarrow CH_3CHO + 3\,H_2O$	0.06	Acetaldehyde
$2\,CO_2 + 12\,H^+ + 12\,e^- \longrightarrow C_2H_4 + 4\,H_2O$	0.08	Ethylene
$2\,CO_2 + 12\,H^+ + 12\,e^- \longrightarrow C_2H_5OH + 3\,H_2O$	0.09	Ethanol
$2\,CO_2 + 14\,H^+ + 14\,e^- \longrightarrow C_2H_64\,H_2O$	0.14	Ethane
$2\,CO_2 + 16\,H^+ + 16\,e^- \longrightarrow C_2H_5CHO + 5\,H_2O$	0.09	Propionaldehyde
$3\,CO_2 + 18\,H^+ + 18\,e^- \longrightarrow C_3H_7OH + 5\,H_2O$	0.10	Propanol
$2\,H^+ + 2\,e^- \longrightarrow H_2$	0.0	Hydrogen Evolution Reaction

Table 1.1: Potential products for the electrochemical reduction of CO_2 in aqueous electrolyte of pH 7 at 25°C and 1 bar of pressure

1.3 Research Motivation

This work focuses on using high-pressure electrochemistry to overcome limitations with traditional CO_2 use in electrochemical organic synthesis. This research aims to provide a sustainable route to synthetic carboxylic acids that utilize CO_2 as a carbon source. Carboxylic acids are precursors to many specialty chemicals such as non-steroidal anti-inflammatory drugs (NSAIDs) like ibuprofen and Naproxin® (Fig. 1.3, b). Initially, the Boots group developed a six step synthesis for ibuprofen starting from isobutylbenzene. This process produces large quantities of waste and often utilizes toxic reagents or heavy metals, complicating the products' purification.[22] The BHC company improved the atom economy of the Boots process for the synthesis of ibuprofen in 1992. Fig. 1.3 a, shows the BHC process starting from isobutyl-acetophenone where the reaction is protonated over a Raney Ni catalyst and carboxylated over a palladium using CO.[27] Though this is a

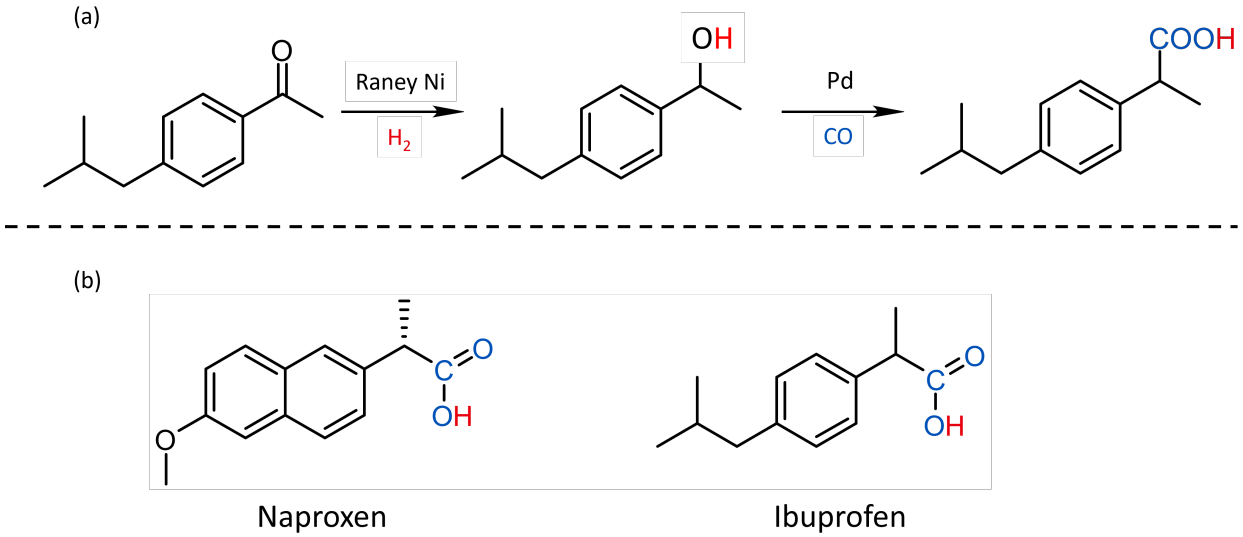

Figure 1.3: a) BHC process for the synthesis of ibuprofen. b) Chemical structure of Naproxen and ibuprofen

massive improvement over the Boots synthesis, this reaction requires two reaction steps, expensive metal catalysts, and the use of hydrogen gas and carbon monoxide most likely produced through petroleum processes.

Further improvements to the sustainability of this reaction can be made by using electrochemical synthesis techniques. Using electrochemical synthesis, the number of reaction steps is reduced, and the number of reagents used decreases, reducing the need for redox agents and improving the atom economy complying with one of the pillars of green chemistry.[28] Additionally, the electrochemistry can be done on inexpensive carbon electrodes and using CO_2 as a feedstock rather than expensive palladium and CO. These changes can further improve the atom economy for the synthesis of ibuprofen and improve the sustainability of its production.

Traditionally, electrochemical carboxylation using CO_2 is done at room temperature and pressure. However, these reaction conditions limit the amount of liquid phase CO_2 available leading to poor selectivity.[29,30] Scialdone *et al.*[30] demonstrated the concentration effects of CO_2 on the production of atrolactic acid. They found a monotonic increase in the selectivity of the reaction as a function of CO_2 pressure; however, they did not test CO_2 concentrations higher than 1.5 M and achieved a maximum selectivity of 80%.[30] Supplying more CO_2 to the system can further improve

selectivity; however, high liquid phase CO_2 concentrations are difficult to achieve.

A novel electrolyte is required to conduct electrochemistry at high CO_2 concentrations. These electrolytes are a special class of solvents known as CO_2 eXpanded Electrolytes or CXEs and enable the study of systems where CO_2 is not the limiting reactant. In addition, CXEs offer tuneable concentrations of CO_2 in the liquid phase from dilute to multi-molar, providing an unprecedented environment to study CO_2 concentration effects. We have found that the CO_2 concentration drastically influences the reaction selectivity. The findings of these studies can then be elaborated upon by utilizing computational tools like COMSOL multiphysics that use regression tools to determine the electrochemical kinetics.

This work also includes a variety of other projects that build on previous knowledge discovered in CXEs. One such project is the development of high surface area gold foam electrodes or noble metal foams for use in the CO_2 reduction reaction. To further enhance the CO production rate in CXEs high surface area electrodes were required. We successfully electrodeposited gold onto nickel foams to develop a high surface area CO_2RR catalyst. In addition, we also studied the effect of surface roughness on the shape of the electrodeposited gold.

Alongside other projects associated with the CO_2 reduction reaction (CO_2RR), the internet of catalysis project focused on developing a machine learning named entity recognition model to read, tag, and extract pertinent data from chemical literature and format it into a database. The goal of developing this tool was to reduce the time investment it takes for researchers to keep up with the relevant literature.

The final project was developing an educational program for students to use science-based approaches to discover and research career plans. Hypothesis-based career planning is a passion project to ensure that students are well-educated and satisfied upon their placement into the workforce. The primary goal for this project was to ensure that the students addressed their assumptions about what it is like to be a professional in their respective discipline. The program was built around the interview and discovery phase of the NSF's I-Corps^{TM} program.

1.4 Organic Electrosynthesis

In the last decade, electrochemistry has been used as a sustainable route toward producing specialty chemicals such as precursors to pharmaceuticals and sensitive reaction intermediates.[31–33] This technique is more widely known as organic electrosynthesis and is a sprawling subfield of electrochemistry covering a vast number of reactions that has grown nearly 300% in the last decade. Fig. 1.4 shows the increase in the number of publications that include the "organic electrosynthesis" keyword. The rise in popularity of this technique is in part due to the rising desire to develop sustainable processes for traditional chemical synthesis and also in part due to the unparalleled reactivity and reaction control afforded by this technique.[34] Organic electrosynthesis uses electrons to activate a substrate that is then converted through a series of either electrochemical or chemical reaction steps to a product. The order and number of these steps can vary greatly depending on the reaction and are generally classified as electrochemical chemical reactions or EC reactions.[35]

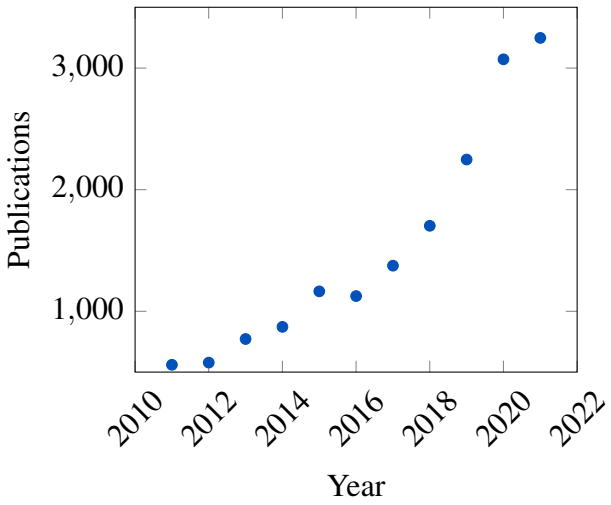

Figure 1.4: Publication volumes for manuscripts with "Organic Electrosynthesis" as a keyword over the last decade indexed by Dimensions.

Many industries have shifted toward the sustainable production of chemicals, and using electrons as redox agents provides many benefits.[36] For chemical synthesis applications, electrification can cut out intermediate steps increasing the atom economy of these reactions and serving as a non-toxic reducing agent.[37] Additionally, the commodity chemical industry can benefit from utilizing cheap electricity and a distributed manufacturing model instead of costly large-scale plants that can reduce the cost of producing chemicals.[6] Furthermore, electrochemistry has proven to be a highly scaleable process. Examples of large-scale electrochemistry processes can be found primarily in the production and plating of metals and in the chloralkali industries.[31] Many types of organic

substrates have been found as suitable starting materials for organic electrosynthesis and several reviews have been published on the state of the art for these reactions.[38]

The primary reaction that will be discussed here is electrochemical carboxylation using CO_2. These types of reactions circumvent the problems with the thermodynamic stability of CO_2 by instead activating an electrochemically active substrate.[39] There have been many example substrates for the breadth of starting materials that can be used in this reaction, including alcohols[40], alkenes[41,42], aldehydes[43], epoxides[44,45], organic halides[46–49], and a few other organic compounds.[50,51] The major pitfall of these reactions is the slow reaction rates and the mass transfer limitations associated with low CO_2 concentrations.[52] Although CO_2 is more soluble in many organic electrolytes when compared to water. The concentration in the liquid phase is still very low, leading to slow reaction rates and low selectivity toward carboxylated products.

1.5 CO_2 eXpanded Electrolytes

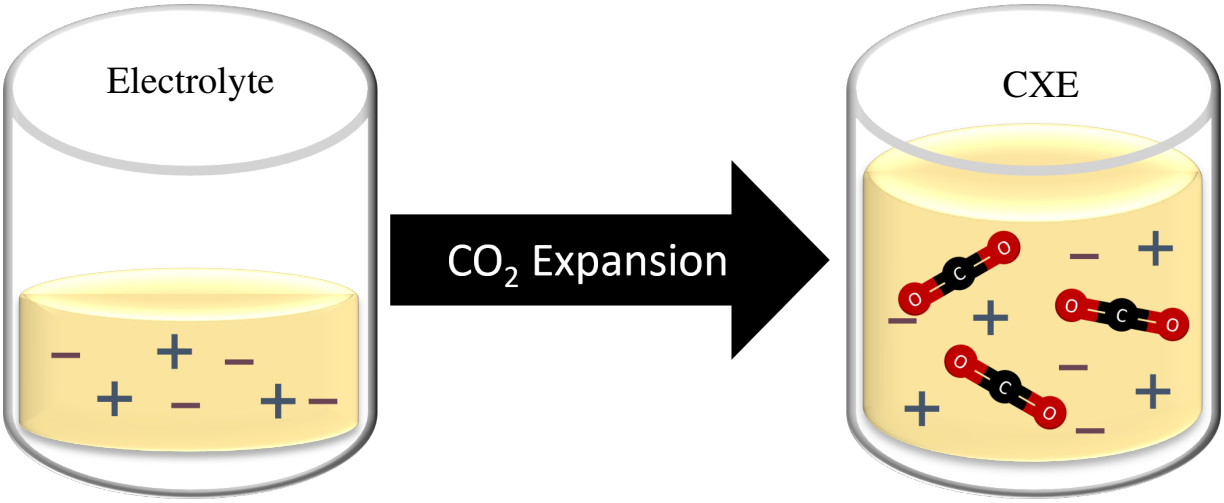

Figure 1.5: Expansion of electrolyte under CO_2 pressure to form a CXE

CO_2 eXpanded Electrolytes or CXEs consist of an organic solvent such as acetonitrile, dimethylformamide, or dimethyl sulfoxide and CO_2. Under CO_2 pressure, the solubility of the gas in the liquid solvent is high enough that the liquid phase volume of the binary mixture increases (Fig. 1.5).[53] This behavior leads to the doubling and even tripling of the liquid volume at moderate CO_2 pres-

sures as seen in data collected by Shaughnessy *et al.*[21] Fig. 1.6, a.[54] Additionally, these solvents enhance the diffusivity of various species by nearly an order of magnitude.[21,55,56] These solvents provide a much higher concentration of CO_2 than in traditional solvents and are critical in CO_2 utilization reactions as seen in Fig. 1.6, b.[57] This class of solvent and its high solubility of CO_2 can be exploited for use in organic electrochemistry with CO_2. The addition of an electrolyte to the solvent, such as an ammonium salt, allows for electrochemistry to be carried out in a medium rich with available CO_2. In traditional electrochemistry, the utilization of CO_2 as a feedstock is met with a major challenge associated with the low concentrations of CO_2 in the liquid phase.[58] These low concentrations contribute greatly to the sluggish reaction kinetics and low achievable current densities. Therefore, it is a worthwhile endeavor to develop an electrolyte media that can sustain higher concentrations of CO_2 while also enabling the transfer of charge. In addition to high CO_2 concentrations, these media also have the advantage of supporting a wide range of organic molecules for organic electrosynthesis. The ability to change solvents to ensure the solubility of reaction intermediates or form easily separable precipitates is another advantage of using CXEs.

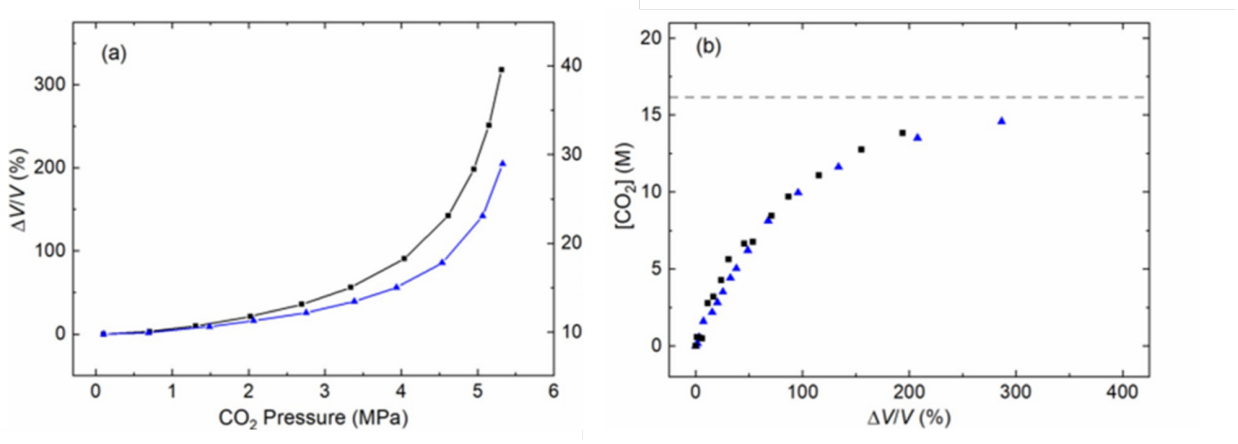

Figure 1.6: Volumetric expansion of acetonitrile (black) and acetonitrile initially containing 0.4 M $TBAPF_6$ (blue) as a function of CO_2 pressure. (b) Increase in the liquid phase CO_2 in Acetonitrile (black) and acetonitrile initially containing 0.4 M $TBAPF_6$ (blue) as a function of CO_2 pressure.[21]

1.6 Fundamentals of Electrochemistry

1.6.1 Cyclic Voltammetry

In electrochemical systems, current and potential are the experimental variables that have been integrated into the experiments. There are many ways that we can learn about these systems by manipulating the current and the potential of the system. One characterization technique discussed here is cyclic voltammetry (CV). This is a scanning potential technique where the potential is swept between two potentials, and the current is measured. A current vs. potential graph is produced and contains a large amount of information regarding the electrochemical system. The electrode surface is sweeping through a range of potentials, and the flux of electrons at that surface determines the shape. Sweeping through a range of potentials initially yields the electrochemical potential or onset potential of the redox event. Once the electrode reaches a potential high enough to activate a redox species, the electron is transferred, resulting in measurable current flow.[59]

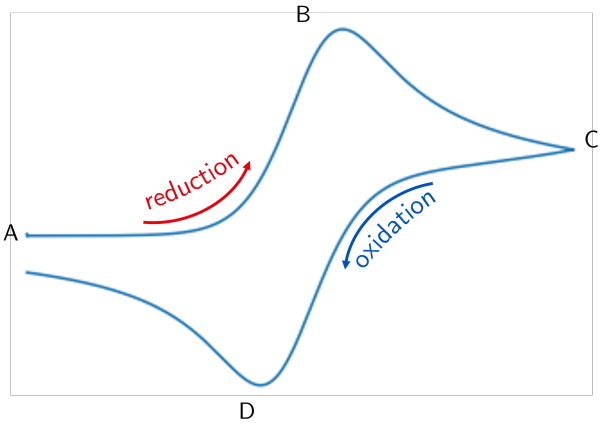

Figure 1.7: General shape of a reversible cyclic voltammogram

CVs are a dynamic process, and as potentials increase, the flux of electrons also increases. The system eventually starves itself of the redox species, and we see a transition from a kinetically limited regime to a mass transfer limited regime (Fig. 1.7, B). This location is known as a peak current and is very important in the characterization of electrochemical systems. For a system where the redox species undergoes reversible electron transfer, once the potential sweep reaches the first endpoint, it begins sweeping in the opposite direction (Fig. 1.7, C). The shape of the CV in the forward sweep will have a peak current and a limiting potential. The peak current is associated with the development of a boundary layer that the redox species must diffuse through. The lim-

iting potential is the steady state current after the boundary layer has been completely developed. Usually, the limiting potential is where the flipping potential is located, and the direction of the sweep is reversed.

For a reversible system, a hysteresis is formed that closely resembles the forward sweep, also having a peak current and a limiting potential (Fig. 1.7, D). The reversibility of a system that exhibits this behavior is determined by the rate of electron transfer and is associated with fast electron transfer kinetics. For a system that does not exhibit reversible electron transfer, the return peak is absent. This absence can be due to various reasons, such as the generation of a stable reaction intermediate or the consumption of the electrogenerated species by a chemical reaction. Traditionally, reversible couples are far more advantageous due to their ease of characterization and the ability to determine diffusion coefficients, reduction potentials, and electron transfer rates.[59] However, these parameters can be estimated through simulation and provide a better understanding of the electrochemical system, making cyclic voltammetry a widely used electrochemical characterization technique.

1.6.2 Electrode Kinetics

Cyclic voltammetry experiments are widely used to study the kinetics of the electrode. In general, the kinetics of electrochemical systems are governed by two chemical phenomena electron transfer and diffusion. To model the electron transfer kinetics, we use the Butler-Volmer kinetic model to govern the flux of electrons across an electrode surface as a function of the electrode potential. Critical parameters in the Butler-Volmer model (eq. (3.2)) are the electrochemical rate constant (k_0), the standard reduction potential (E_0), and the concentration of the reaction species (C_O, C_R). Each of these parameters is critical in the determination of the shape of a voltammogram. During a cyclic voltammetry experiment, the current sweeps through a range of potentials. This results in a flux of electrons from the electrode surface as a function of the cell potential. The Butler-Volmer kinetic model is critical in understanding the kinetics of irreversible electrochemical systems. Each of the parameters discussed affects the shape of the CV, and simulations of the system can be

utilized to regress the kinetic information from experimental data. Producing these models is time-consuming and arduous, but without convenient access to the kinetic information, simulations provide a path to obtain the kinetic information in the case of irreversible electrochemistry.

$$i = FAk^0 \left[C_O(0,t) e^{-\alpha f(E-E^{0'})} - C_R(0,t) e^{(1-\alpha) f(E-E^{0'})} \right] \tag{1.1}$$

1.6.3 Chronoamperometry

Chronoamperetry experiments are often used in conjunction with CV studies. In general, the CV provides necessary information about the electrochemical system, such as the reduction potential and the expected steady-state current. This information is used in chronoamperometry experiments to determine the potential of the electrode to facilitate chemistry. The cell is held at a potential where the electrochemical reaction occurs at a reasonable rate for some amount of time. Over that time, the cell's current is measured as a function of time. These experiments provide several important performance metrics for the reaction. Mainly the reaction rate and the charge passed. From the charge passed, we can calculate the electron efficiency or faradaic efficiency, letting us measure the performance of the reactor over a period of time after the product has been quantified.

Some considerations must be made when developing a system to undergo bulk electrolysis, for example, the size of the sacrificial counter electrode, the concentration of the reactants, and the amount of stirring in the system. The charge passed during the reaction can vary greatly depending on the size of the electrode. Therefore, the size of the sacrificial counter electrode must be sufficiently large to sustain the reaction for its duration; otherwise, the electrolysis will fail.

1.7 High-Pressure Electrochemistry

1.7.1 Reactor Design

Traditional electrochemistry requires a fairly simple setup consisting of an electrochemical cell and three electrodes. Usually, these systems are in a glass compartment with an open top allowing

easy access to each of the components. However, a considerable modification to these systems must be made to transition from atmospheric electrochemistry to a high-pressure system.

The skeleton of the reactor we designed consisted of a 50 ml Parr reactor Fig. 1.8. A new reactor cap had to be fabricated to retrofit this reactor for electrochemical applications. This modified cap contained threaded holes to install specialty electrochemical feedthroughs. The feedthroughs were purchased through CeramTtec (2846-01-A) and consisted of a stainless steel body and a ceramic insulator that contains a copper wire. The copper allowed the connection from the potentiostat to the electrochemical cell. Additionally, the reactor was fitted with a port to collect temperature and pressure information.

A thermocouple and a pressure transducer were installed, and the information they produced was processed through a National Instruments data acquisition device before being viewed in a LabView program. The output provided critical information about the temperature and pressure of the reactor and was also used to ensure the reactor was at equilibrium before electrochemical experiments were conducted. The reactor was also placed in an isothermal jacket to ensure proper temperature control.

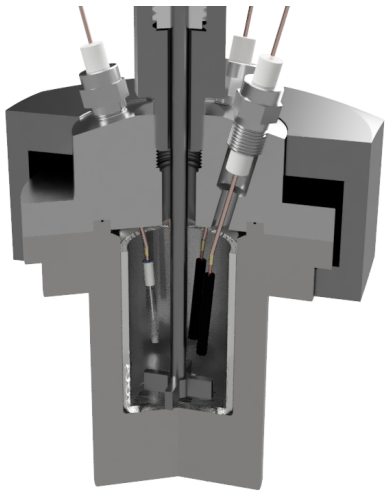

Figure 1.8: High-pressure electrochemical reactor 3d model provided by Ed Atchison

Inside the body of the reactor, a glass electrochemical cell was used to isolate the metal body from the electrochemical system. This is a small optimization from the cell setup described in previous work where a Teflon^{TM} cup was used.[21,55] Teflon^{TM} will expand as CO_2 permeates the cup causing it to be stuck in the reactor body until that gas is released. The permeation behavior could also cause a depreciation in the accuracy of our measurements of products, so the glass vessel removes that source of error.

The copper feedthroughs allow for excellent modularity of the reactor. One feedthrough is dedicated to a reference electrode consisting of a silver wire inside a fritted glass chamber filled with the same electrolyte solution used for electrochemical experimentation. However, the other three feedthroughs can support any other electrode. This is made possible by the use of gold crimp-style clips. These clips slip over the exterior of the copper feedthroughs and establish an electrical connection to the electrode. This design feature allows the system to retain its modularity and facilitate rapid experimental setup changes.

In addition to the larger-scale reactor (50 mL), a smaller-scale reactor (20 mL) was also developed. The reason for its production was twofold. First, waiting for equilibrium in the large reactor is the rate-determining step in using these reactors. A smaller liquid phase would increase the rate of the reactor reaching equilibrium. Additionally, it would serve as redundancy in case of considerable reactor downtime. Often leaks or issues with the electrical feedthroughs would develop, and a backup reactor would ensure that these inconveniences would not impact the ability to produce results.

The development of a smaller reactor would also allow for two reactors to be pressurized in parallel. Similarly to the large reactor, the smaller reactor rested in a single-pass isothermal jacket with identical temperature and pressure sensing equipment. The major difference between the larger and small reactor was the omission of a mechanical stir rod in the smaller cell. Size constraints led to the decision that placing the reactor on a stir plate and outfitting it with a magnetic stir bar would be sufficient. However, the results from the smaller reactor proved to be less consistent than that of its larger clone. This could be due to the inconsistencies in the stirring with a stir bar or having a smaller liquid volume. However, the reactor's use as a training tool is unparalleled. Setting up the larger reactor successfully should not be trivialized. Having a smaller reactor for new graduate and undergraduate students to be trained on is critical in their success when moving to the large reactor while limiting potential downtime if the setup is done incorrectly.

References

[1] NOAA, G. M. L. U. D. o. C. Global Monitoring Laboratory - Carbon Cycle Greenhouse Gases.

[2] Raza, A.; Gholami, R.; Rezaee, R.; Rasouli, V.; Rabiei, M. Significant aspects of carbon capture and storage – A review. *Petroleum* **2019**, *5*, 335–340.

[3] Schiffer, Z. J.; Manthiram, K. Electrification and Decarbonization of the Chemical Industry. *Joule* **2017**, *1*, 10–14.

[4] Houghton, J. The science of global warming. *Interdisciplinary Science Reviews* **2001**, *26*, 247–257.

[5] Song, R.; Zhu, W.; Fu, J.; Chen, Y.; Liu, L.; Zhang, J.; Lin, Y.; Zhu, J. Electrode Materials Engineering in Electrocatalytic CO_2 Reduction: Energy Input and Conversion Efficiency. *Advanced Materials* **2019**, *32*, 1903796.

[6] Sullivan, I.; Goryachev, A.; Digdaya, I. A.; Li, X.; Atwater, H. A.; Vermaas, D. A.; Xiang, C. Coupling electrochemical CO2 conversion with CO2 capture. *Nature Catalysis 2021 4:11* **2021**, *4*, 952–958.

[7] Jin, S.; Hao, Z.; Zhang, K.; Yan, Z.; Chen, J. Advances and Challenges for the Electrochemical Reduction of CO_2 to CO: From Fundamentals to IndSustrialization. *Angewandte Chemie International Edition* **2021**, *60*, 20627–20648.

[8] Jhong, H. R. M.; Ma, S.; Kenis, P. J. Electrochemical conversion of CO_2 to useful chemicals: Current status, remaining challenges, and future opportunities. *Current Opinion in Chemical Engineering* **2013**, *2*, 191–199.

[9] Jiang, X.; Nie, X.; Guo, X.; Song, C.; Chen, J. G. Recent Advances in Carbon Dioxide Hydrogenation to Methanol via Heterogeneous Catalysis. *Chemical Reviews* **2020**, *120*, 7984–8034.

[10] Hori, Y. *Electrochemical CO_2 Reduction on Metal Electrodes*; Springer New York, 2008; pp 89–189.

[11] Loiudice, A.; Lobaccaro, P.; Kamali, E. A.; Thao, T.; Huang, B. H.; Ager, J. W.; Buonsanti, R. Tailoring Copper Nanocrystals towards C2 Products in Electrochemical CO_2 Reduction. *Angewandte Chemie - International Edition* **2016**, *55*, 5789–5792.

[12] Li, C. W.; Kanan, M. W. CO 2 reduction at low overpotential on Cu electrodes resulting from the reduction of thick Cu 2O films. *Journal of the American Chemical Society* **2012**, *134*, 7231–7234.

[13] Roberts, F. S.; Kuhl, K. P.; Nilsson, A. High Selectivity for Ethylene from Carbon Dioxide Reduction over Copper Nanocube Electrocatalysts. *Angewandte Chemie* **2015**, *127*, 5268–5271.

[14] Feng, Q.; Huang, K.; Liu, S.; Wang, X. Electrocatalytic carboxylation of 2-amino-5-bromopyridine with CO 2 in ionic liquid 1-butyl-3-methyllimidazoliumtetrafluoborate to 6-aminonicotinic acid. *Electrochimica Acta* **2010**, *55*, 5741–5745.

[15] Whipple, D. T.; Kenis, P. J. Prospects of CO_2 utilization via direct heterogeneous electrochemical reduction. *Journal of Physical Chemistry Letters* **2010**, *1*, 3451–3458.

[16] Shaughnessy, C. I.; Jantz, D. T.; Leonard, K. C. Selective electrochemical CO_2 reduction to CO using: In situ reduced In2O3 nanocatalysts. *Journal of Materials Chemistry A* **2017**, *5*, 22743–22749.

[17] Sakurai, H.; Tsubota, S.; Haruta, M. Hydrogenation of CO_2 over gold supported on metal oxides. *Applied Catalysis A, General* **1993**, *102*, 125–136.

[18] Tayyebi, E.; Hussain, J.; Abghoui, Y.; Skúlason, E. Trends of Electrochemical CO_2 Reduction Reaction on Transition Metal Oxide Catalysts. *Journal of Physical Chemistry C* **2018**, *122*, 10078–10087.

[19] Bagger, A.; Ju, W.; Varela, A. S.; Strasser, P.; Rossmeisl, J. Electrochemical CO2 Reduction: A Classification Problem. *ChemPhysChem* **2017**, *18*, 3266–3273.

[20] Jones, J.-P.; Prakash, G. K. S.; Olah, G. A. Electrochemical CO_2 Reduction: Recent Advances and Current Trends. *Israel Journal of Chemistry* **2014**, *54*, 1451–1466.

[21] Shaughnessy, C. I.; Sconyers, D. J.; Kerr, T. A.; Lee, H.-J.; Subramaniam, B.; Leonard, K. C.; Blakemore, J. D. Intensified Electrocatalytic CO_2 Conversion in Pressure-Tunable CO_2-Expanded Electrolytes. *ChemSusChem* **2019**, *12*, 3761–3768.

[22] Silvestri, G.; Gambino, S.; Filardo, G. Electrochemical carboxylation of aldehydes and ketones with sacrificial aluminum anodes. *Tetrahedron Letters* **1986**, *27*, 3429–3430.

[23] Isse, A. A.; Galia, A.; Belfiore, C.; Silvestri, G.; Gennaro, A. Electrochemical reduction and carboxylation of halobenzophenones. *Journal of Electroanalytical Chemistry* **2002**, *526*, 41–52.

[24] Feng, Q.; Huang, K.; Liu, S.; Yu, J.; Liu, F. Electrocatalytic carboxylation of aromatic ketones with carbon dioxide in ionic liquid 1-butyl-3-methylimidazoliumtetrafluoborate to -hydroxycarboxylic acid methyl ester. *Electrochimica Acta* **2011**, *56*, 5137–5141.

[25] Zhao, S. F.; Horne, M.; Bond, A. M.; Zhang, J. Electrochemical reduction of aromatic ketones in 1-butyl-3-methylimidazolium-based ionic liquids in the presence of carbon dioxide: the influence of the ketone substituent and the ionic liquid anion on bulk electrolysis product distribution. *Physical Chemistry Chemical Physics* **2015**, *17*, 19247–19254.

[26] Woldu, A. R.; Huang, Z.; Zhao, P.; Hu, L.; Astruc, D. Electrochemical CO2 reduction (CO2RR) to multi-carbon products over copper-based catalysts. *Coordination Chemistry Reviews* **2022**, *454*, 214340.

[27] Agee, B. M.; Mullins, G.; Swartling, D. J. Progress towards a more sustainable synthetic

pathway to ibuprofen through the use of solar heating. *Sustainable Chemical Processes 2016 4:1* **2016**, *4*, 1–9.

[28] Anastas, P.; Eghbali, N. Green Chemistry: Principles and Practice. *Chemical Society Reviews* **2009**, *39*, 301–312.

[29] Chan, A. Asymmetric Catalytic Hydrogenation of Alpha-Arylpropenic Acids. 1991.

[30] Scialdone, O.; Galia, A.; Isse, A. A.; Gennaro, A.; Sabatino, M. A.; Leone, R.; Filardo, G. Electrocarboxylation of aromatic ketones: Influence of operative parameters on the competition between ketyl and ring carboxylation. *Journal of Electroanalytical Chemistry* **2007**, *609*, 8–16.

[31] Kawamata, Y.; Baran, P. S. Electrosynthesis: Sustainability Is Not Enough. *Joule* **2020**, *4*, 701–704.

[32] Zhu, W. *et al.* Monodisperse Au Nanoparticles for Selective Electrocatalytic Reduction of CO_2 to CO. **2013**, *135*.

[33] Chang, X.; Zhang, Q.; Guo, C. Asymmetric Electrochemical Transformations. *Angewandte Chemie International Edition* **2020**, *59*, 12612–12622.

[34] Kingston, C.; Palkowitz, M. D.; Takahira, Y.; Vantourout, J. C.; Peters, B. K.; Kawamata, Y.; Baran, P. S. A Survival Guide for the "Electro-curious". *Accounts of Chemical Research* **2020**, *53*, 72–83, PMID: 31823612.

[35] Bard, A. J. In *Electrochemical methods: fundamentals and applications*, 2nd ed.; Faulkner, L. R., Ed.; Wiley, 2001.

[36] Wiebe, A.; Gieshoff, T.; Möhle, S.; Rodrigo, E.; Zirbes, M.; Waldvogel, S. R. Electrifying Organic Synthesis. *Angewandte Chemie - International Edition* **2018**, *57*, 5594–5619.

[37] Frontana-Uribe, B. A.; Little, R. D.; Ibanez, J. G.; Palma, A.; Vasquez-Medrano, R. No Title. *Green Chemistry* **2010**, *12*, 2099–2119.

[38] Tsuji, Y.; Fujihara, T. Carbon dioxide as a carbon source in organic transformation: carbon-carbon bond forming reactions by transition-metal catalysts. *Chem. Communications* **2012**, *48*, 9956–9964.

[39] Stalcup, M. A.; Nilles, C. K.; Lee, H. J.; Subramaniam, B.; Blakemore, J. D.; Leonard, K. C. Organic Electrosynthesis in CO_2-eXpanded Electrolytes: Enabling Selective Acetophenone Carboxylation to Atrolatic Acid. *ACS Sustainable Chemistry and Engineering* **2021**, *9*, 10431–10436.

[40] Wu, L. X.; Wang, H.; Xiao, Y.; Tu, Z. Y.; Ding, B. B.; Lu, J. X. Synthesis of dialkyl carbonates from CO 2 and alcohols via electrogenerated N-heterocyclic carbenes. *Electrochemistry Communications* **2012**, *25*, 116–118.

[41] Zhang, K.; Xiao, Y.; Lan, Y.; Zhu, M.; Wang, H.; Lu, J. Electrochemical reduction of aliphatic conjugated dienes in the presence of carbon dioxide. *Electrochemistry Communications* **2010**, *12*, 1698–1702.

[42] Steinmann, S. N.; Michel, C.; Schwiedernoch, R.; Wu, M.; Sautet, P. Electro-carboxylation of butadiene and ethene over Pt and Ni catalysts. *Journal of Catalysis* **2016**, *343*, 240–247.

[43] Doherty, A. P. Electrochemical reduction of butyraldehyde in the presence of CO_2. *Electrochimica Acta* **2002**, *47*, 2963–2967.

[44] Xiao, Y.; Chen, B. L.; Yang, H. P.; Wang, H.; Lu, J. X. Electrosynthesis of enantiomerically pure cyclic carbonates from CO 2 and chiral epoxides. *Electrochemistry Communications* **2014**, *43*, 71–74.

[45] Khoshro, H.; Zare, H. R.; Namazian, M.; Jafari, A. A.; Gorji, A. Synthesis of cyclic carbonates through cycloaddition of electrocatalytic activated CO_2 to epoxides under mild conditions. *Electrochimica Acta* **2013**, *113*, 263–268.

[46] Amatore, C.; Jutand, A.; Khalil, F.; Nielsent, M. F. Carbon Dioxide as a C1 Building Block. Mechanism of Palladium-Catalyzed Carboxylation of Aromatic Halides. *Journal of the American Chemical Society* **1992**, *114*, 7076–7085.

[47] Lan, Y. C.; Wang, H.; Wu, L. X.; Zhao, S. F.; Gu, Y. Q.; Lu, J. X. Electroreduction of dibromobenzenes on silver electrode in the presence of CO_2. *Journal of Electroanalytical Chemistry* **2012**, *664*, 33–38.

[48] Isse, A. A.; Durante, C.; Gennaro, A. One-pot synthesis of benzoic acid by electrocatalytic reduction of bromobenzene in the presence of CO_2. *Electrochemistry Communications* **2011**, *13*, 810–813.

[49] Scialdone, O.; Galia, A.; Errante, G.; Isse, A. A.; Gennaro, A.; Filardo, G. Electrocarboxylation of benzyl chlorides at silver cathode at the preparative scale level. *Electrochimica Acta* **2008**, *53*, 2514–2528.

[50] Howell, J. O.; Goncalves, J. M.; Klasinc, L.; Wightman, R. M.; Amatore, C.; Kochi, J. K. Electron Transfer from Aromatic Hydrocarbons and Their -Complexes with Metals. Comparison of the Standard Oxidation Potentials and Vertical Ionization Potentials. *Journal of the American Chemical Society* **1984**, *106*, 3968–3976.

[51] Yang, D. T.; Zhu, M.; Schiffer, Z. J.; Williams, K.; Song, X.; Liu, X.; Manthiram, K. Direct Electrochemical Carboxylation of Benzylic C-N Bonds with Carbon Dioxide. *ACS Catalysis* **2019**, *9*, 4699–4705.

[52] Scialdone, O.; Sabatino, M. A.; Belfiore, C.; Galia, A.; Paternostro, M. P.; Filardo, G. An unexpected ring carboxylation in the electrocarboxylation of aromatic ketones. *Electrochimica Acta* **2006**, *51*, 3500–3505.

[53] Akien, G. R.; Poliakoff, M. A critical look at reactions in class I and II gas-expanded liquids using CO_2 and other gases. *Green Chemistry* **2009**, *11*, 1083–1100.

[54] Jessop, P. G.; Subramaniam, B. Gas-expanded liquids. *Chemical Reviews* **2007**, *107*, 2666–2694.

[55] Sconyers, D. J.; Shaughnessy, C. I.; Lee, H.; Subramaniam, B.; Leonard, K. C.; Blakemore, J. D. Enhancing Molecular Electrocatalysis of CO_2 Reduction with Pressure-Tunable CO_2-Expanded Electrolytes. *ChemSusChem* **2020**, cssc.202000390.

[56] Piskulich, Z. A.; Laird, B. B. Molecular Simulations of Phase Equilibria and Transport Properties in a Model CO_2-Expanded Lithium Perchlorate Electrolyte. *The Journal of Physical Chemistry B* **2021**, acs.jpcb.1c05369.

[57] Wei, M.; Musie, G. T.; Busch, D. H.; Subramaniam, B. CO_2-expanded solvents: Unique and versatile media for performing homogeneous catalytic oxidations. *Journal of the American Chemical Society* **2002**, *124*, 2513–2517.

[58] Chen, Y.; Lewis, N. S.; Xiang, C. Operational constraints and strategies for systems to effect the sustainable, solar-driven reduction of atmospheric CO_2. *Energy and Environmental Science* **2015**, *8*, 3663–3674.

[59] Compton, R.; Banks, C. *Understanding Voltammetry*, 3rd ed.; 2018; pp 255–258.

Chapter 2

Organic Electrosynthesis in CO_2-eXpanded Electrolytes: Enabling Selective Acetophenone Carboxylation to Atrolactic Acid

Organic Electrosynthesis in CO_2-eXpanded Electrolytes: Enabling Selective Acetophenone Carboxylation to Atrolatic Acid

Matthew A. Stalcup, Christian K. Nilles, Hyun-Jin Lee, Bala Subramaniam, James D. Blakemore, and Kevin C. Leonard ACS Sustainable Chemistry Engineering **2021** 9 (31), 10431-10436 DOI: 10.1021/acssuschemeng.1c03073

Abstract

Electrochemical carboxylation is an organic electrosynthesis technique where CO_2 is coupled with an organic molecule to form carboxylic acids. Here we show that process intensification and selectivity enhancements are simultaneously achieved by performing electrochemical carboxylation in CO_2-eXpanded electrolytes (CXE)–a class of media that accommodates multimolar concentrations of CO_2 in organic solvents at modest pressures. We observed that electrochemical carboxylation of acetophenone does not occur at ca. 1 atm (2 bar) CO_2 head-space pressure. Instead, acetophenone hydrogenation was dominant, producing the undesired 1-phenylethanol as the major product. However, in the CXE media (at 14 - 42 bar CO_2 head-space pressure), $(\pm)$-atrolactic acid was the major product with a maximum faradaic efficiency of 72% observed at 28 bar. Achieving the pressure-tunable carboxylation results from the high liquid-phase CO_2 concentrations afforded by the CXE media. At CO_2 pressures exceeding 28 bar, we observed a lower rate of carboxylation, which is attributed to the decreased electrolyte polarity at progressively greater liquid-phase CO_2 concentrations present at higher pressures.

2.1 Introduction

New and sustainable carbon dioxide (CO_2) reaction pathways are needed to leverage CO_2 as a carbon feedstock. CO_2 conversion is challenging because it is both (1) thermodynamically stable, requiring an external input of free energy, and (2) kinetically limited, resulting in the need to overcome large activation energies during its conversion.[1] While several chemocatalytic methods have been reported for converting CO_2 into value-added products,[2,3] electrochemical CO_2 conversion holds promise because it could be powered with renewable wind and solar energy sources. A grand challenge in electrochemical CO_2 conversion is synthesizing high-carbon content products through carbon-carbon coupling.

Copper electrocatalysts have long been known to couple CO_2 with itself to produce a number of C2 (i.e., two-carbon) products in aqueous media.[4–6] It has been suggested that C-C coupling occurs uniquely on Cu because the CO adsorption energy is at an optimum level that enables the surface to be covered by adsorbed CO. This suppresses the hydrogen evolution reaction and promotes the formation of C2 products through dimerization of the adsorbed CO radical intermediate.[7–10] However, because the C-C coupling occurs through CO dimerization, the selectivity and efficiency towards any one product is typically low.[1] Moreover, in aqueous media at ambient pressures, the overall rates are limited by the low solubility of CO_2 in water.[11]

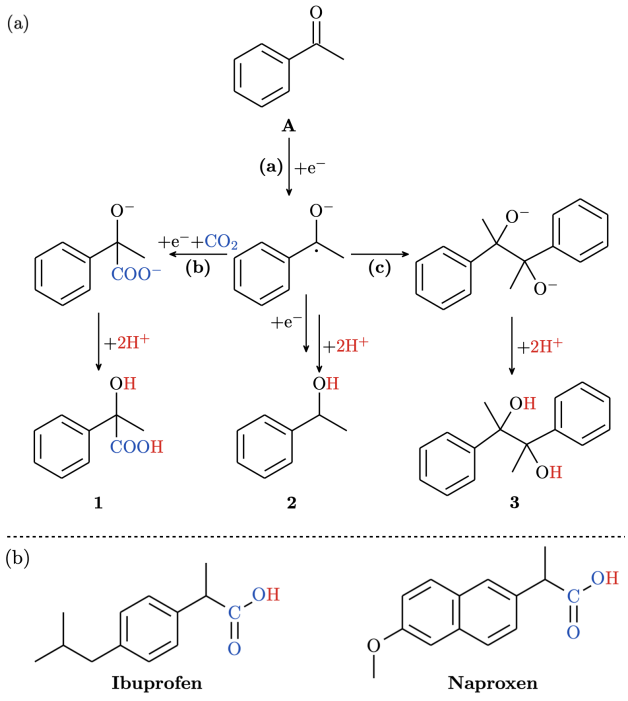

Figure 2.1: (a) Proposed mechanism for the electrocarboxylation of acetophenone resulting in the formation of atrolactic acid (**1**), 1-phenylethanol (**2**), and 2,3-diphenylbutane-2,3-diol (**3**). (b) Chemical structures for Ibuprofen and Naproxen, demonstrating similarities with atrolactic acid.

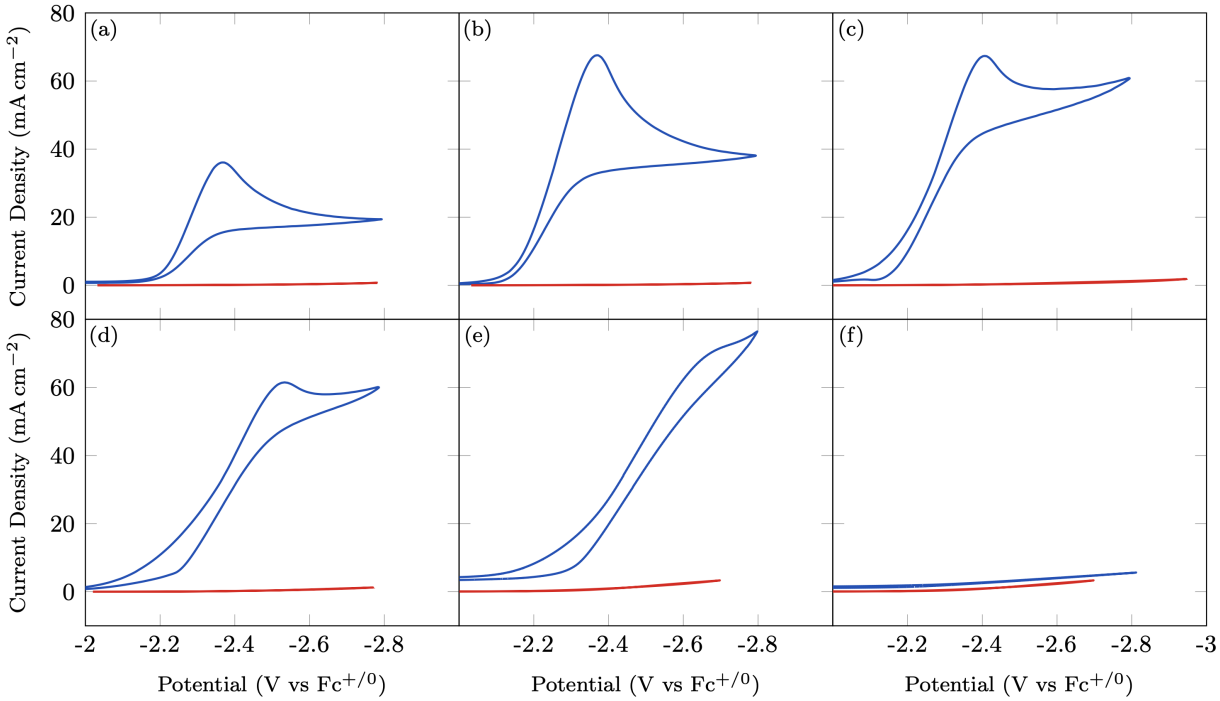

Figure 2.2: Cyclic voltammetry of acetophenone reduction (blue) under both standard and CXE conditions compared to blank electrolytes (red) at various head-space pressures. Panel (a) 2 bar Ar; (b) 2 bar CO_2, (c) 14 bar CO_2; (d) 28 bar CO_2; (e) 42 bar CO_2; (f) 55 bar CO_2. Working electrode: 1 mm diameter glassy carbon; Counter electrode: Mg metal sacrificial anode; Reference electrode: Cu quasi-reference electrode; Scan rate: 50 mV s^{-1}.

Recently, we demonstrated that organic solvent-based CO_2-eXpanded Electrolytes (CXEs) can dissolve multi-molar amounts of liquid CO_2 at moderate pressures while retaining sufficient supporting electrolyte concentrations to facilitate electrochemistry.[12–14] We refer to these as CO_2-eXpanded Electrolytes, because the liquid-phase volume expands with increasing CO_2 pressure (from 14 - 55 bar) due to the dissolution of CO_2 (see Supporting Information, Figure S1). In previous work, we observed (1) an order-of-magnitude enhancement of the catalytic current for CO_2 reduction to CO on heterogeneous catalysts (polycrystalline gold and copper);[12,13] (2) a significant enhancement of catalytic rate for homogeneous ($Re(CO)_3$(bpy)Cl (bpy = 2,2 -bipyridyl)) catalysts;[14] and (3) a maximum in the electrocatalytic current at intermediate CO_2 pressures of $\sim$30 bar.

In this work, we demonstrate that the favorable properties of CXEs enhance the rate and selectivity of producing high-carbon content products via electrochemical carboxylation reaction

pathways. Electrochemical carboxylation is an alternative approach to producing high-carbon-content carboxylic acids via the electrochemical coupling of CO_2 with organic compounds. Organic electrosynthesis has become a promising method to produce a wide variety of chemicals with a high atom economy.[15] Previous studies on electrochemical carboxylation[16] have explored coupling CO_2 with alcohols[17], alkenes[18,19], aldehydes[20], epoxides[21,22], organic halides[23–26], and a few other organic compounds.[27,28] However, elevated liquid-phase CO_2 concentrations have not, to the best of our knowledge, been reported for enhancing electrosynthetic carboxylation, offering an opportunity to improve this important type of otherwise challenging reactivity.

2.2 Results and Discussion

As a model reaction, we demonstrate that CXEs enhance electrochemical carboxylation of acetophenone, selectively producing $(\pm)$-atrolactic acid **1** over either 1-phenylethanol **2** or 2,3-diphenyl-2,3-butanediol **3**. The electrochemical carboxylation of acetophenone is of interest in the production of non-steroidal anti-inflammatory (NSAID) pharmaceuticals such as Ibuprofen and Naproxen (Figure 2.1b). The Monsanto Corporation and others[29–39] had been interested in the electrochemical carboxylation of acetophenone to produce atrolactic acid **1**; however, controlling the reaction to produce the desired carboxylic acid product **1** with high rates and selectivities (i.e, without formation of the alcohol **2** or dimer **3**) has been a challenge.[29,39]

To assess the electrochemical behavior of acetophenone carboxylation in the CXE media, cyclic voltammetry experiments were performed in tetrabutylammonium hexafluorophosphate-supported acetonitrile under 2 bar Ar and CO_2 head-space pressures of 2, 14, 28, 42, and 55 bar with a glassy carbon working electrode and a Mg sacrificial counter electrode (details provided in Supporting Information, subsection 1). The sacrificial Mg/Mg^{2+} counter oxidation reaction (Supporting Information Figure S2) was chosen to charge-balance the acetophenone reduction without oxidizing the electrolyte. In each panel of Figure 2.2, the voltammetry response of acetophenone reduction (blue voltammogram) is compared to a blank (red voltammogram) at identical head-space pressures with no acetophenone present.

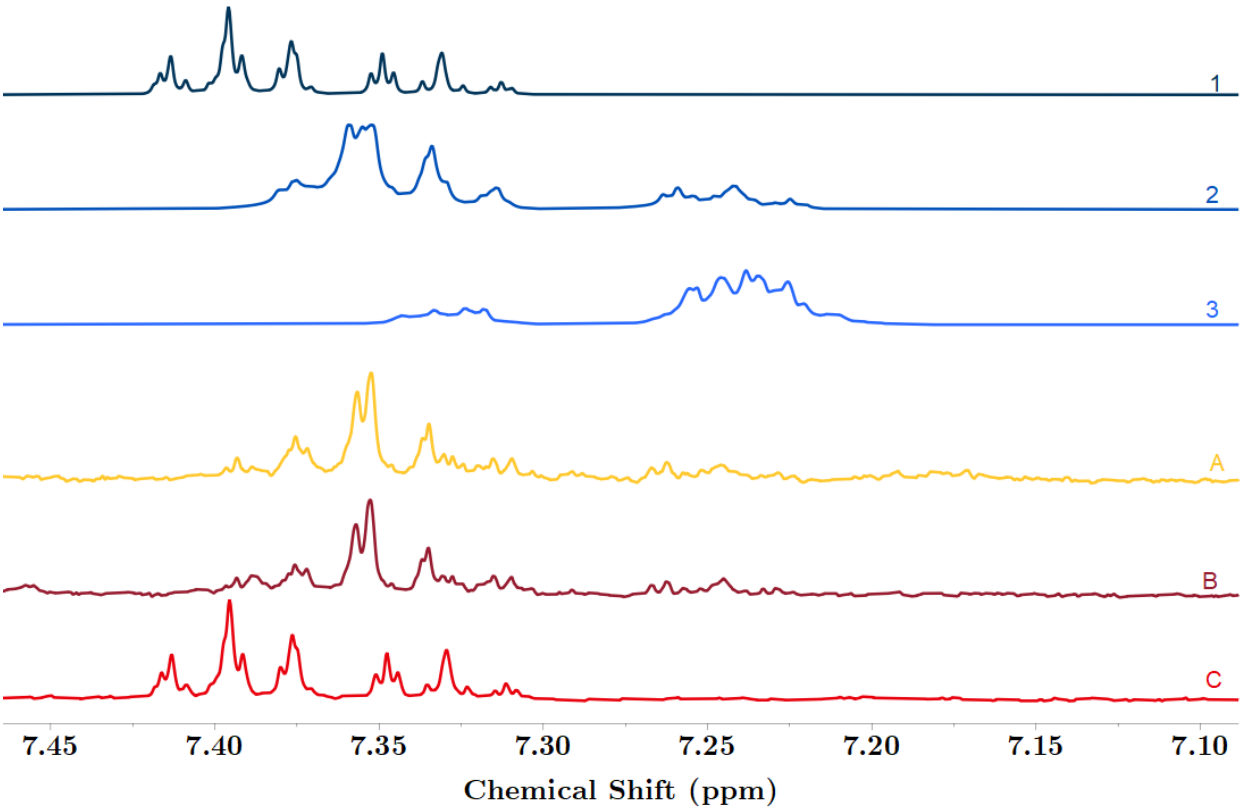

Figure 2.3: ^{1}H-NMR results after 12-hour bulk electrolysis under different reaction conditions at -2.6 V vs Fc/Fc^{+}. (1) (±)-atrolatic acid standard, (2) 1-phenylethanol standard, (3) 2,3-diphenylbutane-2,3-diol standard, (A) 2 bar argon pressure, (B) 2 bar CO_2 pressure, (c) 28 bar CO_2 pressure.

During the electrochemical conversion, we anticipate that acetophenone can undergo a one-electron transfer reduction to form a ketyl radical anion (Fig. 2.1a, reaction **(a)**). This ketyl anion can either react with CO_2 to form a carboxylate anion (Fig. 2.1a, reaction **(b)**), dimerize (Fig. 2.1a, reaction **(c)**), or undergo $H^{+}/H^{\bullet}$ transfer to form an alcohol (Fig. 2.1a,**(2)**). When CO_2 is absent from the system (Figure 2.2a), we observed a voltammetric wave with a peak current of 36.3 $mA\,cm^{-2}$ consistent with a two-electron reduction where the first step is rate determining (See Supporting Information, Section 2).[40] When CO_2 is added to the system (Figure 2.2b), we observed an increase in the peak current of the voltammetric wave to 63.4 $mA\,cm^{-2}$. This increase is consistent with a two-electron reduction where the second electron-transfer step is rate determining suggesting a change in the reaction pathway (See Supporting Information, Section 2). The

CO_2 Pressure (bar)	Liquid-Phase CO_2 (M)	Charged Passed (C)	(±)-Atrolactic acid[a] (mmol)	Rate[b] ($mmol\,h^{-1}\,cm^{-2}$)	Faradaic Efficiency[c] (%)
0	-	39.6	-	-	-
2	0.1	54.2	-	-	-
14	1.7	48.3	0.11 ± 0.01	1.19 ± 0.09	44.9 ± 1.2
28	4.4	46.9	0.18 ± 0.01	1.86 ± 0.14	72.0 ± 1.9
42	8.5	21.7	0.07 ± 0.01	0.73 ± 0.01	60.7 ± 1.6
55	14.0	2.3	-	-	-

[a] Calculated by quantitative ^{1}H-NMR using 1,3,5-trimethoxybenzene as an internal standard.
[b] Calculated from the number of moles of (±)-atrolactic acid, the bulk electrolysis time, and the area of the electrode.
[c] Faradaic efficiency based on moles of product per mole of electron passed assuming two e^- are required.

Table 2.1: Bulk electrolysis data for the electrocarboxylation of acetophenone to (±)-atrolactic in CXEs for 12 hours at -2.6 V vs Fc/Fc^+ on a glassy carbon electrode. (±)-atrolactic acid concentration determined from peak integration of ^{1}H-NMR spectrum. Error analysis from triplicate measurements at 28 bar CO_2-pressure.

absence of an oxidation event on the return sweep is consistent with an electrochemical reduction followed by a homogeneous chemical reaction (e.g., 'EC', 'EEC', or 'ECE') where the kinetics of the homogeneous chemical reaction are fast and the product is not redox active.[40,41]

A unique feature of the CXE media is the ability to pressure-tune the liquid-phase CO_2 concentration enabling us to study its effect on the electrochemical carboxylation of acetophenone. Under CXE conditions, when acetophenone is absent (Figure 2.2 c-f, red voltammograms), we do not observe significant current flow above background levels at the potentials investigated. This demonstrates that acetophenone reduction does not compete with direct CO_2 reduction on glassy carbon in the CXE, even though CO_2 is present in high liquid-phase concentrations.

As the head-space CO_2 pressures increase beyond ambient conditions, we observed a near identical peak current of ca. 63 $mA\,cm^{-2}$ in the voltammograms. We also observed a slight shift of the peak potential to more negative potentials, with the largest shift occurring at pressures exceeding 28 bar. This indicates that the electron-transfer kinetics slow as the CXE medium becomes more non-polar, attributed to the high liquid-phase CO_2 concentrations. In fact, at 55 bar CO_2 pressure, the acetophenone reduction wave is not present at the potentials investigated. The observed effect

for acetophenone carboxylation appears to be similar to what we observed during electrochemical CO_2 reduction to CO in the CXE media.[12]

To quantify the liquid-phase CO_2 concentrations effect on acetophenone carboxylation, bulk electrolysis experiments were performed under both standard and CXE conditions with the results summarized in Table 3.1 (bulk electrolysis chronoamperograms shown in Appendix A). After the bulk electrolysis experiments, hydrochloric acid was added in excess to protonate the liquid-phase products and make them visible via ^{1}H-NMR. Figure 2.3 shows the ^{1}H-NMR spectra obtained after 12-hour bulk electrolysis experiments under 28 bar CO_2, 2 bar CO_2, and 2 bar Ar. These are compared to ^{1}H-NMR spectra measured for purchased standards of **1**, **2**, and **3**. Additional ^{1}H-NMR spectra from the other CO_2 pressures tested are shown in the Supporting Information.

Under 2 bar Ar, the major observed product is the alcohol **2**. The resonance peaks present at 7.35 ppm are characteristic of the 1-phenylethanol standard (Fig. 2.3, **2**). When Ar is replaced with 2 bar of CO_2, 1-phenylethanol **2** remains the major product observed. Clearly, the multiplet at 7.35 ppm is present in both 2 bar Ar (Fig. 2.3, **A**) and in 2 bar CO_2 (Fig. 2.3,**B**). However, at higher CO_2 pressures, we observed a change in selectivity towards $(\pm)$-atrolactic acid, **1**. Evidence of this shift in selectivity is represented by different resonance peaks emerging between 7.38 and 7.45 ppm accompanied by a shift in resonance lined between 7.3 and 7.35 ppm (Fig. 2.3, **C**). Additionally, the characteristic resonance of 1-phenolethanol at 7.35 ppm is diminished in the 28 bar sample.

The rate of $(\pm)$-atrolactic acid production was determined via quantification of the ^{1}H-NMR signal using a 1,3,5-trimethoxybenzene internal standard. Interestingly, we observed a maximum in both production rate and faradaic efficiency at 28 bar CO_2- head-space pressure (1.9 $\mathrm{mmol\,h^{-1}\,cm^{-2}}$ and 72%, respectively). At head-space pressures exceeding 42 bar, we observed an attenuation in the $(\pm)$-atrolactic acid production rate (Figure 2.4). Similar to our previous studies on electrochemical CO_2 reduction,[12–14] we attribute the decrease in rate to a decrease in the polarity of the electrolyte as the liquid-phase CO_2 concentrations approach that of pure liquid CO_2. Gas chromatography analysis of the head-space after bulk electrolysis showed only trace

gas-phase products (e.g., H_2 or CO), revealing total faradaic efficiencies that are less than unity (Supporting Information Table S1). Interestingly, we also observed similar faradaic efficiencies for CO_2 reduction to CO in our previous work using the same reactor setup (74% on Au[13], 70% with $Re(CO)_3(bpy)Cl$[14]). This was attributed to the use of a single-compartment electrochemical cell, which may allow some reduced species formed at the working electrode to be potentially oxidized at the counter electrode (or vice versa) resulting in lower faradaic yields.

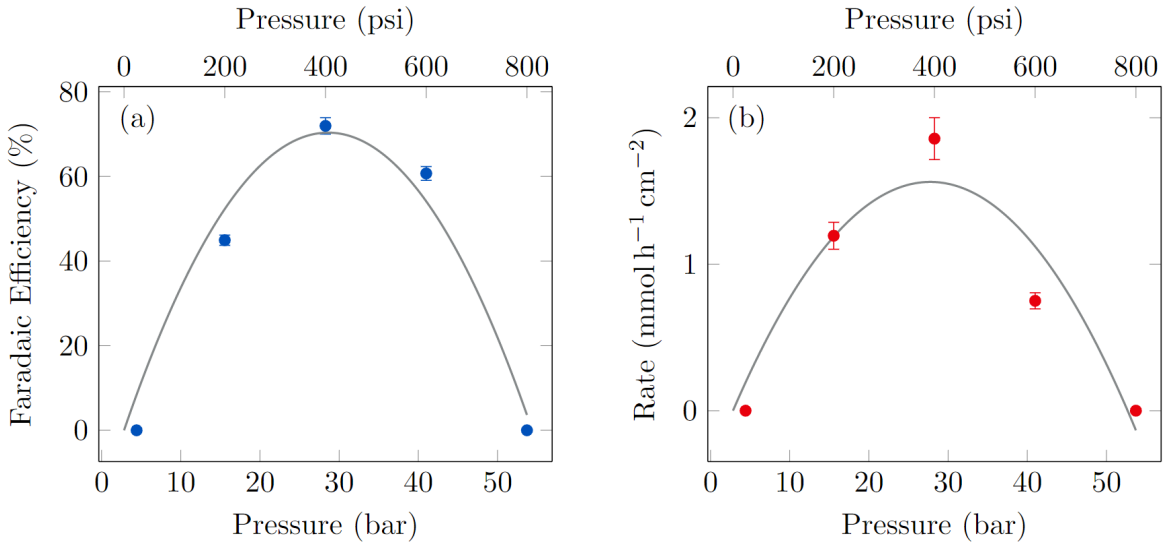

Figure 2.4: Faradaic efficiency (a) and rate of reaction (b) for the electrocarboxylation of acetophenone to atrolactic acid as a function of pressure for 12 hour bulk electrolysis experiments.

Under Ar-saturated conditions, the measured and expected product is **2**, which corresponds to a two-electron/two-proton reduction product. At present, the exact mechanistic route in the aprotic media is still ambiguous. It is possible that a dianion is formed via a two-electron reduction that is stabilized by Mg^{2+} formed on the sacrificial anode. Alternatively, proton transfer could occur from trace water, the supporting electrolyte, or other organic molecules after the first electron step. Under standard CO_2 conditions (2 bar CO_2 head-space pressure, Figure 2.2b), the increase in the peak current in voltammetry experiments compared to Ar-saturated conditions suggests a possible change in the reaction pathway. However, the desired product **1** was not observed as the major product in bulk electrolysis experiments for 2 bar CO_2. Under near atmospheric CO_2 pressures the ratio of the number of moles of CO_2 in the reactor compared to the number of electrons passed dur-

ing the bulk electrolysis experiment is ca. 3:1. In contrast, the CO_2-to-e^- ratio is ca. 170:1 under CXE conditions at a head-space pressure of 28 bar. This demonstrates that the high liquid-phase CO_2 concentrations afforded in the CXE media are necessary to sustain electrochemical carboxylation of acetophenone to (±)-atrolactic acid over the 12-hour bulk electrolysis experiment.

2.3 Conclusion

This experimental study clearly demonstrates that process intensification and selectivity enhancements in electrochemical carboxylation can be achieved in CXE media. Interestingly, the optimum liquid phase CO_2 concentration (ca. 4.5 M), with respect to the rate of reaction, is identical for both electrochemical carboxylation and electrochemical CO_2 reduction to CO in acetonitrile-based CXE media. This represents an instance where the decrease in the polarity of the electrolyte at higher liquid-phase CO_2 concentrations dictates the optimum pressure. Fortunately, the optimum pressure is relatively modest favoring the practical viability of CXE-based electrochemical carboxylations.

2.4 Acknowledgments

This work was made possible through collaboration with Christian Nilles, Bala Subramaniam, and James Blakemore. Without their insight and chemical expertise, this work would not have been published in The American Chemical Society journal of Sustainable Chemistry and Engineering in 2021.

Organic Electrosynthesis in CO2-eXpanded Electrolytes: Enabling Selective Acetophenone Carboxylation to Atrolactic Acid

Matthew A. Stalcup, Christian K. Nilles, Hyun-Jin Lee, Bala Subramaniam, James D. Blakemore, and Kevin C. Leonard

ACS Sustainable Chemistry & Engineering **2021** *9* (31), 10431-10436

DOI:10.1021/acssuschemeng.1C03073

2.5 Supporting Information

2.5.1 Electrochemical Methods

High-pressure electrochemical experiments were performed in a single-cell electrochemical vessel as described elsewhere.[13] This vessel was custom-built from a Parr reactor fitted with a modified cap and electrical feed-throughs capable of withstanding the operating pressure of the reactor. Inside the reaction vessel, a Teflon sleeve separated the electrochemical solution from the metal body of the reactor. The reactor was fitted with temperature and pressure sensing equipment that is monitored with a NI LabVIEW Data Acquisition system. The reactor is jacketed by a custom-built single-pass heat exchanger piped to a water bath allowing for precise temperature control.

All electrochemical experiments were performed with a Gamry Reference 3000 Potentiostat/ Galvanostat at various CO_2 pressures (Matheson 99.999% purity) and a constant temperature of 25 °C using a glassy carbon working electrode (0.0079 cm^2), a sacrificial magnesium counter electrode (99.9% purity), and a copper wire quasi-reference (99.9% purity). The reaction medium consisted of acetonitrile, 0.4 M tetrabutylammonium hexafluorophosphate ($TBAPF_6$), 4 mM ferrocene (Fc), and 100 mM acetophenone. All components of the solution were thoroughly dried to remove trace water impurities.

Previous work has shown that the ferrocene redox couple can be used as an internal reference over the pressure and potential ranges studied.[13] The potential of the Cu quasi-reference electrode was calibrated against the potential of the $Fc^{+/0}$ redox couple for each electrochemical experiment.

The Mg sacrificial anode was employed to enable the study of the electrochemical carboxylation reduction reactions without drastically changing the reaction media. Without the use of a sacrificial anode, the supporting electrolyte and/or solvent may be oxidized on a more conventional Pt counter electrode, which disrupts the system and produces unwanted side products visible in the ^{1}H-NMR experiments. Figure 2.6 shows the oxidation potential of the Mg electrode in the CXE media. Here, the Mg electrode oxidizes at ca. -1 V vs $Fc^{+/0}$. Since acetophenone reduces at ca. -2.2 V vs $Fc^{+/0}$, the total cell voltage of the system is approximately 1.2 V.

2.5.2 Volumetric Expansion Methods

In the CXE media, the liquid phase volume increases as a function of CO_2 head-space pressure. Expansion experiments were performed in a Jergenson view cell at a reaction temperature similar to our previous studies.[13] This enables visualization and quantification of the liquid phase expansion as a function of CO_2 pressure. A calibration curve from the expansion data was created to calculate the final volume of the CXE in the reactor at various CO_2 head-space pressures. This calibration curve was used to adjust the initial acetophenone concentration so that the concentration under CXE conditions was maintained to be 0.1 M at all CO_2 head-space pressures. The supporting electrolyte concentration of 0.4 M was not adjusted due to the concentration of $TBAPF_6$ being higher than the typical 0.1 M even at the highest pressure tested.[40]

2.5.3 Product Detection and ^{1}H-NMR

Bulk electrolysis experiments were conducted at a potential of -2.6V vs Fc/Fc^+ for 12 hours, with agitation provided by a mechanical stirrer. An aliquot of the reacted solution was prepared for ^{1}H-NMR (Bruker AVIIIHD 400 MHz NMR) by dilution in deuterated acetonitrile. 1,3,5-trimethoxybenzene was added as an internal standard for the quantification of products and concentrated hydrochloric acid was added to protonate any product species.

^{1}H-NMR spectra were analyzed using MestreNova. The spectra were cropped to include only the internal standard and the analyte enabling the most accurate baseline correction and integration. The known concentration and signal strength for the internal standard could then be compared to the signal strength of the unknown $(\pm)$-atrolactic acid concentration using:

$$\frac{M_r}{M_a} = \frac{I_r N_a}{I_a N_r} \tag{2.1}$$

where M, I, and N correspond to the molarity, signal strength, and the number of hydrogen molecules integrated for the analyte (a) and the internal reference (r). From Equation (2.1), the total number of moles of atrolactic acid present in the reactor can be calculated.

To calculate the faradaic efficiency, we used the two-electron carboxylation of acetophenone as shown in Scheme 2.1.

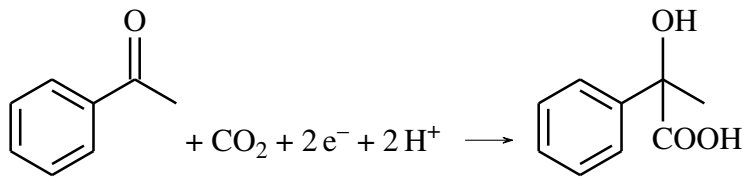

Acetophenone Atrolactic acid

Scheme 2.1: Two-electron two-proton carboxylation of acetophenone

The theoretical yield of this reaction is proportional to the charge passed at the culmination of the reaction. The total charge was calculated by integrating the chronoamperometry experiments using Gamry Echem Analyst software. The total charge was then divided by Faraday's constant to determine the moles of electrons required for the reduction reaction.

$$\frac{Q}{F} = \text{moles of } e^- \tag{2.2}$$

Scheme 2.1 shows that two moles of electrons are needed to form one mole of atrolactic acid. The theoretical number of moles of atrolactic acid formed was calculated by multiplying by the stoichiometric ratio. Assuming the reaction media has a uniform concentration of atrolactic acid, the theoretical concentration of the bulk and the ^{1}H-NMR sample can be determined. Dividing the actual number of moles by the theoretical number of moles of atrolactic acid formed gives the faradaic efficiency.

2.6 Peak Current Calculations for Cyclic Voltammetry Experiments

$$I_{peak} = -0.496\sqrt{n' + \alpha_{n'+1}}nFA[A_{bulk}]\sqrt{\frac{F\nu D}{RT}} \tag{2.3}$$

It is well known[40] that Equation 2.3 represents a peak current calculation for multiple electron steps with different kinetics where $n^{'}$ is the number of electrons transferred prior to the rate-determining step, $\alpha = 0.5$ is the transfer coefficient, n is the total number of electrons transferred, F is the Faraday constant (96485 $\mathrm{C\,mol^{-1}}$), A is the surface area of the electrode, A_{bulk} is the concentration of the substrate in the bulk, v is the scan rate ($\mathrm{mV\,s^{-1}}$), D is the diffusion coefficient 1.5×10^{-5} $\mathrm{cm\,s^{-1}}$, R is the gas constant (8.314 $\mathrm{J\,mol^{-1}\,K^{-1}}$), and T (in K) is the temperature.[40] Both major products (atrolactic acid, and 1-phenylethanol) are two-electron transfer reactions. When n' equals 0 and n equals 2, meaning the first electron transfer is rate-determining and there are two electron transfers, the peak current density calculated from Equation 2.3 is 36.6 $\mathrm{mA\,cm^{-2}}$ matching the Ar saturated conditions. When n' equals 1 and n equals 2, meaning the second electron transfer is rate-determining and there are 2 electron transfers, the peak current density calculated from Equation 2.3is 63.4 $\mathrm{mA\,cm^{-2}}$ matching the CO_2 saturated conditions.

Additionally to investigate the change in selectivity at elevated CO_2 pressures the relationship between CO_2 availability and electron availability. The equation refeqn:molese gives the total moles of electrons after the Q charge is passed. For the CO_2 saturated bulk electrolysis experiment, 54.2 C of charge is passed resulting in approximately 0.28 mmol of electrons transferred. Using the concentration of CO_2 in the reactor and the reactor size (19 mL), the molar ratio of CO_2 to e^- was determined to be ca. 3:1. However, when CO_2 pressure is 28 bar analogous calculations yield a CO_2:e^- molar ratio of ca. 170:1.

2.7 Supporting Information Figures

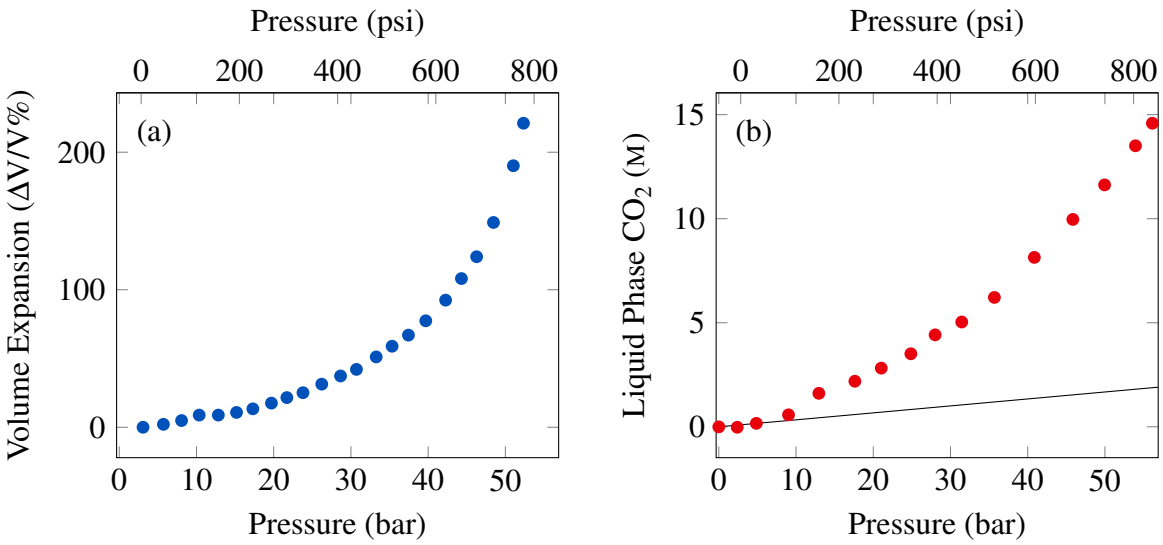

Figure 2.5: Volumetric expansion of acetonitrile (a), and liquid phase CO_2 concentrations (b), at CO_2 pressures up to 56 bar at 25 °C.

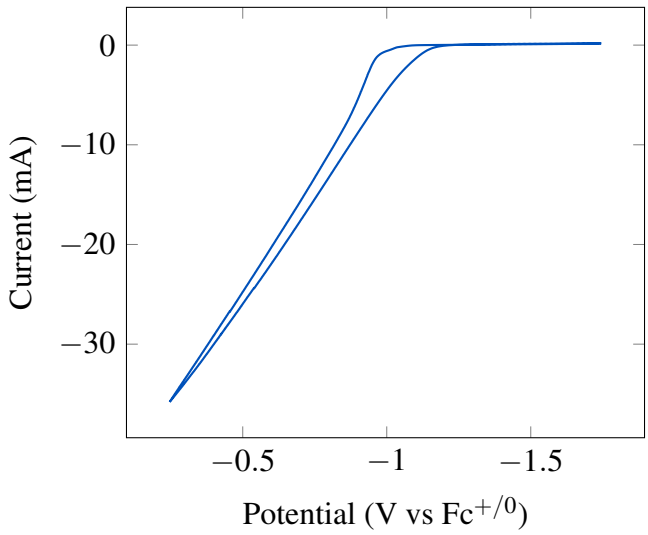

Figure 2.6: Verification of the Mg oxidation potential for the CXE system at a scan rate of 100 $mV\,s^{-1}$ using platinum counter and reference electrodes.

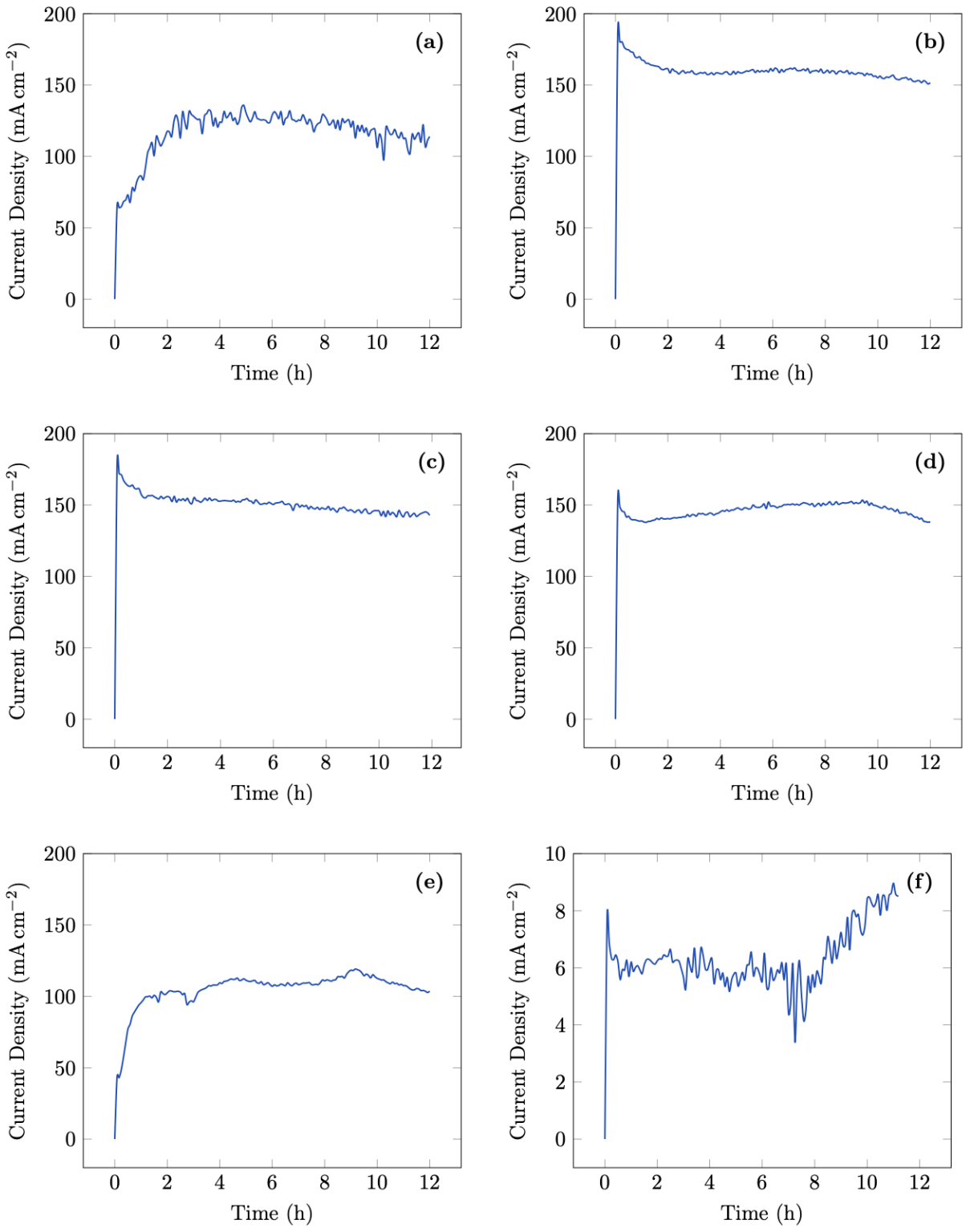

Figure 2.7: Twelve hour chronoamperometry experiments for electrochemical acetophenone reduction at -2.6V vs Fc/Fc^{+} with glassy carbon working, magnesium counter, and copper pseudo-reference electrodes at 2 bar Ar (a), 2 bar CO_2 (b), 14 bar CO_2 (c), 28 bar CO_2 (d), 42 bar CO_2 (e), and 55 bar CO_2 pressures (f).

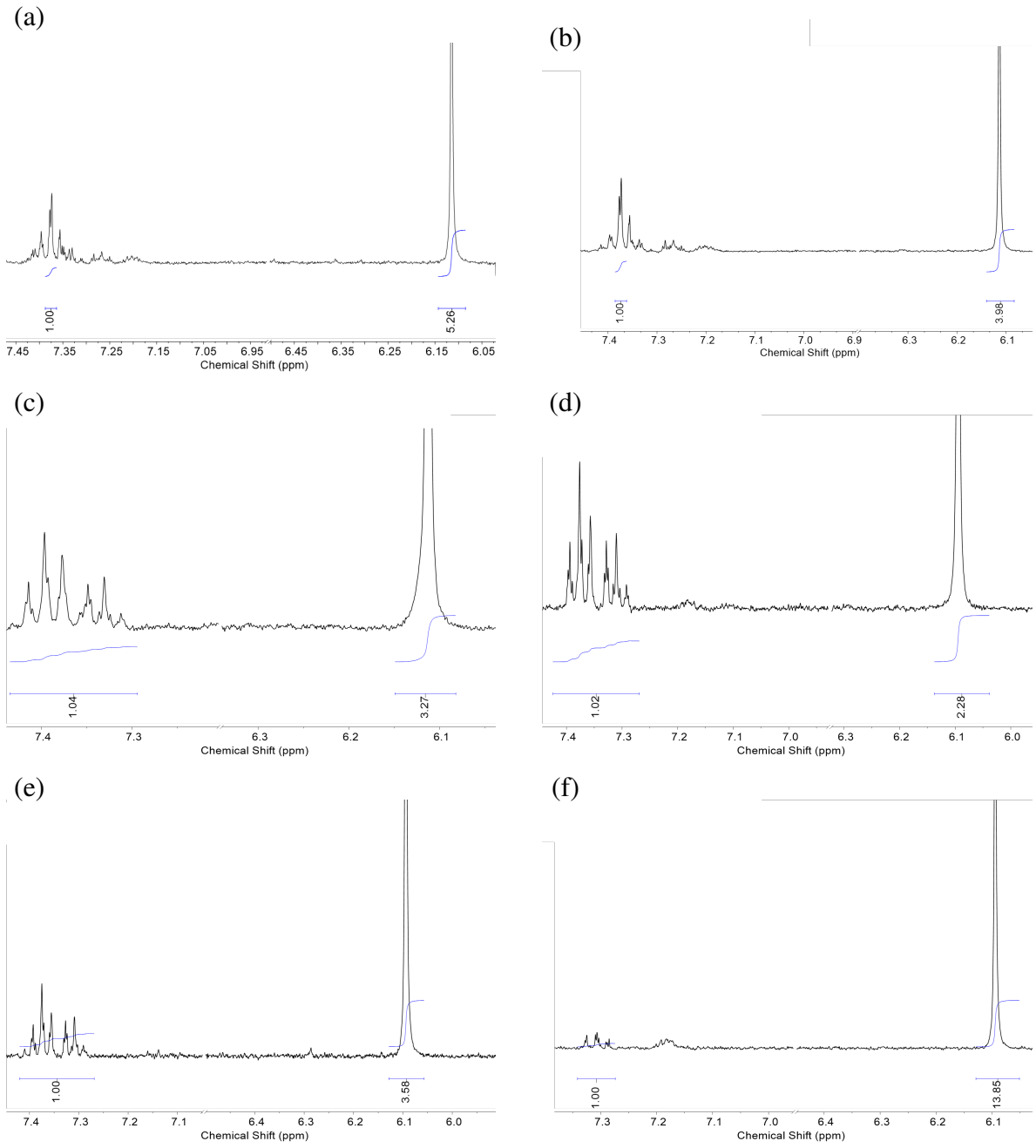

Figure 2.8: ^{1}H-NMR results for 12 hour bulk electrolysis experiments at 2 bar Ar (a), 2 bar CO_2 (b), 14 bar CO_2 (c), 28 bar CO_2 (d), 42 bar CO_2 (e), and 55 bar CO_2 pressures (f).

CO_2 Pressure (bar)	(±)-Atrolactic acid (%)	1-phenylthanol (%)	2,3-diphenylbutane-2,3-diol (%)	H_2 (%)	CO (%)
0	Not Detected	47	Observed	-	-
2	Not Detected	66	Observed	Observed	Observed
14	45	Observed	Not Detected	Observed	Observed
28	72	Not Detected	Not Detected	Observed	Observed
42	60	Not Detected	Not Detected	Observed	Observed
55	Observed	Not Detected	Not Detected	-	-

Table 2.2: Faradaic Efficiency of both liquid-phase ((±)-Atrolactic acid, 1-phenylethanol, and 2,3-diphenylbutane-2,3-diol) and possible gas-phase products (H_2 and CO) as a function of CO_2 headspace pressure. Numbers represent % Faradaic Efficiency determined via quantitative ^{1}H-NMR. 'Observed' indicates that the species was observed in the ^{1}H-NMR spectra or gas chromatogram, but not quantifiable. 'Not Detected' indicates that the species was not detected in either the ^{1}H-NMR spectra or gas chromatogram.

References

[1] Bushuyev, O. S.; Luna, P. D.; Dinh, C. T.; Tao, L.; Saur, G.; van de Lagemaat, J.; Kelley, S. O.; Sargent, E. H. What Should We Make with CO_2 and How Can We Make It? *Joule* **2018**, *2*, 825–832.

[2] Jhong, H. R. M.; Ma, S.; Kenis, P. J. Electrochemical conversion of CO_2 to useful chemicals: Current status, remaining challenges, and future opportunities. *Current Opinion in Chemical Engineering* **2013**, *2*, 191–199.

[3] Jiang, X.; Nie, X.; Guo, X.; Song, C.; Chen, J. G. Recent Advances in Carbon Dioxide Hydrogenation to Methanol via Heterogeneous Catalysis. *Chemical Reviews* **2020**, *120*, 7984–8034.

[4] Feng, X.; Jiang, K.; Fan, S.; Kanan, M. W. Grain-Boundary-Dependent CO_2 Electroreduction Activity. *Journal of the American Chemical Society* **2015**, *137*, 4606–4609.

[5] Roberts, F. S.; Kuhl, K. P.; Nilsson, A. High Selectivity for Ethylene from Carbon Dioxide Reduction over Copper Nanocube Electrocatalysts. *Angewandte Chemie* **2015**, *127*, 5268–5271.

[6] Loiudice, A.; Lobaccaro, P.; Kamali, E. A.; Thao, T.; Huang, B. H.; Ager, J. W.; Buonsanti, R. Tailoring Copper Nanocrystals towards C2 Products in Electrochemical CO_2 Reduction. *Angewandte Chemie - International Edition* **2016**, *55*, 5789–5792.

[7] Clark, E. L.; Hahn, C.; Jaramillo, T. F.; Bell, A. T. Electrochemical CO_2 Reduction over Compressively Strained CuAg Surface Alloys with Enhanced Multi-Carbon Oxygenate Selectivity. *Journal of the American Chemical Society* **2017**, *139*, 15848–15857.

[8] Hori, Y.; Murata, A.; Yoshinami, Y. Adsorption of CO, intermediately formed in electrochemical reduction of CO_2, at a copper electrode. *Journal of the Chemical Society, Faraday Transactions* **1991**, *87*, 125–128.

[9] Hori, Y.; Koga, O.; Yamazaki, H.; Matsuo, T. Infrared spectroscopy of adsorbed CO and intermediate species in electrochemical reduction of CO_2 to hydrocarbons on a Cu electrode. *Electrochimica Acta* **1995**, *40*, 2617–2622.

[10] Genovese, C.; Ampelli, C.; Perathoner, S.; Centi, G. Electrocatalytic conversion of CO_2 to liquid fuels using nanocarbon-based electrodes. *Journal of Energy Chemistry* **2013**, *22*, 202–213.

[11] Chen, Y.; Lewis, N. S.; Xiang, C. Operational constraints and strategies for systems to effect the sustainable, solar-driven reduction of atmospheric CO_2. *Energy and Environmental Science* **2015**, *8*, 3663–3674.

[12] Shaughnessy, C. I.; Sconyers, D. J.; Lee, H.-J.; Subramaniam, B.; Blakemore, J. D.; Leonard, K. C.; Co, E. Insights into pressure tunable reaction rates for electrochemical reduction of CO 2 in organic electrolytes †. **2020**,

[13] Shaughnessy, C. I.; Sconyers, D. J.; Kerr, T. A.; Lee, H.-J.; Subramaniam, B.; Leonard, K. C.; Blakemore, J. D. Intensified Electrocatalytic CO_2 Conversion in Pressure-Tunable CO_2-Expanded Electrolytes. *ChemSusChem* **2019**, *12*, 3761–3768.

[14] Sconyers, D. J.; Shaughnessy, C. I.; Lee, H.; Subramaniam, B.; Leonard, K. C.; Blakemore, J. D. Enhancing Molecular Electrocatalysis of CO_2 Reduction with Pressure-Tunable CO_2-Expanded Electrolytes. *ChemSusChem* **2020**, cssc.202000390.

[15] Kingston, C.; Palkowitz, M. D.; Takahira, Y.; Vantourout, J. C.; Peters, B. K.; Kawamata, Y.; Baran, P. S. A Survival Guide for the "Electro-curious". *Accounts of Chemical Research* **2020**, *53*, 72–83, PMID: 31823612.

[16] Tsuji, Y.; Fujihara, T. Carbon dioxide as a carbon source in organic transformation: carbon-carbon bond forming reactions by transition-metal catalysts. *Chem. Communications* **2012**, *48*, 9956–9964.

[17] Wu, L. X.; Wang, H.; Xiao, Y.; Tu, Z. Y.; Ding, B. B.; Lu, J. X. Synthesis of dialkyl carbonates from CO 2 and alcohols via electrogenerated N-heterocyclic carbenes. *Electrochemistry Communications* **2012**, *25*, 116–118.

[18] Zhang, K.; Xiao, Y.; Lan, Y.; Zhu, M.; Wang, H.; Lu, J. Electrochemical reduction of aliphatic conjugated dienes in the presence of carbon dioxide. *Electrochemistry Communications* **2010**, *12*, 1698–1702.

[19] Steinmann, S. N.; Michel, C.; Schwiedernoch, R.; Wu, M.; Sautet, P. Electro-carboxylation of butadiene and ethene over Pt and Ni catalysts. *Journal of Catalysis* **2016**, *343*, 240–247.

[20] Doherty, A. P. Electrochemical reduction of butyraldehyde in the presence of CO_2. *Electrochimica Acta* **2002**, *47*, 2963–2967.

[21] Xiao, Y.; Chen, B. L.; Yang, H. P.; Wang, H.; Lu, J. X. Electrosynthesis of enantiomerically pure cyclic carbonates from CO 2 and chiral epoxides. *Electrochemistry Communications* **2014**, *43*, 71–74.

[22] Khoshro, H.; Zare, H. R.; Namazian, M.; Jafari, A. A.; Gorji, A. Synthesis of cyclic carbonates through cycloaddition of electrocatalytic activated CO_2 to epoxides under mild conditions. *Electrochimica Acta* **2013**, *113*, 263–268.

[23] Amatore, C.; Jutand, A.; Khalil, F.; Nielsent, M. F. Carbon Dioxide as a C1 Building Block. Mechanism of Palladium-Catalyzed Carboxylation of Aromatic Halides. *Journal of the American Chemical Society* **1992**, *114*, 7076–7085.

[24] Lan, Y. C.; Wang, H.; Wu, L. X.; Zhao, S. F.; Gu, Y. Q.; Lu, J. X. Electroreduction of dibromobenzenes on silver electrode in the presence of CO_2. *Journal of Electroanalytical Chemistry* **2012**, *664*, 33–38.

[25] Isse, A. A.; Durante, C.; Gennaro, A. One-pot synthesis of benzoic acid by electrocatalytic

reduction of bromobenzene in the presence of CO_2. *Electrochemistry Communications* **2011**, *13*, 810–813.

[26] Scialdone, O.; Galia, A.; Errante, G.; Isse, A. A.; Gennaro, A.; Filardo, G. Electrocarboxylation of benzyl chlorides at silver cathode at the preparative scale level. *Electrochimica Acta* **2008**, *53*, 2514–2528.

[27] Howell, J. O.; Goncalves, J. M.; Klasinc, L.; Wightman, R. M.; Amatore, C.; Kochi, J. K. Electron Transfer from Aromatic Hydrocarbons and Their -Complexes with Metals. Comparison of the Standard Oxidation Potentials and Vertical Ionization Potentials. *Journal of the American Chemical Society* **1984**, *106*, 3968–3976.

[28] Yang, D. T.; Zhu, M.; Schiffer, Z. J.; Williams, K.; Song, X.; Liu, X.; Manthiram, K. Direct Electrochemical Carboxylation of Benzylic C-N Bonds with Carbon Dioxide. *ACS Catalysis* **2019**, *9*, 4699–4705.

[29] Scialdone, O.; Sabatino, M. A.; Belfiore, C.; Galia, A.; Paternostro, M. P.; Filardo, G. An unexpected ring carboxylation in the electrocarboxylation of aromatic ketones. *Electrochimica Acta* **2006**, *51*, 3500–3505.

[30] Isse, A. A.; Scialdone, O.; Galia, A.; Gennaro, A. The influence of aluminium cations on electrocarboxylation processes in undivided cells with Al sacrificial anodes. *Journal of Electroanalytical Chemistry* **2005**, *585*, 220–229.

[31] Zhang, K.; Wang, H.; Zhao, S.-F.; Niu, D.-F.; Lu, J.-X. Asymmetric electrochemical carboxylation of prochiral acetophenone: An efficient route to optically active atrolactic acid via selective fixation of carbon dioxide. **2009**,

[32] Matthessen, R.; Fransaer, J.; Binnemans, K.; Vos, D. E. D. Electrocarboxylation: Towards sustainable and efficient synthesis of valuable carboxylic acids. *Beilstein Journal of Organic Chemistry* **2014**, *10*, 2484–2500.

[33] Wawzonek, S.; Gundersen, A. Polarographic Studies in Acetonitrile and Dimethylformamide. *Journal of The Electrochemical Society* **1960**, *107*, 537.

[34] Datta, A. K.; Marron, P. A.; King, C. J.; Wagenknecht, J. H. Process development for electrocarboxylation of 2-acetyl-6-methoxynaphthalene. *Journal of Applied Electrochemistry* **1998**, *28*, 569–577.

[35] Chen, B.-L. L.; Xiao, Y.; Xu, X.-M. M.; Yang, H.-P. P.; Wang, H.; Lu, J.-X. X. Alkaloid induced enantioselective electroreduction of acetophenone. *Electrochimica Acta* **2013**, *107*, 320–326.

[36] Chan, A. S. C.; Huang, T. T.; Wagenknecht, J. H.; Miller, R. E. A Novel Synthesis of 2-Aryllactic Acids via Electrocarboxylation of Methyl Aryl Ketones. *J. Org. Chem* **1995**, *60*, 742–744.

[37] Muchez, L.; Vos, D. E. D.; Kim, M. J. Sacrificial Anode-Free Electrosynthesis of -Hydroxy Acids via Electrocatalytic Coupling of Carbon Dioxide to Aromatic Alcohols. *ACS Sustainable Chemistry and Engineering* **2019**, *7*, 15860–15864.

[38] Wagenknecht, J. H.; Kirkwood, M. Electrochemical carboxylation of p-isobutylacetophenone and other aryl ketones. 1985.

[39] Chan, A. Asymmetric Catalytic Hydrogenation of Alpha-Arylpropenic Acids. 1991.

[40] Compton, R.; Banks, C. *Understanding Voltammetry*, 3rd ed.; 2018; pp 255–258.

[41] Bard, A. J. In *Electrochemical methods: fundamentals and applications*, 2nd ed.; Faulkner, L. R., Ed.; Wiley, 2001.

Chapter 3

Distinguishing the Mechanism of Electrochemical Carboxylation in CO_2 eXpanded Electrolytes

Abstract

We shed light on the mechanism and rate-determining steps of the electrochemical carboxylation of acetophenone as a function of CO_2 concentration, by using a robust finite element analysis model that incorporates each reaction step. Specifically, we show that the first electrochemical reduction of acetophenone is followed by the homogeneous chemical addition of CO_2. The electrochemical reduction of the acetophenone-CO_2 adduct is more facile than that of acetophenone, resulting in an electrochemical chemical electrochemical (ECE) reaction pathway that appears as a single voltammetric wave. These modeling results provide new fundamental insights on the complex microenvironment in CO_2-rich media that produces an optimum electrochemical carboxylation rate as a function of CO_2 pressure

3.1 Introduction

Electrochemical CO_2 fixation is a grand challenge in sustainability science and is also significant in the context of the electrification of the chemical industry.[1,2] Specifically, selective synthesis of multicarbon products via electrochemical coupling of CO_2 remains challenging.[3] However, organic electrosynthesis has recently received increased attention due to its ability to precisely control reaction conditions and achieve novel reactivity patterns providing access to c-c bond formation.[4–6] Electrocarboxylation is a sub-class of organic electrosynthesis reactivity in which CO_2 is coupled to an organic backbone, enabling the formation of C-C bonds. In particular, electrocarboxylation of acetophenone produces atrolactic acid, a useful precursor for production of nonsteroidal anti-inflammatory drugs (NSAIDs) such as ibuprofen and naproxen. This electrochemical route provides a greener alternative to the traditional production of hydroxyl carboxylic acids, which requires the use of cyanohydrins and the corresponding ketones.[7–14] However, achieving selective production of the carboxylic acid product remains difficult under most conditions due to competing alcohol production in protic solvents and reductive dimerization in aprotic solvents.[12,15–17] Additionally, the elementary steps involved in electrocarboxylation are not well understood, impeding further use of this reactivity mode to utilize waste CO_2 for production of more useful chemicals.

In a prior report,[18] we demonstrated that CO_2-eXpanded Electrolytes (CXEs), electrochemical reaction media that support multi-molar CO_2 concentrations, enable the selective carboxylation of acetophenone to produce atrolactic acid. We also observed that the selectivity of the reaction can be optimized by tuning the CO_2 concentration.[18] At low (near atmospheric pressure) CO_2 concentrations, the rate of atrolactic acid production was low, and the reaction primarily produced 1-phenyl ethanol by net hydrogenation reactivity. At higher CO_2 concentrations, a dramatic increase in production of atrolactic acid occurred. Additionally, in our system, electrokinetic data collected as a function of CO_2 concentration revealed a surprising maximum rate of atrolactic acid production at 28 bar—the very highest CO_2 concentration resulted in diminished rates, despite the role of CO_2 as a substrate in the overall reactivity.

To gain insight into this counterintuitive CO_2 concentration dependence and shed light more

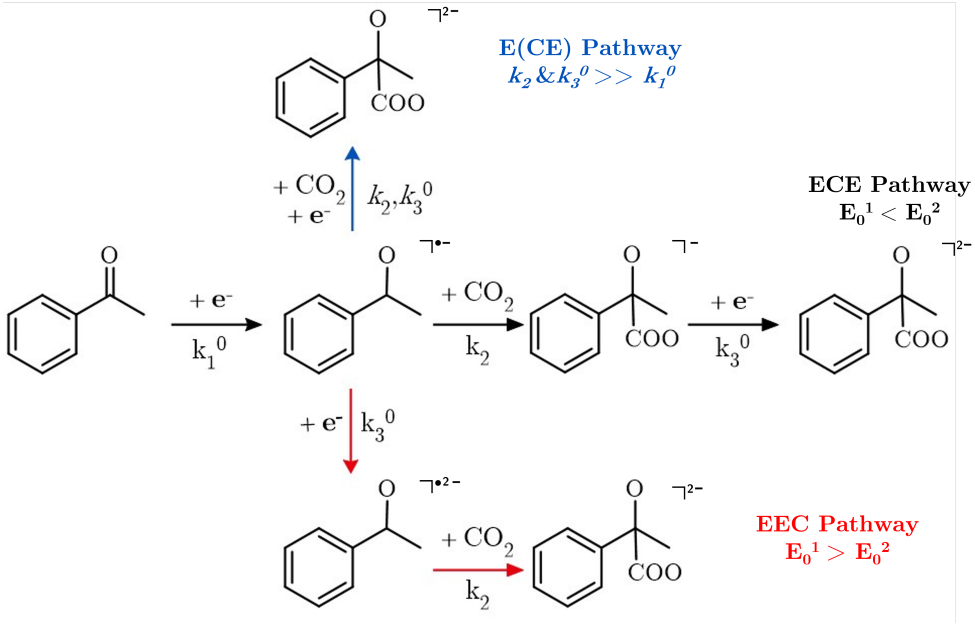

Figure 3.1: Proposed reaction mechanisms for the electrochemical carboxylation of acetophenone for three different electrochemical reaction pathways EEC, ECE, and E(CE).

broadly on the little-investigated mechanism of electrochemical carboxylation, we now report the development of a robust finite element analysis (FEA) model that incorporates the possible individual reaction step and enables distinguishing the operative mechanism in CXE media. The modeling results provide insight into the mechanistic pathway, overcoming the typical opacity of irreversible electrochemistry by global analysis of data across varying scan rate and CO_2 concentration. We find that the mechanism involves an initial, rate-limiting electron transfer to acetophenone that is followed by a homogeneous chemical reaction of the acetophenone radical anion with CO_2, the step that forges a new C–C bond. Critically, electron transfer to the nascent acetophenone-CO_2 adduct is thermodynamically less demanding than to acetophenone, resulting in potential inversion of the second electron transfer. Thus, the reaction is shown to proceed via an ECE-type pathway which results in measurement of only a single voltammetric wave under all conditions.

In this work, we considered three possible schemes[19,20] for the two-electron carboxylation reaction (Fig. 3.1): – (i) two electrochemical steps followed by a homogeneous chemical step (EEC), (ii) a homogeneous chemical step occurring between the electrochemical steps (ECE), (iii) and an electrochemical step followed by a concerted chemical-electrochemical step (E(EC)).

While several studies often treat the second electron transfer and carboxylation steps as a combined reaction step (E(EC)),[7,11,21] it was unclear at the outset of this work which of the three possible mechanisms best describes this optimum in rate versus CO_2 pressure

3.2 Results and Discussion

We began development of our FEA model by collecting cyclic voltammograms for the reduction/-carboxylation of acetophenone at five different scan rates across five different CO_2 concentrations in CXEs. The electrochemical cell was a custom 50 mL Parr reactor modified for electrochemical use.[22] The electrolyte consisted of dry acetonitrile with dissolved tetrabutylammonium hexafluorophosphate ($TBAPF_6$) as the supporting electrolyte. A three-electrode system was used consisting of a glassy carbon working electrode (1 mm diameter), a Mg sacrificial counter electrode, and a glass-fritted silver reference electrode. The concentration of acetophenone remained constant at 0.1 M, accounting for the increase in volume as a function of pressure.[22,23] The reactor headspace pressure was varied from an argon atmosphere to CO_2 pressures ranging from 3.4 - 41.4 bar at 25°C. Under an argon atmosphere (Fig. 3.2, Ar sat) the reduction wave consisted of a single reduction wave with no oxidation occurring on the reverse scan. The introduction of CO_2 (Fig. 3.2, 3.4 bar CO_2) results in a slight shift in the reduction wave in the less negative direction. Additionally, a significant increase in peak current is also observed.

Inspection of the voltammetry data shows that the carboxylation of acetophenone does not proceed via the EEC reaction pathway, as sequential reduction waves were not measured. In the absence of CO_2, the two-electron reduction of acetophenone and many other aromatic ketone molecules undergo sequential electron transfer with two distinct peaks in the voltammetry data.[10,21,24] This is typically believed to be attributable to the observation that the second electron transfer is more thermodynamically challenging than the first electron transfer. The absence of sequential electron transfer behavior in the voltammetry data thus speak against the EEC reaction pathway in our system. To probe the ECE reaction pathway, COMSOL Multiphysics was used to model the physicochemical processes underlying the carboxylation of acetophenone. The rate

equations for the individual reactions (as given in Figure 1) were represented with individual elementary kinetic steps. Such an empirical kinetic modeling approach is necessary because it is very difficult, if not impossible, to experimentally measure the irreversible kinetics associated with this system. Without the presence of a return oxidation in the CV, it is not possible to determine parameters such as peak-to-peak separation that provide insights into the kinetics. Zhao *et al.*[24] used extremely fast scan rates (10 $Vs^{-}1$) to measure quasi-reversible electrochemical data in ionic liquids in which the diffusion coefficient of acetophenone (D_{ace}) was several orders of magnitude slower compared to its conversion rate. However, in CXE systems, the diffusion and/or reactivity of acetophenone is larger than in this prior work, resulting in the fully irreversible behavior measured here.

Details of the numerical model can be found in the Supporting Information. Briefly, the model relies on the actual experimental electrode geometry and calculates the predicted current accounting for the mass transfer properties of all species involved, the kinetics of both electron-transfer steps, and the kinetics of the homogeneous chemical step. The adjustable parameters which could be shifted to fit the simulation to the actual experimental cyclic voltammograms include the electrochemical rate constants (k_0^1 and k_0^2), the standard reduction potential (E_1^0 and E_3^0), and the homogeneous reaction rate coefficient (k_2). The results of these simulations can be found in the center and bottom rows of Fig. 3.2. Supporting Information table S1 shows the simulated kinetic information for the experiments at various CO_2 pressures.

We have found reasonable agreement between the COMSOL simulation results and the experimental voltammetric data at various CO_2 pressures. The correspondence of the simulated and experimental voltammograms at the various scan rates and at each pressure is shown in Figures 3.5-3.9 in the Supporting Information. Under Ar-saturated conditions, the model predicted a single one-electron transfer voltammetric wave, as was observed experimentally (Figure S2). The absence of CO_2 made the reaction unable to proceed through the proposed ECE reaction pathway, and our simulation predicts this expected behavior

At CO_2 pressures of 3.4 bar, 13.8 bar, and 28.6 bar the model predicts an increase in the peak

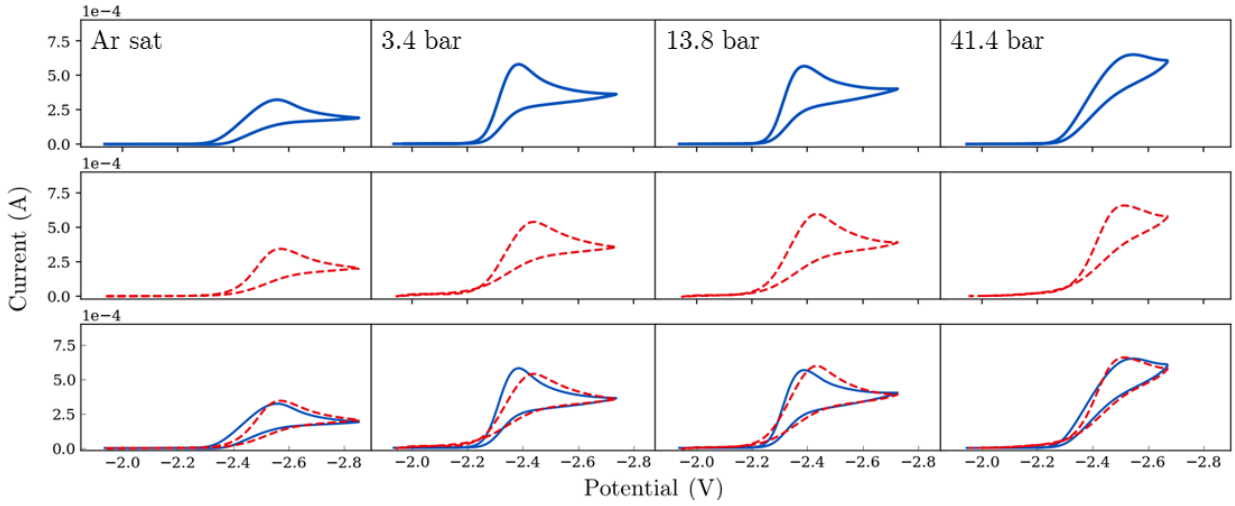

Figure 3.2: Cyclic voltammetry of acetophenone carboxylation at 200 mV/s under argon saturated, 3.4 bar, 13.8 bar, and 41.4 bar CO_2 pressures on a 1 mm diameter glassy carbon electrode (solid line) vs COMSOL simulated data (dashed) where the potential is measured vs the Fc^+/Fc redox couple.

current and a slightly less negative shift in the onset, as was observed experimentally in each case. Examination of the simulated kinetic rate constants and standard reduction potentials for the electron transfer reactions show that the second reduction of the radical acetophenone-CO_2 adduct is more facile than the first reduction of acetophenone. This is a notable finding because the simulation shows that no direct CO_2 electrochemistry occurs during electrocarboxylation (i.e., no $CO_2^{\bullet-}$ radical is formed) and that the addition of CO_2 to the organic structure enables the second electron transfer. While a more detailed molecular dynamic model may be necessary to determine involvement of concerted mechanisms, the second electron transfer can be reliably concluded to be significant faster than the first. Additionally, the extracted kinetics for the homogeneous chemical step and the second electron-transfer step point to the ECE mechanism over the concerted mechanism. Both our simulation showing a moderate lifetime for the acetophenone-CO_2 anion, and the size of a CO_2 molecule make a concerted mechanism less plausible.

As seen in the experimental data (Fig. 3.2, 41.4 bar CO_2), the voltammetric wave changes shape when the CO_2 pressure is increased to 41.4 bar. The simulation for the ECE mechanism can be made to fit the unique shape at this elevated pressure by decreasing the values of the kinetic

rate constants for the electron transfer reactions while keeping their standard reduction potentials constant. Interestingly, we observed a similar pattern at higher CO_2 pressures during direct CO_2 electroreduction on a model polycrystalline gold catalyst in CXE media.[25] The COMSOL simulation predicted an attenuation of the electron transfer kinetic rate constant in this system as well. This suggests that the rate inhibition in the electrochemical reactions studied here and in our prior work[18,23,26] may be linked to a change in bulk property of the CXE medium (such as a lower polarity or conductivity) at higher CO_2 pressures that affects the mobility of available electrolyte ions and/or the structure of the electrochemical double layer.

Within the overall reaction paradigm described above, sensitivity analysis was performed by varying E_1^0, E_3^0, k_0^1, k_2, and k_0^2 to discern possible rate-determining step(s). The coefficient of determination, R^2, was used to infer the extent of sensitivity of the COMSOL simulation to various paramaters, as shown in supporting information (Figures 3.10 – 3.14, Supporting Information). The parameters E_1^0 and k_0^1 were found to be most sensitive to changes in their values suggesting that the first electron transfer is the rate-determining step.

As shown in Fig. 3.3a, the measured rate of production of atrolactic acid (red points in Figure 3(a)) shows a non-monotonic dependence on CO_2 headspace pressure (i.e., CO_2 concentration in the liquid phase).[18] A plot of the product of k_0^1 and the liquid phase CO_2 concentration shows a similar trend (Fig. 3.3a, blue points). However, a plot of the regressed rate constant (k_0^1) vs. CO_2 head pressure (Fig. 3.3b) shows that while the rate constant remains virtually independent of CO_2 head pressure until 28 bar, it decreases rather steeply beyond this CO_2 pressure. Thus, a decrease in the rate of the first electron transfer dictates the behavior of our CXE-based system for electrocarboxylation, a reasonable conclusion since the analysis described above suggests that this step is rate determining. We attribute this drop to inhibition of ion transport in the CXE microenvironment, which could be dominated by non-polar CO_2 at the higher pressures of CO_2. Consequently, CO_2 can be viewed to inhibit the facile generation of acetophenone radicals at high CO_2 concentrations, resulting in an optimum CO_2 pressure that maximizes the rate of atrolactic acid formation by providing sufficient CO_2 to react while not using such high pressures that electron transfer is

decelerated significantly through dissolution of very large quantities of CO_2.

In conclusion, the detailed modeling of the physicochemical processes underlying the electrochemical acetophenone carboxylation described here highlights the role of the CXE microenvironment at the electrode in governing reaction outcomes in CXEs. Our elucidation of a plausible rate determining step in the mechanistic model also helps unravel the origin of the non-monotonic dependence of rate on CO_2 pressure. These insights provide guidance for future interrogation of CXE microenvironments; these would have been inaccessible without global simulation of the voltammetry data to its irreversible nature. We emphasize that electrochemical carboxylation of acetophenone can occur in the CXE environment without direct CO_2 reduction, contributing to high rates and selectivities when sufficient liquid-phase CO_2 is present. These conditions thus avoid the need for production of $CO_2^{\bullet-}$, a species well known to be difficult to access under most conditions.[27–29] On the other hand, the complexity of the microenvironment under ultra-high CO_2 concentrations (e.g., exceeding 5 M) results in a trade-off between CO_2 availability and enabling fast electron transfer. For the current system, this optimum pressure (ca. 30 bar) is fairly mild from an industrial and practical standpoint, making CXE media ideal for further development of practical electrocarboxylation

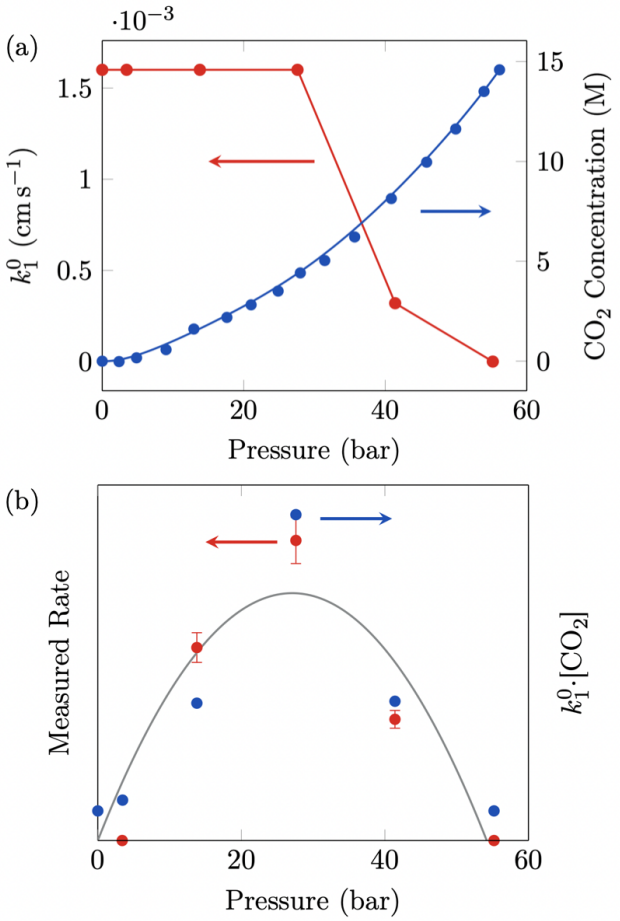

Figure 3.3: Relationship between the electron-transfer kinetics (red) and CO_2 concentration (blue) as a function of CO_2 head-space pressure (a). The measured rate of atrolactic acid production from bulk electrolysis (red) versus the product of the electron transfer kinetics and the CO_2 concentration (blue) as a function of CO_2 head-space pressure (b).

systems.

3.3 Detailed Description of Experimental Methods and Equipment

3.3.1 Electrochemical Methods

High-pressure electrochemical experiments were performed in a single-cell electrochemical vessel as described elsewhere.[26] Briefly, this vessel was custom-built from a Parr reactor fitted with a modified cap and electrical feed-throughs capable of withstanding the operating pressure of the reactor. Inside the reaction vessel, a glass cylinder separated the electrochemical solution, consisting of 0.4 M tetrabutylammonium hexafluorophosphate in acetonitrile, from the metal body of the reactor. The reactor was fitted with temperature and pressure sensing equipment that is monitored with a National Instruments LabVIEW Data Acquisition system. The reactor is jacketed by a custom-built single-pass heat exchanger piped to a water bath allowing for precise temperature control ensuring isothermal reaction conditions.

All electrochemical experiments were performed with a Gamry Reference 3000 Potentiostat/ Galvanostat at various CO_2 pressures (Matheson 99.999% purity) and a constant temperature of 25 °C using a glassy carbon working electrode (0.0079 cm^2), a sacrificial magnesium counter electrode (99.9% purity), and a Silver wire inside a fritted chamber quasi-reference (99.9% purity). The reaction medium consisted of acetonitrile, 0.4 M tetrabutylammonium hexafluorophosphate ($TBAPF_6$), 4 mM ferrocene (Fc), and 100 mM acetophenone. All components of the solution were thoroughly dried to remove trace water impurities.

Previous work has shown that the ferrocene redox couple can be used as an internal reference over the pressure and potential ranges studied.[26] The potential of the Ag quasi-reference electrode was calibrated against the potential of the $Fc^{+/0}$ redox couple for each electrochemical experiment.

The Mg sacrificial anode was used to enable the study of the electrochemical carboxylation reduction reactions without drastically changing the reaction media. Without the use of a sacrificial anode, the supporting electrolyte and/or solvent may be oxidized on a more conventional platinum

counter electrode, which disrupts the system and produces unwanted side products.[30]

3.3.2 COMSOL Multiphysics Simulation of Voltammetry

COMSOL (COMSOL Multiphysics® v. 6.0) simulations were used to model the electrochemical carboxylation of acetophenone on a glassy carbon electrode in CO_2 expanded electrolytes. The simulation field is shown in Fig. 3.4. The simulated reactor geometry was created as a 2D axial-symmetric domain with the electrode size (0.5 mm radius), insulating sheath size (100 μm width), and reactor dimensions (5 mm radius, 8 mm height). This reactor size was chosen because it is sufficiently larger than the boundary layer surrounding the electrode. Thus the CO_2 and the acetophenone concentration at the outer boundary is the same as the reactor bulk concentration because of the size of the diffusion profile around the electrode. A free triangular mesh using COMSOL's built-in 'normal' element size was used for the bulk of the reactor, with a 'fine' mesh used for the area near the electrode (1 mm × 1 mm). An edge mesh was incorporated with a maximum mesh element of 1e–3 mm and a minimum mesh element of 1e-4 mm for increased spatial resolution near the electrode. The transport of the reactants to and from the electrode surface was simulated by the "transport of diluted species" module in COMSOL. This module evaluates Fick's Second Law of diffusion, eq. (3.1), to model the concentration gradients and the development of the diffusion layer near the electrode.

$$\frac{\partial C_i}{\partial t} = D_i \nabla^2 C_i \tag{3.1}$$

Previous studies have provided us with accurate measurements of the CO_2 concentration as a function of the headspace pressure.[26] These experimentally determined values were used as initial conditions for the concentration of the CO_2 species in the simulated system. The acetophenone concentration was also fixed at 100 mM for each pressure. Experimentally, the concentration of acetophenone initially added to the reactor accounts for the increase in volume as a function of pressure and was calculated using expansion curves from previous studies.[26] Additionally, 'No

Flux" boundary conditions were placed at the boundaries of the reactor geometry to define the areas where a mass transfer can occur. A "Flux" boundary condition was placed at the surface of the electrode to allow the flow of electrons to the substrate.

CO_2 Pressure bar	[CO_2] M	[Acetophenone] M	k_1^0 cm/s	E_1^0 V vs. Fc^+/Fc	k_2 m^3/(s mol)	k_3^0 cm/s	E_3^0 V vs. Fc^+/Fc
0	0	0.1	1.6E-3	-2.26	0.1	1.0E-3	-1.93
3.4, 13.8, 28.6	1.16-4.4	0.1	1.6E-3	-2.26	0.1	1.0E-3	-1.93
41.4	8.14	0.1	3.2E-4	-2.26	0.1	3.2E-5	-1.93

Table 3.1: Optimized parameters for the simulation of cyclic voltammetry experiments of the acetophenone reduction reaction.

Butler-Volmer kinetics were then used to model the electrochemical behavior as a function of electrode potential and traditional reaction kinetics to simulate the addition of CO_2 to the acetophenone radical. The Butler-Volmer kinetic model, eq. (3.2), handles the change in the reaction rate as the electrode potential changes. Constants for this equation fundamentally influence the shape of the voltammetry. This equation also contains the fundamental kinetic information that can be used to model this system accurately. The electrochemical rate constants(k_0^1, k_0^2) in addition to the standard reduction potentials (E_0^1, E_0^3) are critical in ensuring the model agrees with experimental data. Once these parameters are inputted into the system the current flowing from the electrode becomes a function of the potential and the concentration of the redox species.

$$i = FAk^0 \left[C_O(0,t) e^{-\alpha f(E-E^{0'})} - C_R(0,t) e^{(1-\alpha) f(E-E^{0'})} \right] \tag{3.2}$$

Aside from electrochemical kinetics, chemical kinetics must also be simulated to model the chemical reaction step that occurs between electron transfer reactions. The rate of this reaction depends on the concentration of acetophenone, the reaction rate constant k_2, and most importantly the concentration of liquid phase CO_2. Each of these parameters is required to accurately simulate the pressure-dependent effects of CO_2 concentration in the liquid phase on the electrochemical carboxylation of acetophenone. Initial estimates for both the electrochemical and chemical rate con-

stants as well as the standard reduction potentials for eq. (3.2) were used to begin the simulation of the system.

$$r = k_2[\mathrm{CO_2}][Ace]^{\cdot -} \tag{3.3}$$

The manual optimization of each parameter was initially carried out at one pressure and scan rate. Once the fit was accurate further optimization was done using different scan rates (50, 100, 200, and 500 $\mathrm{mVs^{-}}$) at 28.6 bar to validate the fit to the experimental data. Further testing of the model was carried out at various CO_2 pressures where the only changes to the model were scan rate and the concentration of CO_2 in the liquid phase.

3.4 Sensitivity Analysis

To ensure that the parameters in the model were representative of the electrochemical system a sensitivity analysis was performed. The electrochemical rate constants, electrochemical potentials, and the chemical rate constant were all parameters that were optimized by hand for the simulation. Each of these parameters can influence the shape of the cyclic voltammogram. 13.8 bar was selected as a model pressure and 200 mVs^{-} as the scan rate we would test the perturbations. In our COMSOL multiphysics® model, a parametric sweep was created and iterated over different values of the parameters. The output was a simulated CV of the experimental data overlayed with the simulated data. This CV provided a graphical representation of which parameters influenced the shape of the CV the most. E_0^1 and k_0^1 are the parameters associated with the initial electron transfer (rate-determining) step and changes in their value led to the greatest change in CV shape. The fit visibly worsened when the values for these parameters were either increased or decreased; however, a more concrete method of quantifying the results as desired. To quantify the accuracy of the fit, a python script was developed that would calculate the r^2 value between the simulated data and the experimental data. The r^2 value or coefficient of determination is determined by eq. (3.4) where the sum squared regression is the sum of the residuals squared and the total sum of squares is the sum of the distance the data is from the mean all squared. The closer the r^2 value is to 1 the better the fit between the model and experimental data.

$$r^2 = 1 - \frac{\text{sum squared regression}}{\text{total sum of squares}} = 1 - \frac{\sum(y_i - \hat{y})^2}{\sum(y_i - \bar{y})^2} \tag{3.4}$$

Once the coefficient of determination was calculated, we could plot it vs the value of the parameter to visualize the changes in the quality of the fit vs changes in the parameter. The results from the optimization are found in figures Fig. 3.10-Fig. 3.14. This shows that our initial judgment of the changes in quality of fit being sensitive to the constants associated with the initial electrochemical reaction was correct

3.5 Supporting Information Figures

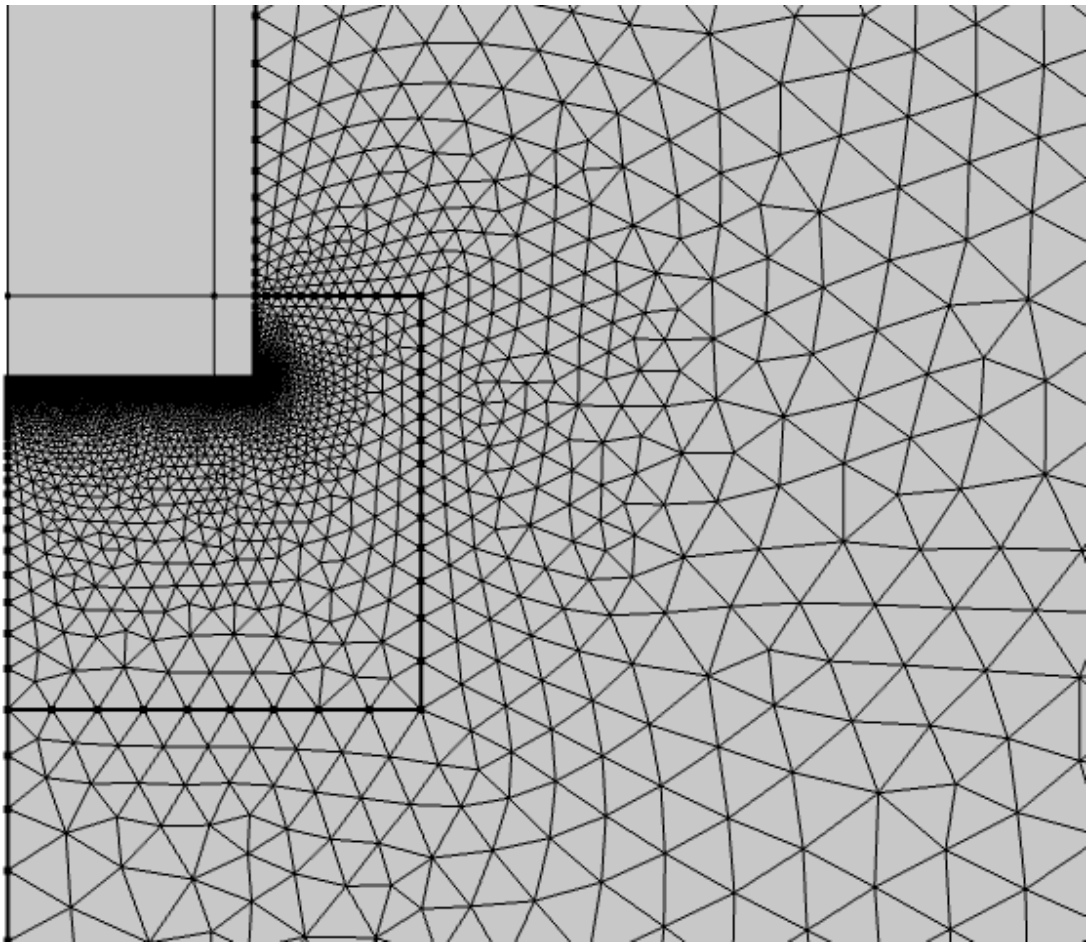

Figure 3.4: Simulation geometry for the COMSOL model used to represent the glassy carbon working electrode and its surrounding region.

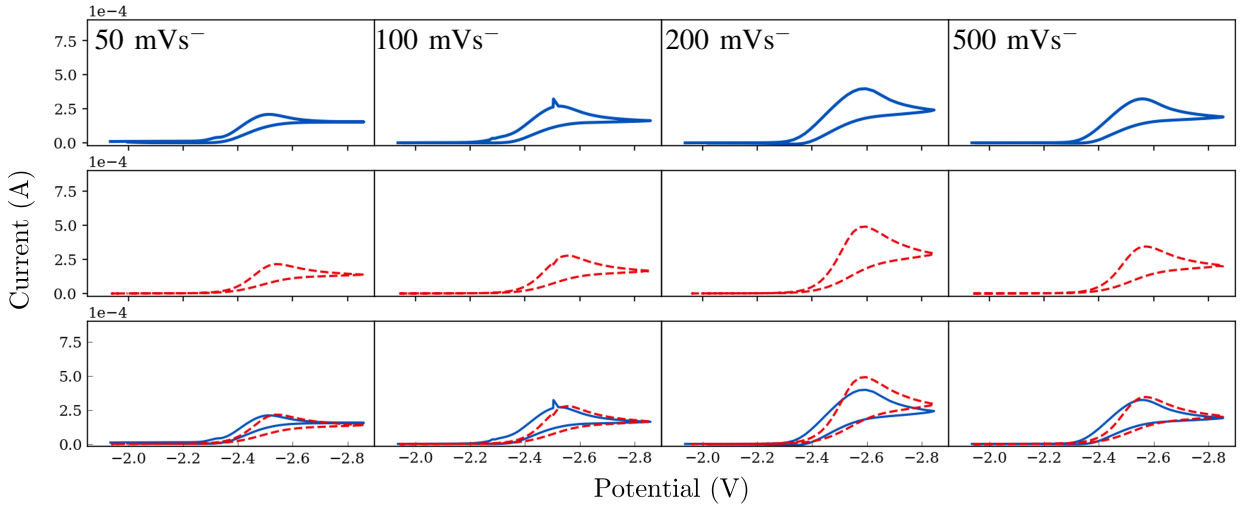

Figure 3.5: Cyclic voltammetry of acetophenone carboxylation at Ar saturated pressure on a 1mm diameter glassy carbon electrode (solid line) vs COMSOL simulated data (dashed) at various scan rates (50, 100, 200 and 500 mVs^{-})

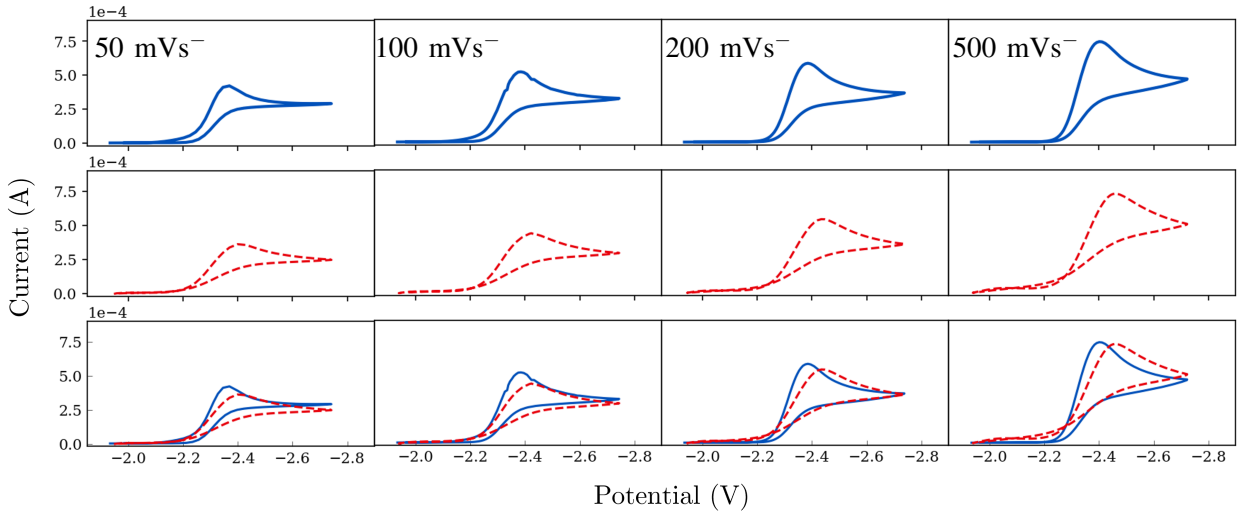

Figure 3.6: Cyclic voltammetry of acetophenone carboxylation at 3.4 bar CO_2 pressure on a 1 mm diameter glassy carbon electrode (solid line) vs COMSOL simulated data (dashed) at various scan rates (50, 100, 200 and 500 mVs^{-})

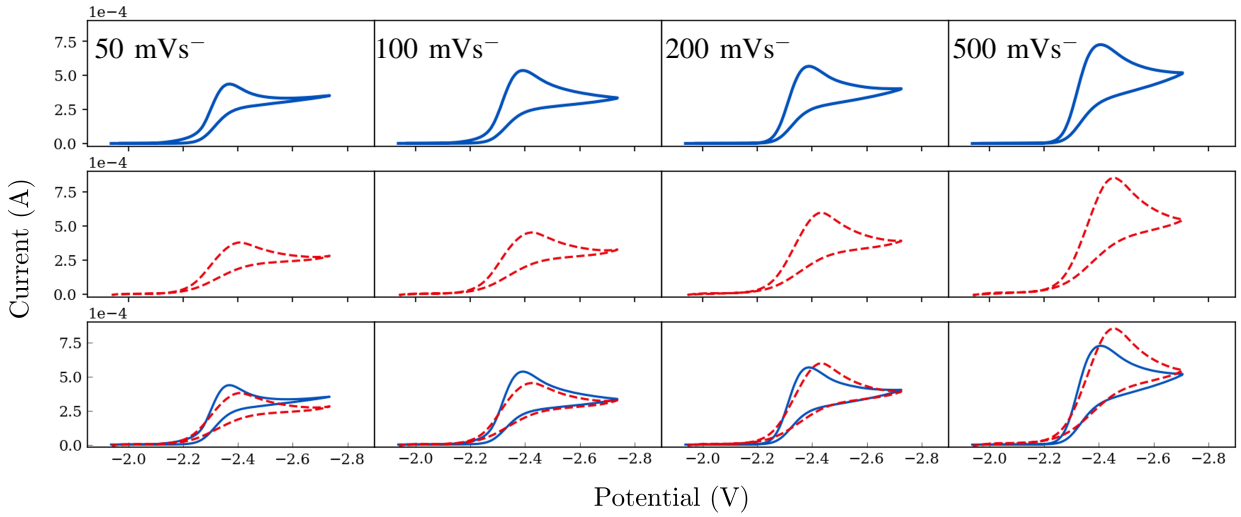

Figure 3.7: Cyclic voltammetry of acetophenone carboxylation at 13.8 bar CO_2 pressure on a 1 mm diameter glassy carbon electrode (solid line) vs COMSOL simulated data (dashed) at various scan rates ((50, 100, 200 and 500 mVs^{-})

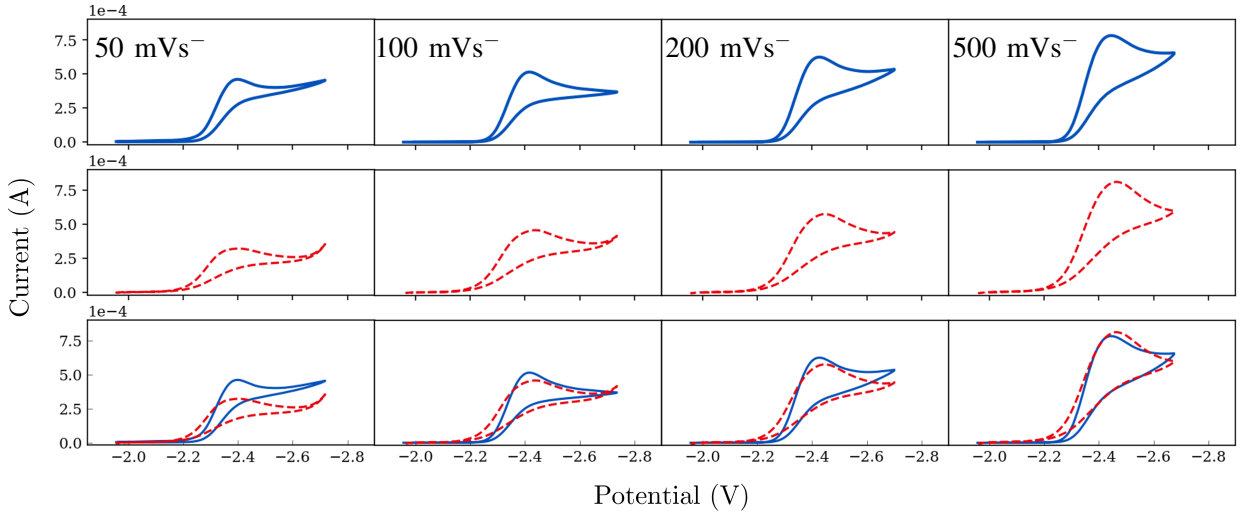

Figure 3.8: Cyclic voltammetry of acetophenone carboxylation at 28.8 bar CO_2 pressure on a 1 mm diameter glassy carbon electrode (solid line) vs COMSOL simulated data (dashed) at various scan rates (50, 100, 200 and 500 mVs^{-})

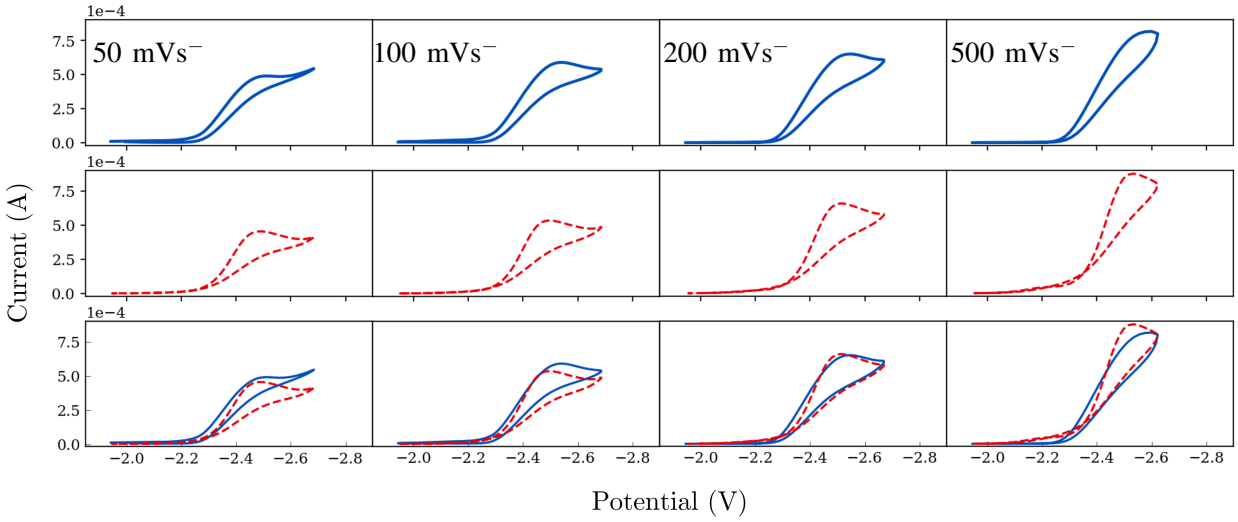

Figure 3.9: Cyclic voltammetry of acetophenone carboxylation at 41.4 CO_2 pressure on a 1 mm diameter glassy carbon electrode (solid line) vs COMSOL simulated data (dashed) at various scan rates (50, 100, 200 and 500 mVs^{-})

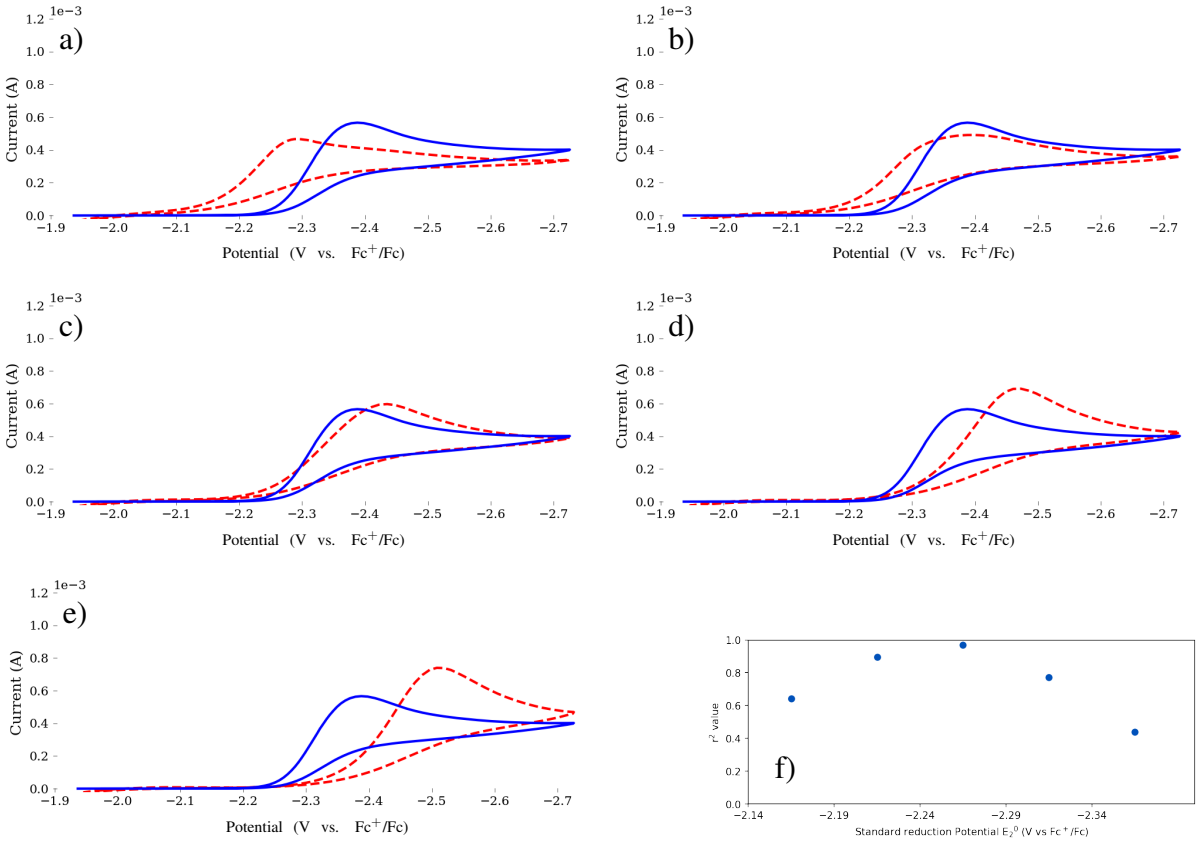

Figure 3.10: Sensitivity of the COMSOL model to changes in the value of E_1^0 (dashed) vs experimental cyclic voltammetry data (solid) for values (a) -2.17, (b) -2.22, (c) -2.27, (d) -2.32, and (e) -2.37 (V vs. Fc^+/Fc) at 13.8 bar CO_2 pressure and 200 mVs^-. The r^2 results as a function of the value are shown in panel (f).

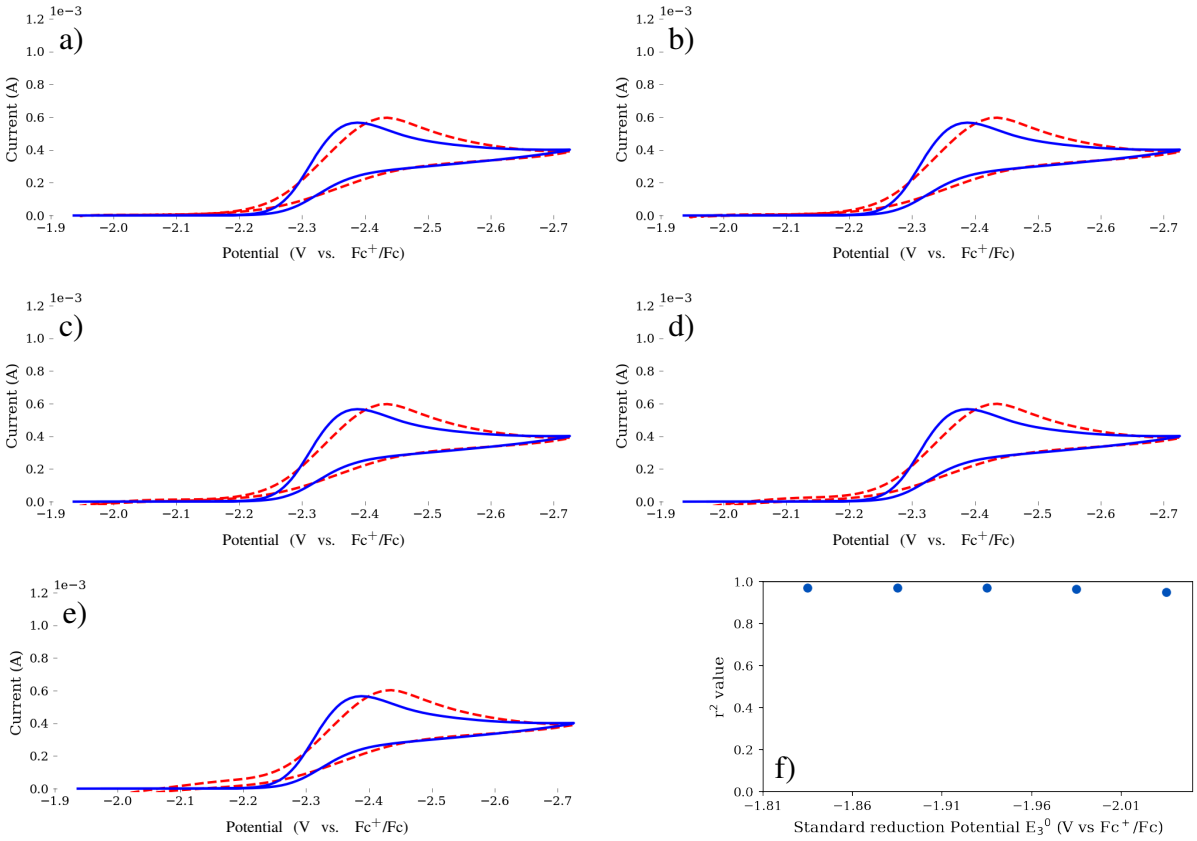

Figure 3.11: Sensitivity of the COMSOL model to changes in the value of E_3^0 (dashed) vs experimental cyclic voltammetry data (solid) for values (a) -1.84, (b) -1.89, (c) -1.94, (d) -1.99, and (e) -2.04 (V vs. Fc^+/Fc) at 13.8 bar CO_2 pressure and 200 mVs^-. The r^2 results as a function of the value are shown in panel (f).

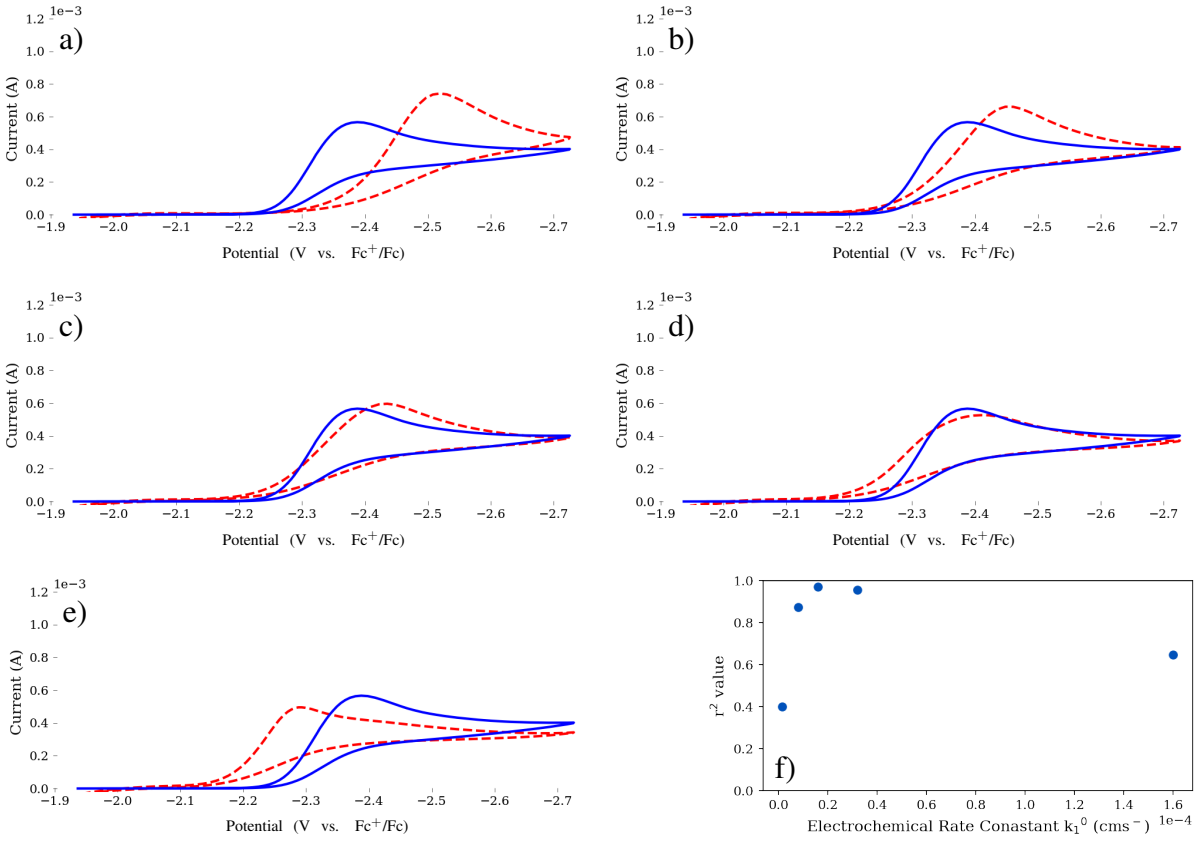

Figure 3.12: Sensitivity of the COMSOL model to changes in the value of k_0^1 (dashed) vs experimental cyclic voltammetry data (solid) for values (a) 1.6e-6, (b) 8e-6, (c) 1.6e-5, (d) 3.2e-5, and (e) 1.6e-4 (cm/s) at 13.8 bar CO_2 pressure and 200 mVs^{-}. The r^2 results as a function of the value are shown in panel (f).

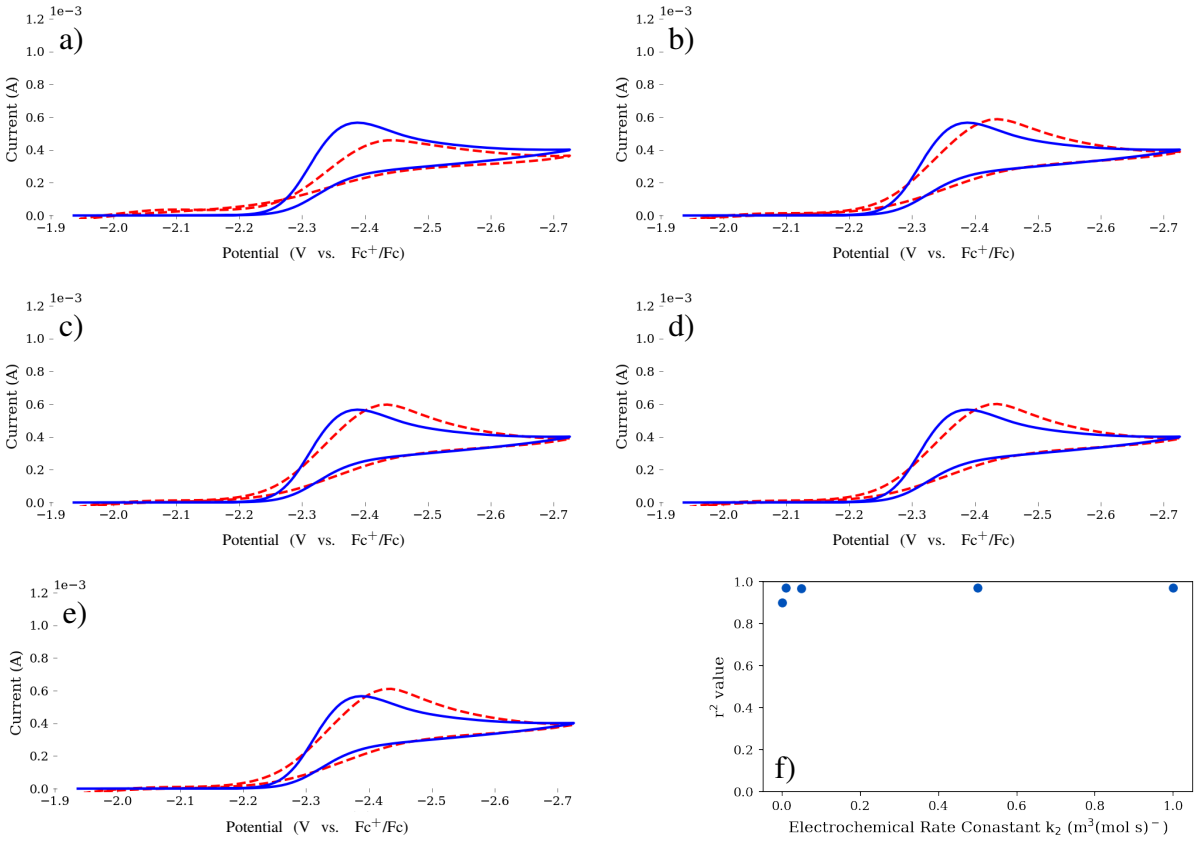

Figure 3.13: Sensitivity of the COMSOL model to changes in the value of k_2(dashed) vs experimental cyclic voltammetry data (solid) for values (a) 1e-3, (b) 5e-2, (c) 1e-1, (d) 2e-1, and (e) 1 (m^3/(s mol)) at 13.8 bar and 200 mVs^-. The r^2 results as a function of the value are shown in panel (f).

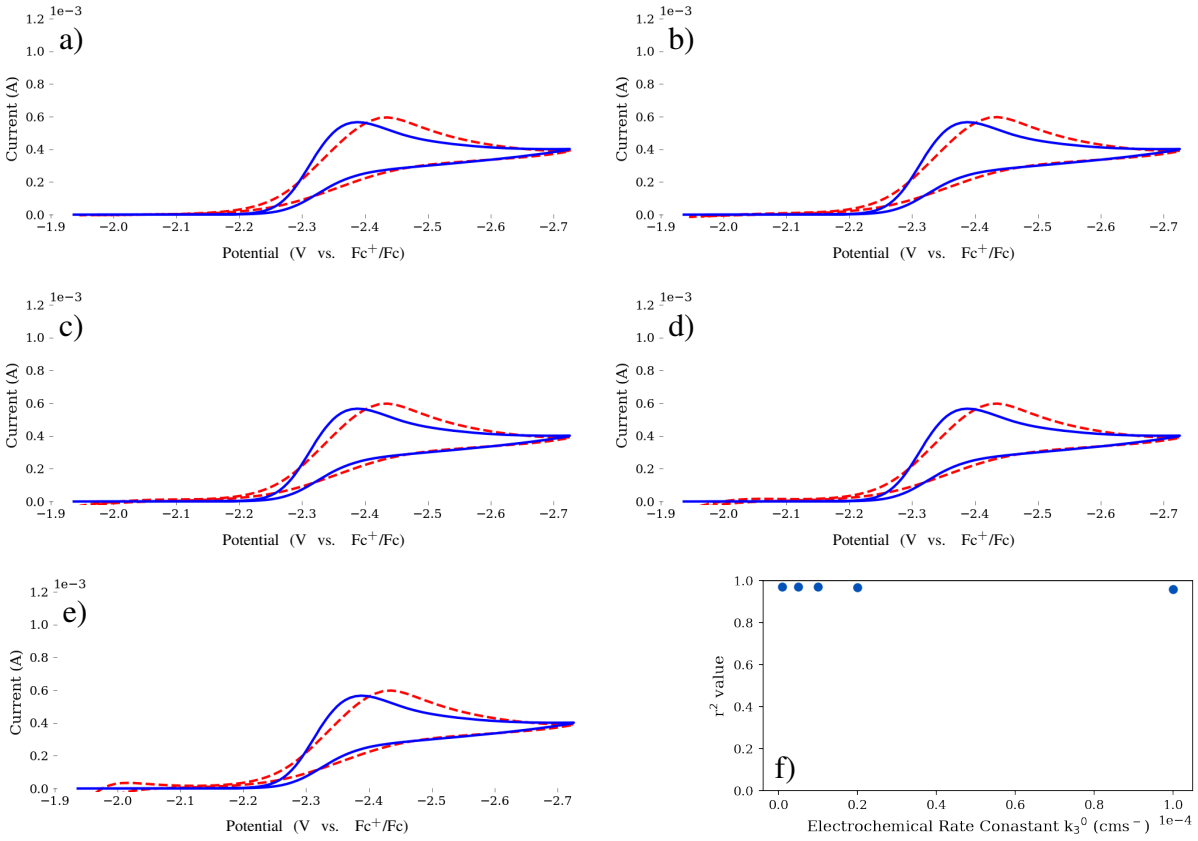

Figure 3.14: Sensitivity of the COMSOL model to changes in the value of k_0^2 (dashed) vs experimental cyclic voltammetry data (solid) for values (a) 1e-6, (b) 5e-6, (c) 1e-5, (d) 2e-5, and (e) 1e-4 (cm/s) at 13.8 bar CO_2 pressure and 200 mVs^{-}. The r^2 results as a function of the value are shown in panel (f).

References

[1] Bushuyev, O. S.; Luna, P. D.; Dinh, C. T.; Tao, L.; Saur, G.; van de Lagemaat, J.; Kelley, S. O.; Sargent, E. H. What Should We Make with CO_2 and How Can We Make It? *Joule* **2018**, *2*, 825–832.

[2] Zhang, W.; Hu, Y.; Ma, L.; Zhu, G.; Wang, Y.; Xue, X.; Chen, R.; Yang, S.; Jin, Z. Progress and Perspective of Electrocatalytic CO_2 Reduction for Renewable Carbonaceous Fuels and Chemicals. *Advanced Science* **2018**, *5*.

[3] Roberts, F. S.; Kuhl, K. P.; Nilsson, A. High Selectivity for Ethylene from Carbon Dioxide Reduction over Copper Nanocube Electrocatalysts. *Angewandte Chemie* **2015**, *127*, 5268–5271.

[4] Kawamata, Y.; Baran, P. S. Electrosynthesis: Sustainability Is Not Enough. *Joule* **2020**, *4*, 701–704.

[5] Chang, X.; Zhang, Q.; Guo, C. Asymmetric Electrochemical Transformations. *Angewandte Chemie International Edition* **2020**, *59*, 12612–12622.

[6] Frontana-Uribe, B. A.; Little, R. D.; Ibanez, J. G.; Palma, A.; Vasquez-Medrano, R. No Title. *Green Chemistry* **2010**, *12*, 2099–2119.

[7] Isse, A. A.; Galia, A.; Belfiore, C.; Silvestri, G.; Gennaro, A. Electrochemical reduction and carboxylation of halobenzophenones. *Journal of Electroanalytical Chemistry* **2002**, *526*, 41–52.

[8] Wawzonek, S.; Gundersen, A. Polarographic Studies in Acetonitrile and Dimethylformamide. *Journal of The Electrochemical Society* **1960**, *107*, 537.

[9] Amatore, C.; Jutand, A. Activation of Carbon Dioxide by Electron Transfer and Transition Metals. Mechanism of Nickel-Catalyzed Electrocarboxylation of Aromatic Halides. *Journal of the American Chemical Society* **1991**, *113*, 2819–2825.

[10] Zhang, K.; Wang, H.; Zhao, S.-F.; Niu, D.-F.; Lu, J.-X. Asymmetric electrochemical carboxylation of prochiral acetophenone: An efficient route to optically active atrolactic acid via selective fixation of carbon dioxide. **2009**,

[11] Chan, A. S. C.; Huang, T. T.; Wagenknecht, J. H.; Miller, R. E. A Novel Synthesis of 2-Aryllactic Acids via Electrocarboxylation of Methyl Aryl Ketones. *J. Org. Chem* **1995**, *60*, 742–744.

[12] Zhao, S. F.; Wu, L. X.; Wang, H.; Lu, J. X.; Bond, A. M.; Zhang, J. A unique proton coupled electron transfer pathway for electrochemical reduction of acetophenone in the ionic liquid [BMIM][BF4] under a carbon dioxide atmosphere. *Green Chemistry* **2011**, *13*, 3461–3468.

[13] Feng, Q.; Huang, K.; Liu, S.; Yu, J.; Liu, F. Electrocatalytic carboxylation of aromatic ketones with carbon dioxide in ionic liquid 1-butyl-3-methylimidazoliumtetrafluoborate to -hydroxy-carboxylic acid methyl ester. *Electrochimica Acta* **2011**, *56*, 5137–5141.

[14] Zhao, S. F.; Horne, M.; Bond, A. M.; Zhang, J. Electrochemical reduction of aromatic ketones in 1-butyl-3-methylimidazolium-based ionic liquids in the presence of carbon dioxide: the influence of the ketone substituent and the ionic liquid anion on bulk electrolysis product distribution. *Physical Chemistry Chemical Physics* **2015**, *17*, 19247–19254.

[15] Zhang, L.; Xiao, L. P.; Niu, D. F.; Luo, Y. W.; Lu, J. X. Electrocarboxylation of acetophenone to 2-hydroxy-2-phenylpropionic acid in the presence of CO_2. *Chinese Journal of Chemistry* **2008**, *26*, 35–38.

[16] Matthessen, R.; Fransaer, J.; Binnemans, K.; Vos, D. E. D. Electrocarboxylation: Towards sustainable and efficient synthesis of valuable carboxylic acids. *Beilstein Journal of Organic Chemistry* **2014**, *10*, 2484–2500.

[17] Scialdone, O.; Galia, A.; Isse, A. A.; Gennaro, A.; Sabatino, M. A.; Leone, R.; Filardo, G. Electrocarboxylation of aromatic ketones: Influence of operative parameters on the competi-

tion between ketyl and ring carboxylation. *Journal of Electroanalytical Chemistry* **2007**, *609*, 8–16.

[18] Stalcup, M. A.; Nilles, C. K.; Lee, H. J.; Subramaniam, B.; Blakemore, J. D.; Leonard, K. C. Organic Electrosynthesis in CO_2-eXpanded Electrolytes: Enabling Selective Acetophenone Carboxylation to Atrolatic Acid. *ACS Sustainable Chemistry and Engineering* **2021**, *9*, 10431–10436.

[19] Bard, A. J.; Bard Allen J,; Faulkner, L. R. *Electrochemical Methods : Fundamentals and Applications*, 2nd ed.; Wiley: New York, 2001; p 236.

[20] Compton, R.; Banks, C. *Understanding Voltammetry*, 3rd ed.; 2018; pp 255–258.

[21] Chen, B.-L. L.; Xiao, Y.; Xu, X.-M. M.; Yang, H.-P. P.; Wang, H.; Lu, J.-X. X. Alkaloid induced enantioselective electroreduction of acetophenone. *Electrochimica Acta* **2013**, *107*, 320–326.

[22] Shaughnessy, C. I.; Jantz, D. T.; Leonard, K. C. Selective electrochemical CO_2 reduction to CO using: In situ reduced In2O3 nanocatalysts. *Journal of Materials Chemistry A* **2017**, *5*, 22743–22749.

[23] Sconyers, D. J.; Shaughnessy, C. I.; Lee, H.; Subramaniam, B.; Leonard, K. C.; Blakemore, J. D. Enhancing Molecular Electrocatalysis of CO_2 Reduction with Pressure-Tunable CO_2-Expanded Electrolytes. *ChemSusChem* **2020**, cssc.202000390.

[24] Zhao, S. F.; Horne, M.; Bond, A. M.; Zhang, J. Electrocarboxylation of acetophenone in ionic liquids: The influence of proton availability on product distribution. *Green Chemistry* **2014**, *16*, 2242–2251.

[25] Shaughnessy, C. I.; Sconyers, D. J.; Lee, H.-J.; Subramaniam, B.; Blakemore, J. D.; Leonard, K. C.; Co, E. Insights into pressure tunable reaction rates for electrochemical reduction of CO 2 in organic electrolytes †. **2020**,

[26] Shaughnessy, C. I.; Sconyers, D. J.; Kerr, T. A.; Lee, H.-J.; Subramaniam, B.; Leonard, K. C.; Blakemore, J. D. Intensified Electrocatalytic CO_2 Conversion in Pressure-Tunable CO_2-Expanded Electrolytes. *ChemSusChem* **2019**, *12*, 3761–3768.

[27] Haynes, L. V.; Sawyer, D. T. Electrochemistry of Carbon Dioxide in Dimethyl Sulfoxide at Gold and Mercury Electrodes. *Analytical Chemistry* **1967**, *39*, 332–338.

[28] Morgenstern, D. A.; Wittrig, R. E.; Fanwick, P. E.; Kubiak, C. P. Photoreduction of Carbon Dioxide to Its Radical Anion by [Ni3(μ3-I)2(dppni)3]: Formation of Two Carbon-Carbon Bonds via Addition of CO2• to Cyclohexene. *Journal of the American Chemical Society* **1993**, *115*, 6470–6471.

[29] Morris, A. J.; Meyer, G. J.; Fujita, E. Molecular approaches to the photocatalytic reduction of carbon dioxide for solar fuels. *Accounts of Chemical Research* **2009**, *42*, 1983–1994.

[30] Silvestri, G.; Gambino, S.; Filardo, G. Electrochemical carboxylation of aldehydes and ketones with sacrificial aluminum anodes. *Tetrahedron Letters* **1986**, *27*, 3429–3430.

Chapter 4

A Study of Structure-Property relationships in Organic Electrosynthesis

Abstract

A long-standing grand challenge in organic electrochemistry is forming carbon bonds between carbon dioxide (CO_2) and itself or other substrates, providing a sustainable route toward chemical production. The major challenge with CO_2 utilization is the thermodynamic stability of CO_2 since it requires considerable energy inputs to activate. However, some recent developments in methods and tools have allowed researchers to form carbon-carbon bonds using CO_2 as a carbon source with a technique called organic electrosynthesis. Researchers have selectively formed carboxylic acids on various substrates using CO_2 as a reactant. We have recently demonstrated that acetophenone's electrochemical carboxylation is enhanced in CO_2 eXpanded Electrolytes or CXEs. These media consist of solvents and supporting electrolytes with a high affinity for dissolved CO_2, yielding multi-molar concentrations in the liquid phase. To further study the electrochemical carboxylation in CXEs, we chose to study the effect of electron-withdrawing groups on the reducibility of aromatic molecules used in electrochemical carboxylation reactions. In addition to changes in the substrate, the concentration of CO_2 in the liquid phase can also be studied to understand the interaction between substrate and CO_2 concentration.

4.1 Introduction

For the past decade, scientists have been focused on developing technologies and techniques that will lead to the more sustainable production of chemicals. The global green house gas emissions from petrochemical processes topped one gigatonne of carbon dioxide equivalent in 2010.[1] Due to the incredible amount of CO_2 generated per year through chemical manufacturing, there is a significant desire to begin closing the carbon loop.

Currently, our work is at the intersection of sustainable chemistry and CO_2 utilization. The intersection of traditional chemical synthesis and its potential enhancement in CO_2 rich media has led to many exciting studies about CO_2 concentration effects and electron transfer kinetics in such a unique media.[2–4] For example, electrochemical carboxylation in CO_2 eXpanded Electrolytes (CXEs) has enabled the study of CO_2 concentration effects on electrochemical carboxylation reactions. However, the breadth of potential reactants and the effects of substituents are not well understood, especially in a media with tuneable CO_2 concentration. In particular, we wanted to study the electrochemical carboxylation of styrene and 4'-trifluoromethyl acetophenone.

Styrene was chosen as a reactant for several reasons. First, unlike acetophenone, styrene does not have a strong electron-withdrawing group. We hypothesized that the absence of the electron-withdrawing oxygen would require more negative potentials for the reduction to take place. Understanding how electron-donating/withdrawing species interact in electrochemical carboxylation can aid in selecting reactants that lend themselves to this type of reaction. Additionally, The carboxylation of styrene could yield hydrocynammic acid, a widely used chemical in the food and drug industries as a preservative and a flavoring agent. An electrochemical pathway to valuable chemicals can further promote the use of sustainable electrochemistry in chemical synthesis.

In addition to styrene, understanding the effects of electron-withdrawing groups on the electrochemical behavior of acetophenone could lead to tuneable reactivity by adding electron-withdrawing groups. 4'-Trifluoromethyl acetophenone was selected as a model chemical to study the effect of electron-withdrawing groups on electrochemical reduction. We anticipated that the trifluoromethyl group would make the electrochemical reduction begin at less negative potentials when compared

to acetophenone. Studying substitution effects for electrochemical carboxylation reactions is critical if a direct synthesis route to certain carboxylic acid products, such as ibuprofen, is desirable.

4.2 Experimental Methods

As described previously, high-pressure electrochemical experiments were conducted in a single-cell electrochemical vessel.[5] This custom-built vessel consisted of a Parr reactor (50 mL) base fitted with a modified cap and electrical feed-throughs capable of withstanding the operating pressure of the reactor. Inside the reaction vessel, a glass sleeve separated the electrochemical solution from the metal body of the reactor. The reactor was equipped with temperature and pressure sensing equipment that monitored reaction conditions through a NI LabVIEW Data Acquisition system. In addition, the reactor is jacketed to ensure isothermal conditions.

All electrochemical experiments were performed using a Gamry Reference 3000 Potentiostat/Galvanostat at various CO_2 pressures (Matheson 99.999% purity) and a constant temperature of 25 °C using a glassy carbon working electrode (0.0079 cm^2) or a platinum wire electrode (99.99% purity), a sacrificial magnesium counter electrode (99.9% purity), and a quasi-reference electrode consisting of a fritted glass chamber with a silver wire (99.9% purity).

The reaction medium for the styrene studies consisted of dimethylformamide (DMF), 0.4 M tetrabutylammonium hexafluorophosphate ($TBAPF_6$), 4 mM ferrocene (Fc), and 100 mM styrene. All components of the solution were thoroughly dried to remove trace water impurities. DMF had to be used in the reduction of styrene due to the solvent window being stable at highly negative potentials.

The reaction medium for the 4'-trifluoromethyl acetophenone studies consisted of acetonitrile, 0.4 M tetrabutylammonium hexafluorophosphate ($TBAPF_6$), 4 mM ferrocene (Fc), and 100 mM 4'-trifluoromethyl acetophenone. All components of the solution were thoroughly dried to remove trace water impurities.

Previous work has shown that the ferrocene redox couple can be used as an internal reference over the pressure and potential ranges studied.[5] The potential of the Ag quasi-reference electrode

was calibrated against the potential of the $Fc^{+/0}$ redox couple before each electrochemical experiment.

The Mg sacrificial anode was employed to enable the study of the electrochemical carboxylation reduction reactions without drastically changing the reaction media. Without a sacrificial anode, the supporting electrolyte and/or solvent may be oxidized on a more conventional Pt counter electrode, disrupting the system and producing unwanted side products visible in the ^{1}H-NMR experiments. In addition, the Mg ions stabilize the divalent anions and precipitate to ease the characterization of products.

4.3 Styrene Carboxylation

Styrene is an aromatic alkene widely produced as a monomer for polystyrene. However, the carbon-carbon double bond in styrene makes it very reactive, and we hypothesized that styrene would exhibit similar behavior to acetophenone regarding the carboxylation of a radical anion.[6] Yuan *et al.*[7] and[8] proposed the mechanism found in Fig. 4.1 where there are several potential reaction pathways. They proposed that the electrochemical carboxylation could either be facilitated by the reduction of CO_2 forming a radical anion that attacks the carbon double bond of the styrene. Without a proton source, a second CO_2 radical can terminate the radical anion generating a divalent carboxylic acid. Additionally, the styrene can be activated through an electrochemical reduction reaction and carboxylated by CO_2 nucleophilic attack. This pathway also generates a styrene-CO_2 adduct that requires further carboxylation to form the dicarboxylate product. The origin of this split pathway is in the electrochemical reduction potentials for each component. The standard reduction potential (E^0) for styrene is -3.04 V vs. Fc^+/Fc in dry DMF where in similar conditions E^0 for CO_2 is -2.66 V vs. Fc^+/Fc.

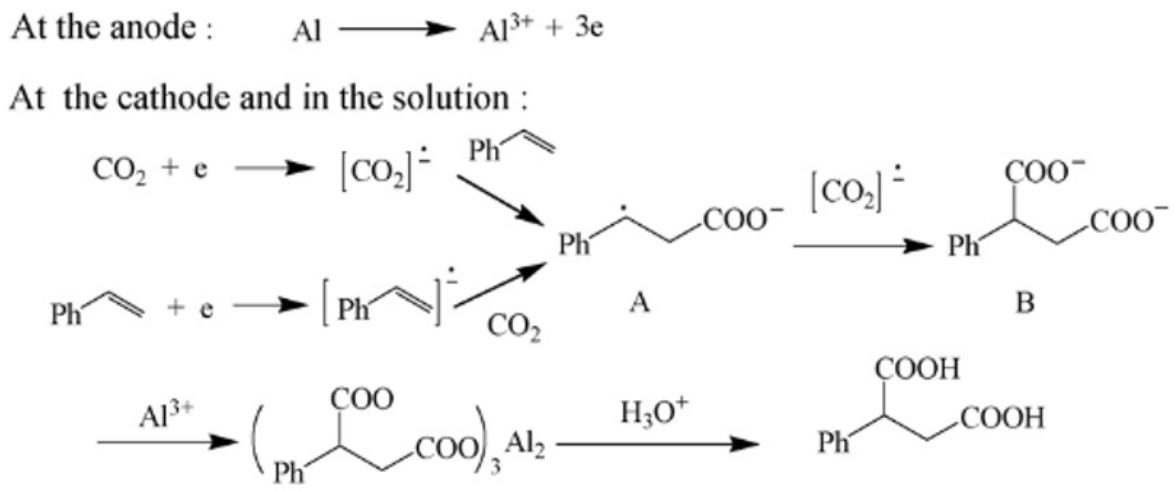

Figure 4.1: Electrochemical carbxylation of strene proposed by Yuan *et al.*[7].

Each of the aforementioned pathways could not be disseminated because Yuan *et al.*[7] did not have access to tuneable CO_2 concentrations. In CXEs, the pressure tuneable concentration of CO_2 enables the study of concentration effects on this reduction. Therefore, it is hypothesized that the CO_2 concentration must be sufficiently low to ensure that there is not a substantial generation of CO_2 reduction reaction (CO_2RR) products. However, this is only the case if the CO_2 activated pathway is the primary pathway toward carboxylation. Otherwise, the rate of intermediate formation directly depends on the concentration of available CO_2.

The electrochemical steps are the initial steps of the reaction mechanism. Thus changes in voltammetry as a function of CO_2 pressure and styrene concentration will provide insight into the nature of the reduction. Changing the styrene concentration and observing changes in the shape of the cyclic voltammetry can confirm that the styrene is being reduced. Since the styrene reduction occurs more negatively than the CO_2RR, an electrode with a low activity toward the CO_2RR reaction must be used. Cyclic voltammetry experiments were carried out using a platinum wire electrode. Other electrode materials like copper and glassy carbon were also used. However, copper can make faradaic quantification challenging, and glassy carbon did not yield a substantial reduction of either reactant.

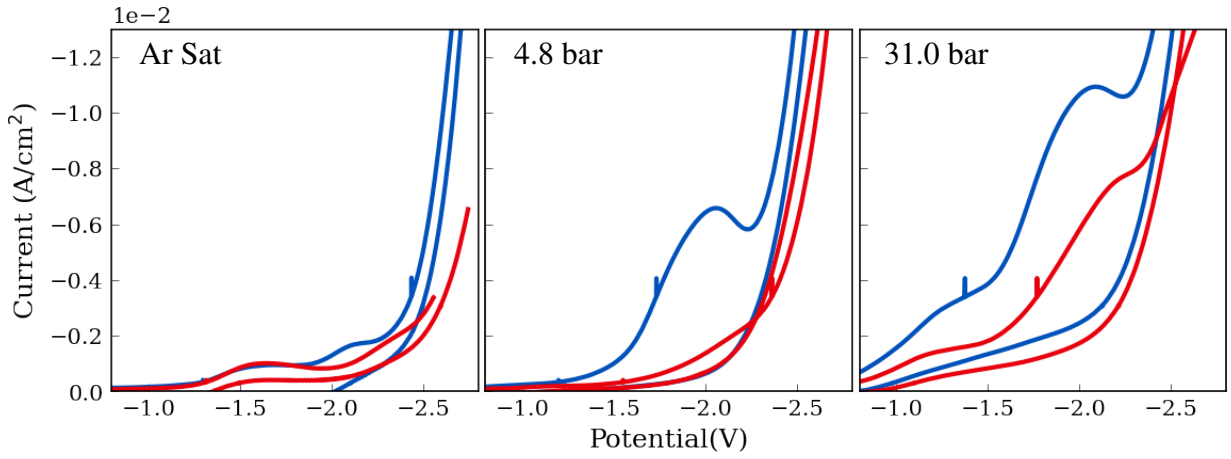

Figure 4.2: Cyclic Voltammetry experiments in GXEs with (blue) and without (red) styrene. CV's were performed on a platinum wire electrode at 100 mVs^{-} at argon saturated and various CO_2 headspace pressures all potentials are measured vs the Ferrocenium/Ferrocene redox couple.

Fig. 4.2 shows the results of the reduction of styrene in the DMF-based CXE as a function of CO_2 pressure. The prominent feature that changes as a function of CO_2 pressure is the emergence of a reduction event with a peak current around -2.0 V vs. Fc^+/Fc. This reduction is irreversible and may be due to the activation of the styrene substrate generating a stable radical anion intermediate. In the argon saturated experiment, this peak has a small peak current; however, when CO_2 is introduced at mild pressures, that current increases substantially. It is even further enhanced at 31 bar CO_2 pressure. The absence of this peak when styrene is not present provides evidence that this reduction event is related to the styrene. The increase in the peak current as a function of CO_2 pressure may suggest enhanced diffusion of the styrene. Additionally, the onset potential also decreases in the presence of CO_2. This shows that the interaction with the CO_2 and the styrene provides similar enhancements to what was seen in acetophenone.

To further confirm that this reduction is a result of the styrene. Concentration-dependent experiments were conducted. These experiments can be found in Appendix C1 and show that as the styrene concentration increases, so does the magnitude of the reduction event.

These results do not show the mechanism presented by Yuan *et al.*[7]. If the pathway proceeded through the styrene's electrochemical activation, the peak current would not depend on CO_2 pres-

sure for the reduction of acetophenone. Additionally, if the CO_2 reduction pathway were preferred, there would not be a peak current at these elevated CO_2 concentrations. Instead, the mechanism most supported would be an electrochemical chemical, electrochemical reaction (ECE). Wherein the styrene is reduced and forms a CO_2-styrene adduct. The formation of this intermediate can facilitate another electron transfer to occur. This additional electron transfer would result in a larger peak current. Additionally, the intermediate would be more easily reducible than the styrene starting material resulting in a single waveform. Fig. 4.3 is the proposed mechanism of the ECE reaction for the reduction of styrene where the dianion would be stabilized by a magnesium counter or be further reduced. These findings are consistent with others found in the literature.[8]

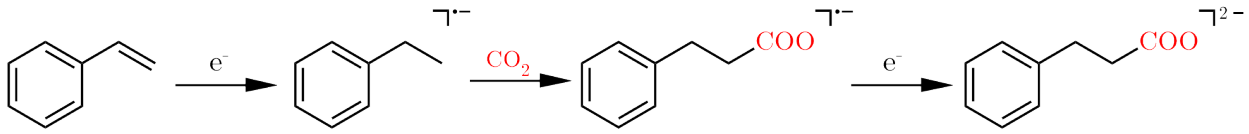

Figure 4.3: Electrochemical chemical electrochemical (ECE) reaction mechanism of styrene in the presence of CO_2.

The next step was to perform bulk electrolysis experiments on the system to generate a quantifiable amount of product for analysis through ^{1}H-NMR. The electrochemical cell was held at a constant potential of -2.0 V vs. Fc^+/Fc for 12 hours. After electrolysis, the system was depressurized and a precipitate formed as a result of the electrolysis. This precipitate was thought to be the product of the carboxylation and was collected through filtration. The supposed Mg salt of the divalent carboxylate was then treated with concentrated hydrochloric acid to protonate the acid for analysis.

Unfortunately, the resulting compounds proved incredibly challenging to characterize due to precipitation and the sample size being small. Many techniques were used to quantify the resulting solids; however, none were successful.

4.4 4'-(Triflouromethyl)acetophenone Carboxylation

In addition to stretching the carboxylation to styrene, we investigated the effects of electron-withdrawing substitutions to acetophenone. Having a strong electron withdrawing group in the *para* position to the carbonyl on the acetophenone could have dramatic effects on the electrochemical behavior of the system. These behaviors are fundamental to study in this system because we need to know what kind of substrates support this reaction. Furthermore, understanding the substituents that support electrochemical carboxylation can lead to the direct electrochemical synthesis of pharmaceuticals such as ibuprofen. We chose to investigate 4'-(trifluoromethyl)acetophenone to test the effects of electron-withdrawing substituents. The hypothesis when studying this system was that the electron-withdrawing nature of the trifluoromethyl group would shift the onset potential of the reduction less negatively when compared to the acetophenone reduction. However, the radical anion generated through the electrochemical reduction may have less energy due to the less negative reduction potential making the activation of the CO_2 during carboxylation slower. The slower rate of carboxylation could potentially generate side reactants such as the dimerization product.

The proposed mechanism follows a similar ECE reaction pathway as acetophenone. The initial reduction of the substrate is followed by the chemical addition of CO_2 and subsequent reduction. Fig. 4.4 outlines the three major reaction pathways that the reaction could proceed depending on the concentration of CO_2, protons, and other substrate molecules. We anticipate a similar behavior regarding the peak current and the shift in onset potential as we had seen in acetophenone.

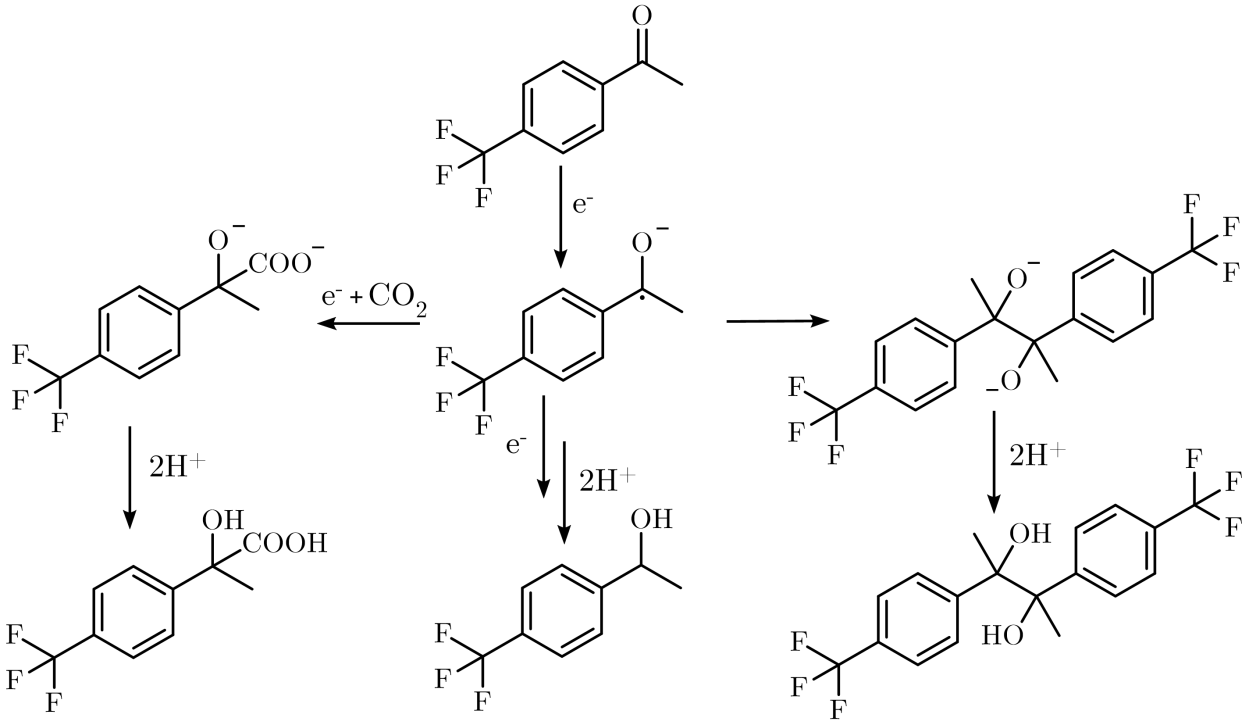

Figure 4.4: Proposed electrochemical reduction pathways of 4'-(triflouromethyl)acetophenone.

To study the effect of the electron-withdrawing group on the electrochemical behavior, cyclic voltammetry experiments were conducted at various CO_2 headspace pressures. The results can be found in Fig. 4.5. The reduction consists of a single irreversible reduction event. The irreversible reduction indicates the generation of a stable radical anion that can be further reduced after carboxylation in the presence of CO_2. The previous insights from simulations of the acetophenone reduction can be extended here, where the chemical reaction step in this electrochemical chemical reaction allows for the second electron transfer to occur.

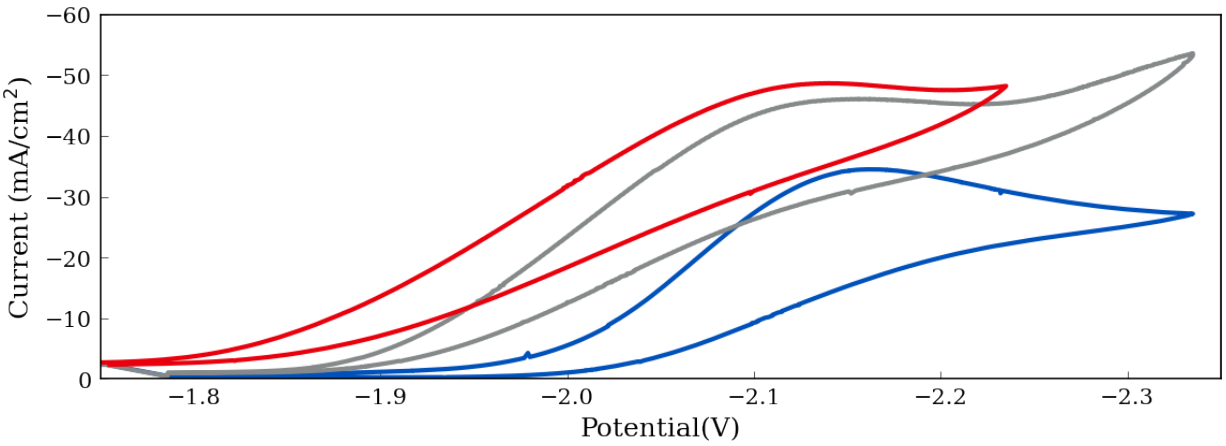

Figure 4.5: Electrochemical reduction of 4'-(triflouromethyl)acetophenone on a 1 mm diameter glassy carbon working electrode under Ar atmosphere (blue), 4.8 bar (grey), and 28.6 bar (red) CO_2 pressures at 100 mVs^{-}.

Furthermore, the peak current increases in the presence of CO_2, and a significant change in the onset potential is observed. The increase in peak current and the shift in onset potential are also observed in acetophenone.[2] The shift to less negative potentials with respect to the acetophenone supports the hypothesis that the electron-withdrawing group decreases the potential required to reduce the 4'-(trifluoromethyl)acetophenone. Additionally, the separation between the onset potential and the peak current could indicate a slower carboxylation rate; however, this could also be representative of the slower diffusion of 4'-(trifluoromethyl)acetophenone vs. acetophenone at elevated pressures. This phenomenon can be tested by measuring the rate of carboxylation of 4'-(trifluoromethyl)acetophenone against the carboxylation of acetophenone using a bulk electrolysis experiment.

Bulk electrolysis experiments were conducted over 12 hours on a glassy carbon disk electrode 1 mm in diameter. After 12 hours at -2.1 V vs. Fc^{+}/Fc, the resulting precipitate was separated through filtration. This precipitate was assumed to be the magnesium salt of the divalent product. After treatment with concentrated hydrochloric acid ^{1}H-NMR and ^{19}F-NMR were conducted in deuterated water. Unfortunately, the precipitate would not remain in the solution and quickly precipitated. The resulting NMR experiments show a lack of an aromatic region we would associate with both the product and the residual starting material. These results lead to the abandonment of

this research effort to pursue other areas of discovery.

4.5 Conclusion

The extension of organic electrosynthesis in CXEs can lead to a better fundamental understanding of how CO_2 interacts with these systems that are traditionally limited by CO_2 concentration. However, in an effort to minimize the impact on the electrochemical system during the bulk electrolysis experiments, the use of a magnesium counter electrode could generate salts of the products that are difficult to redissolve and analyze. Others have used other metals as counter ions, such as aluminum. Potentially, the dissociation constant for the electrogenerated species for both the styrene and the 4'-(trifluoromethyl)acetophenone and another metal cation can be more soluble, allowing for analysis using ^{1}H-NMR.

In the case of 4'-(trifluoromethyl)acetophenone, it exhibits very similar behavior to what we see in acetophenone. The less negative shift in onset potential can be attributed to the electron-withdrawing nature of the trifluoromethyl group. The next step would be looking at electron-donating groups such as isobutyl. 4'-(Isobutyl)acetophenone could be used as a starting material for the electrochemical synthesis of ibuprofen. The primary concern is that the carboxylation could occur in an unwanted position or that the reduction potential with an electron-donating group like tertbutyl could be more negative than the boundaries of our solvent window.

In general, we learned that the CO-activated pathway for the electrochemical carboxylation of styrene is most likely not the route of carboxylation. This makes intuitive sense since the CO_2RR occurs at less negative potentials than the styrene reduction. More support for this is the lack of CO_2RR products in the reactor headspace for styrene carboxylation. We also learned that the reduction potential of these reactions is tuneable using different chemical substitutions. Unfortunately, without product quantification, these results are just observations made based on previous experience in a similar media and have not resulted in the generation of publishable data.

4.6 Supporting Information Figures

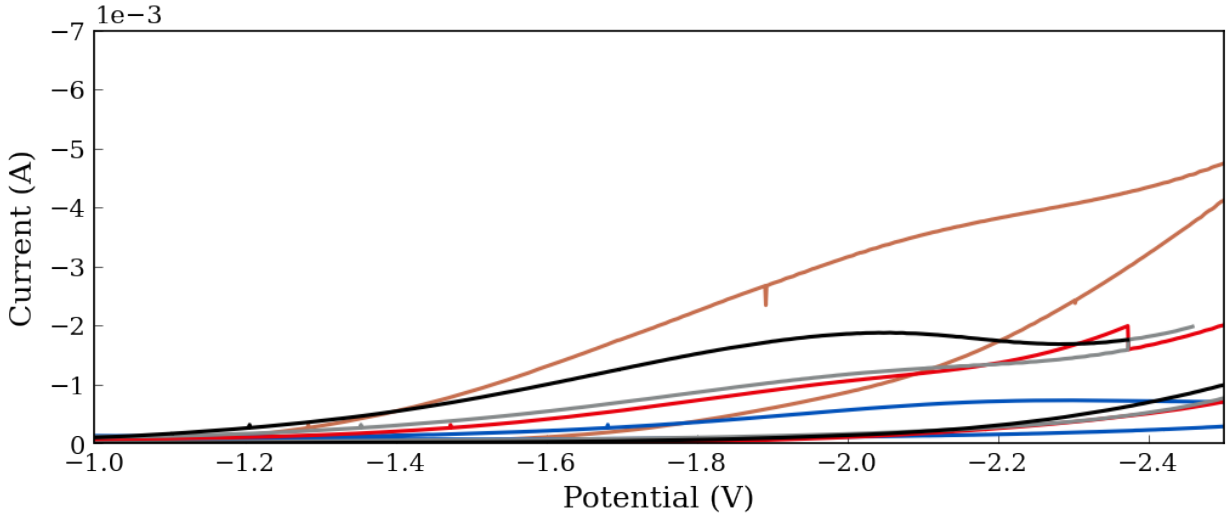

Figure 4.6: Cyclic voltammetry data for the electrochemical reduction of styrene at 0 mM (blue), 10 mM (red), 50 mM (black), and 100 mM (orange) in DMF at 27.6 bar of CO_2 pressure on a platinum wire at 100 mVs^{-}.

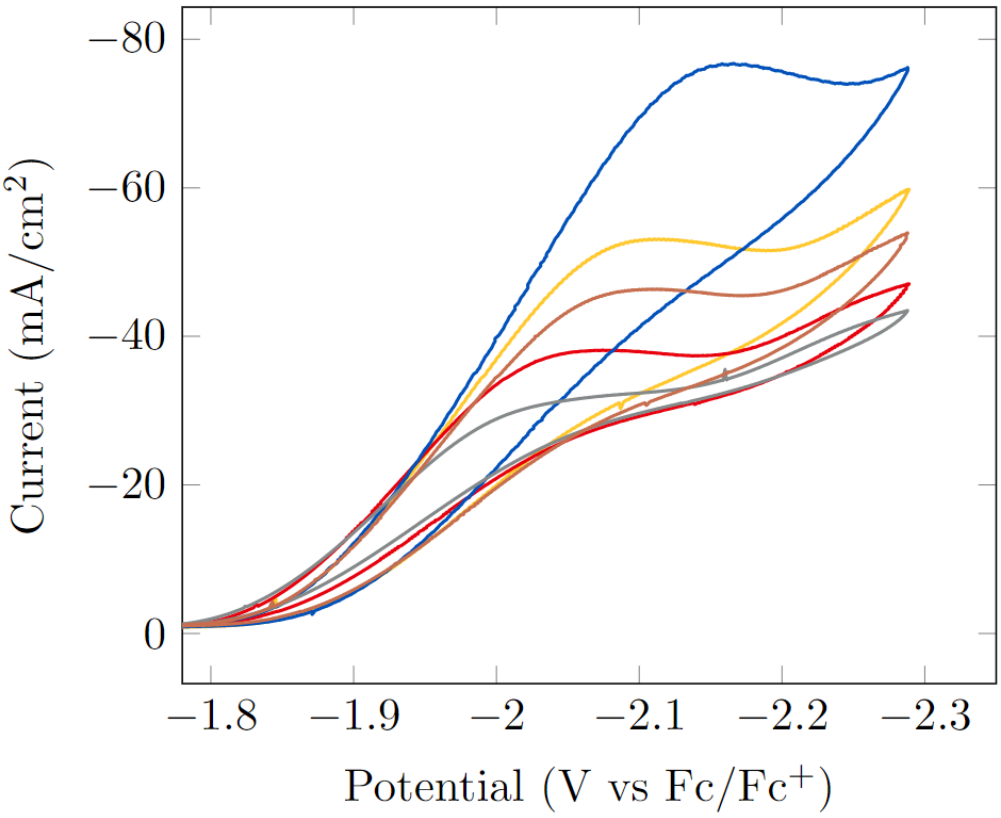

Figure 4.7: Cyclic voltammetry data for the electrochemical reduction of 4'-(trifluoromethyl) acetophenone at 100 mM in acetonitrile at 4.8 bar of CO_2 pressure on a glassy carbon disk at 20 mVs^- (grey), 50 mVs^- (red), 100 mVs^- (orange), 200 mVs^- (yellow), 500mVs^- (blue).

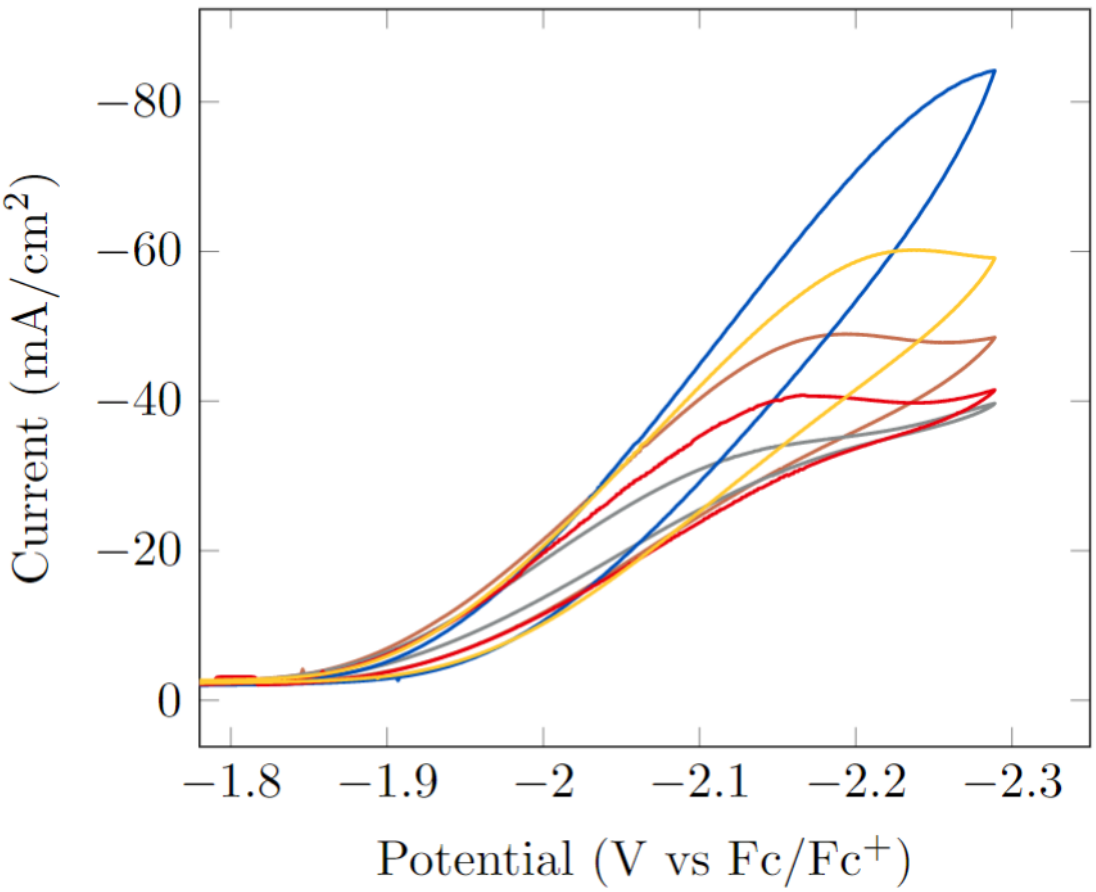

Figure 4.8: Cyclic voltammetry data for the electrochemical reduction of 4'-(trifluoromethyl) acetophenone at 100 mM in acetonitrile at 27.6 bar of CO_2 pressure on a glassy carbon disk at 20 mVs$^-$ (grey), 50 mVs$^-$ (red), 100 mVs$^-$ (orange), 200 mVs$^-$ (yellow), 500mVs$^-$ (blue).

References

[1] Schiffer, Z. J.; Manthiram, K. Electrification and Decarbonization of the Chemical Industry. *Joule* **2017**, *1*, 10–14.

[2] Stalcup, M. A.; Nilles, C. K.; Lee, H. J.; Subramaniam, B.; Blakemore, J. D.; Leonard, K. C. Organic Electrosynthesis in CO_2-eXpanded Electrolytes: Enabling Selective Acetophenone Carboxylation to Atrolatic Acid. *ACS Sustainable Chemistry and Engineering* **2021**, *9*, 10431–10436.

[3] Shaughnessy, C. I.; Sconyers, D. J.; Lee, H.-J.; Subramaniam, B.; Blakemore, J. D.; Leonard, K. C.; Co, E. Insights into pressure tunable reaction rates for electrochemical reduction of CO 2 in organic electrolytes †. **2020**,

[4] Sconyers, D. J.; Shaughnessy, C. I.; Lee, H.; Subramaniam, B.; Leonard, K. C.; Blakemore, J. D. Enhancing Molecular Electrocatalysis of CO_2 Reduction with Pressure-Tunable CO_2-Expanded Electrolytes. *ChemSusChem* **2020**, cssc.202000390.

[5] Shaughnessy, C. I.; Sconyers, D. J.; Kerr, T. A.; Lee, H.-J.; Subramaniam, B.; Leonard, K. C.; Blakemore, J. D. Intensified Electrocatalytic CO_2 Conversion in Pressure-Tunable CO_2-Expanded Electrolytes. *ChemSusChem* **2019**, *12*, 3761–3768.

[6] Quan, Y.; Yu, R.; Zhu, J.; Guan, A.; Lv, X.; Yang, C.; Li, S.; Wu, J.; Zheng, G. Efficient carboxylation of styrene and carbon dioxide by single-atomic copper electrocatalyst. *Journal of Colloid and Interface Science* **2021**, *601*, 378–384.

[7] Yuan, G. Q.; Jiang, H. F.; Lin, C.; Liao, S. J. Efficient electrochemical synthesis of 2-arylsuccinic acids from CO_2 and aryl-substituted alkenes with nickel as the cathode. *Electrochimica Acta* **2008**, *53*, 2170–2176.

[8] Kim, Y.; Park, G. D.; Balamurugan, M.; Seo, J.; Min, B. K.; Nam, K. T. Electrochemical -Selective Hydrocarboxylation of Styrene Using CO_2 and Water. *Advanced Science* **2020**, *7*.

Chapter 5

Electrodeposition of Gold on Nickel Foams to form Electrocatalytic Nobel Metal Foams

Abstract

Over the past decade, a substantial amount of work has been done in the electrochemical reduction of carbon dioxide. The effort has been focused on closing the carbon cycle associated with the combustion of fuels by taking CO_2 and converting it into fuels and chemicals. However, the thermodynamic stability and low selectivity toward higher carbon-containing compounds have continuously challenged this field of sustainable chemistry. In addition to the intrinsic difficulties with CO_2 reduction, mass transport, and solubility difficulties also plague these systems. In traditional atmospheric electrochemistry cells, the solubility of CO_2 is very low; however, using CO_2 eXpanded Electrolytes of CXEs to provide multimolar concentrations of CO_2 can overcome these issues. Unfortunately, the clever design of electrolytes is not enough. For the electrochemical reduction of CO_2 to become an industrially relevant technique, the development of high current density electrodes is a critical milestone in the progression of this technology. Herein, we show the development and characterization of a gold-plated nickel Nobel Metal Foam (NMF) designed to increase current density for the CO_2 Reduction Reaction (CO_2RR).

5.1 Introduction

The environmental impact of CO_2 on the climate has led researchers to invest significant effort in innovative and sustainable processes for energy generation. The CO_2 reduction reaction (CO_2RR) has a wide distribution of products with selectivities that are strongly dependent on electrode material. Specifically, the CO_2 binding energy is particularly important when designing electrocatalysis for CO_2RR.[1] Three types of electrode materials are characterized by their primary product pictured in Fig. 5.1. The first are species where CO_2 strongly adsorbs the selectivity and efficiency for the production of CO (e.g., Au & Ag)[1–7] is very high. In contrast, the second type has weaker binding energies, and the selectivity of the reaction favors the formation of formate (e.g., Sn and Pb[1,6,8–10] or Bi.)[11,12] Finally, the third type balances strong and weak adsorption enabling C2 product formation.

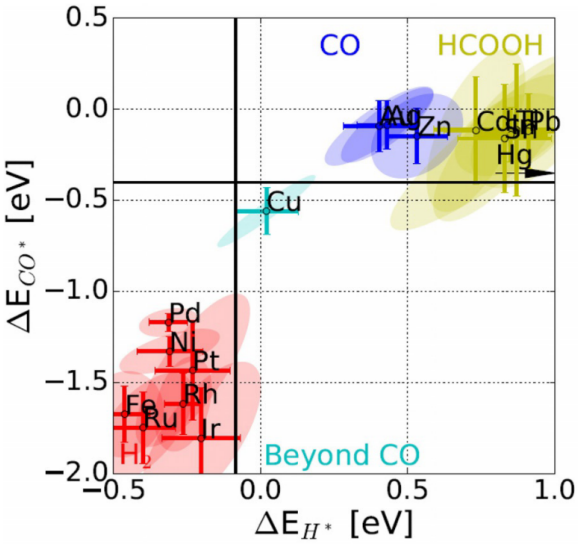

Figure 5.1: The binding energies of the intermediates can be used to separate the Cu metal catalyst into its own group, and hence, ex- plain the beyond CO* group. Where the beyond CO* group bind CO* while not having hydrogen under potential deposition. Furthermore, the black lines show the thermodynamics of adsorbed or none-adsorbed hydrogen.[1]

Enhancement of experimental parameters such as electrode material, substrate concentration, and electrolyte can be studied to optimize the performance and efficiency of CO_2RR. Surface engineering of electrode materials to tailor the selectivity of the reaction or lower the overpotential are common enhancements.[13–15] Investigating surface structure, particle size, and support material of electrocatalysts has increased the understanding of these systems[16]. However, when enhancing electrodes, researchers have chosen to maximize one of several performance metrics. Jhong *et al.*[17] has compiled a review of electrochemical catalytic publications and demonstrated that authors decided to optimize energy efficiency, faradaic efficiency, or current density. It is paramount

for the success of CO_2RR that, when developing catalysts, the optimization of each of these facets are considered. It is hypothesized that CO_2RR catalysts that produce CO as the primary product must reach current densities of 200 mA/cm^2 and have a selectivity above 90% to be considered industrially relevant electrocatalysts.[14]

Increasing the surface area of the electrode could produce CO at rates relevant for industrial applications, specifically on gold. Metal wires, bars, and foils can be shaped to provide as much surface area as possible but are still orders of magnitude smaller than those found in traditional catalysis. Traditionally, catalysis utilizes porous substrates with catalysts deposited onto them to achieve very high surface areas per gram. Taking inspiration from conventional chemical catalysis, we have developed a high surface area electrode by plating gold onto a nickel foam substrate. This class of high surface area electrodes are known as Nobel Metal Foams or NMFs. These foams provide a stable nanostructured electrode surface in various Nobel metal compositions, including Au, Ag, Ag-Pt, Au-Ag, and others.[16,18,19] NMFs are an excellent platform for electrocatalysts because the enhanced surface area provides easier access to active sites (such as defects and facets), yielding higher overall catalyst activity.[20,21] Moreover, the ability to control the molar ratio in multimetallic systems allows customization of the catalyst composition.[22] It is reasonable to consider that once the NMF is generated, many different types of traditional catalysts can be fixed to its surface. Du *et al.*[18] has mentioned that the unexplored potential of NMFs is due to the difficulty of tuning the nanoscale geometry of NMFs. Furthermore, they discuss the excellent control over noble metal nanocrystals, but difficulties in scaling to more macroscopic systems such as NMFs have proven challenging. Metal foams could be used as a framework to deposit other electrocatalysts, potentially further enhancing CO_2RR.

We have shown that we can grow structured gold dendrites on mesoporous nickel meshes. Additionally, we can tune the gold deposit's structure by changing the Ni foam's smoothness. This development can potentially circumvent the issues with using NMFs for large-scale electrocatalysis. We chose gold as a proof of concept for developing these foams. The main reason for this choice is that gold is selective in producing CO from the CO_2RR.[3,7] The high selectivity will elim-

inate the chance of losing current density to other side reactions and will allow us to accurately determine the catalyst's efficiency and current density toward CO production. In addition, nickel was chosen as a substrate because it is a commercially available foam that is relatively inexpensive.

The experimental setup for electroplating the gold on the nickel foam was reasonably straightforward. A single chamber aqueous electrochemical cell was set up with a sodium chloride supporting electrolyte. The concentration of the supporting electrolyte was 0.4 M to ensure the mitigation of migration effects. In addition, A 0.1 wt% solution of $AuCl_4$ was used as the source of the gold. The working electrode consisted of approximately a 1 cm^2 strip of Ni foam. That foam was cleaned in acetone and ethanol and dried thoroughly before use in the reactor. A platinum counter electrode was used to split water as the counter-reaction. The gold salt is very hygroscopic and requires fast work to measure the mass accurately. Finally, a saturated potassium chloride reference electrode was used as a reference. This reference was calibrated against the ferrocenemethanol redox couple to ensure no reference shifts occurred.

After the electrochemical cell was constructed, chronoamperometry experiments were conducted at a constant cell potential of 0.8 V vs. saturated KCl. The maximum time allotted on the CH instruments potentiostat was 600 seconds resulting in the chronoamperometry experiments being carried out twice to ensure proper coverage. The samples were then thoroughly washed in water. Dark discoloration of Ni foam indicated electrodeposition of the gold. The foams were dried in an oven overnight, then fixed to scanning electron microscope (SEM) stages, and further prepared for analysis.

5.2 Imaging and Characterization

Imaging through scanning electron microscopy provided information on the surface morphology of the gold-plated nickel foam. Fig. 5.2 shows the results of the SEM imaging done on a FEI versa 3-D dualbeam field emission/low vacuum scanning electron microscope. We can see that when we compare the bare nickel foam (Fig. 5.2, a) to the coated under similar magnification (Fig. 5.2, b), there is a significant change in the surface morphology. This is because the electrodeposited

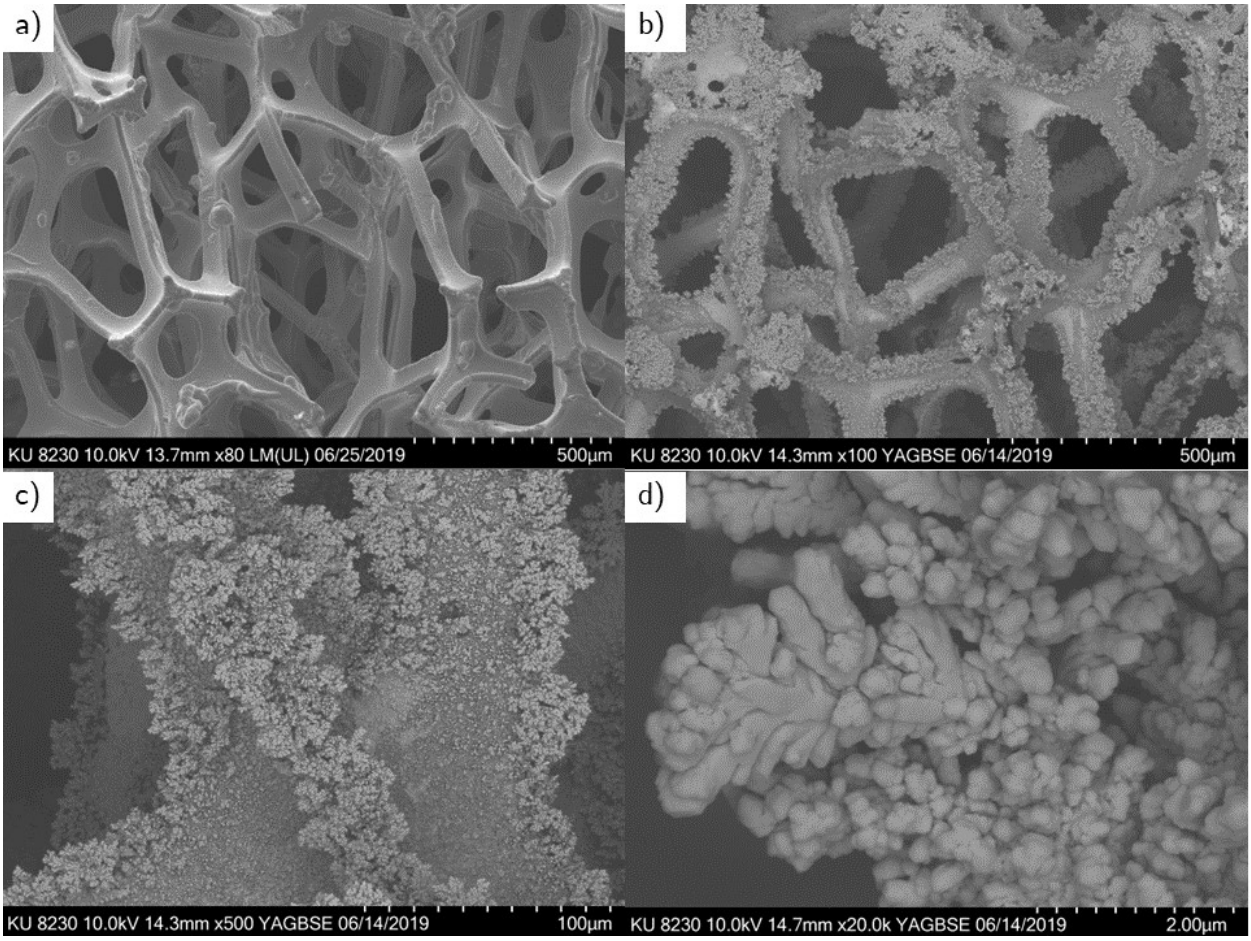

Figure 5.2: Scanning electron microscope (SEM) image of bare Ni Foam (a) vs. Au dendrites on a Ni foam at magnifications of 100x (b), 500x (c), and 20,000x (d).

gold has grown dendritic structures on the Ni foam. This result has taken a high surface area material in the Ni foam and further increased the surface area by depositing gold on the surface. An excellent view of the gold structure can be viewed in Fig. 5.2, d. where the size of the dendrites is approaching the nanoscale. The surface coverage also appears to be quite good and coating nearly all the Ni foam; however, some areas are left bare. The bareness could be due to that area being more smooth than the surrounding areas, so there are fewer nucleation sites for the gold to deposit.

Alongside SEM imaging, we can confirm the presence of gold on the foam using energy dispersive spectroscopy, an electron scattering technique used to determine the identity of atomic species. Fig. 5.3 shows the results from those experiments on a small area of the dendritic gold

foam depicting a high percentage of the surface coated in gold (92.8%). Additionally, the other components of the spectrum can be explained by adsorbed surface oxygen (<3%), uncoated Ni (<3%), and residual Na from the supporting electrolyte (<2%). This evidence shows that this is an effective method for the electrodeposition of Au on Ni foam and creating a high surface area NMF. The foam coverage is good; however, some places are bare. Appendix D1 shows an area of the foam that is not evenly covered by the deposited gold prompting an investigation into the condition of the surface on the structure of the electrodeposited gold.

From the SEM images of the foam before and after electrodeposition (Fig. 5.2 a & b), we observed preferential deposition and growth of dendrites near the edges of the foams. This preference may be due to the abundance of nucleation sites near the edge of the foam. To test this hypothesis, we etched the foam at various times in a solution of aqua regia. Three etchings were done on different samples before gold deposition. The times of the etchings were short to ensure that the significant structure of the foams remained intact. The first sample was etched for 30 seconds, the second for 60 seconds, and the third for 120 seconds. Then, using SEM to image the surface, we could see that they were progressively smoother as the etch duration increased. The images that led to this observation can be found in Appendix D2. The etching process reduces the roughness in the thicker portions of the structure rather than on the edges.

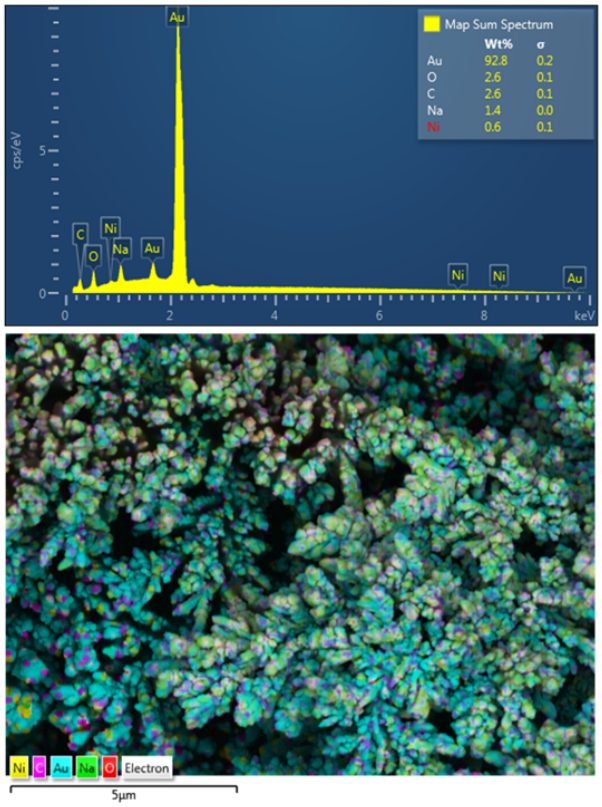

Figure 5.3: Results from EDS experiments on the dendritic Au plated Ni foam.

With this information, we electrodeposited gold on the smoothest surface. There was no observable change in the electrochemical behavior during the electrodeposition of the gold between

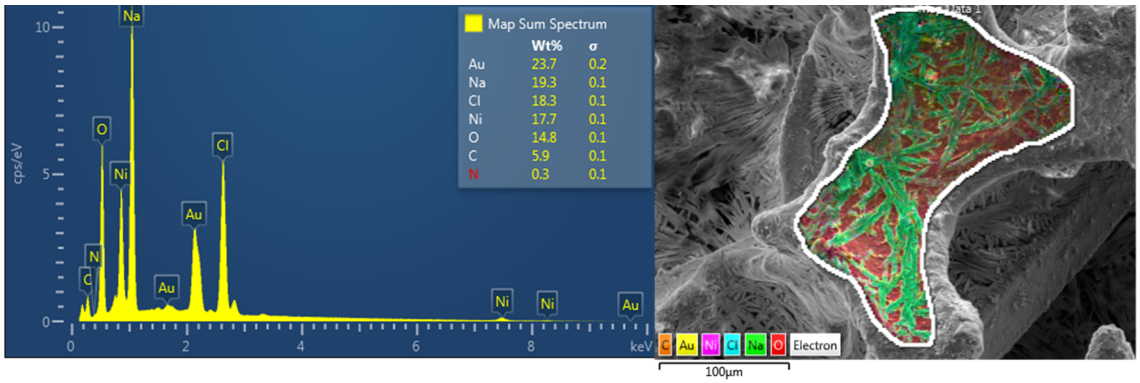

Figure 5.4: Results from EDS experiments on the dendritic Au plated Ni foam after etching.

the different etches. However, we observed a major change in the surface geometry. The surface went from being dendritic after deposition to having a "fuzzy" appearance. Otherwise, the surface resembled the uncoated Ni foam from lower magnifications. However, when the magnification was increased, we began to see that the surface of the foam had a substantial amount of NaCl crystals. This is most likely due to improper sample cleaning before preparation for SEM experiments. However, if surface contamination is neglected, a substantial amount is also present in EDS measurements. Fig. 5.4 shows that over the mapped area, the larger needle-like structures are identified as NaCl, but gold is also present in the sample. Unfortunately, the ion beam was unavailable, resulting in being unable to etch the surface to remove the contamination and determine the thickness of the gold layer.

5.3 Electrochemical Behavior

After the surface was characterized, the gold NMF was tested as a CO_2RR catalyst. As previously stated, gold electrodes almost exclusively produce CO as the product of the CO_2RR.[7,23] Additionally, it has recently been shown that exploiting the increased solubility of CO_2 in CO_2 eXpanded Electrolytes of CXEs can overcome the mass transfer limitations associated with traditional electrochemical systems. When this physical phenomenon is paired with the enhanced surface area of gold NMF, there is a general enhancement of the CO_2RR.

The electrochemical behavior of the dendritic gold was chosen to study due to the higher sur-

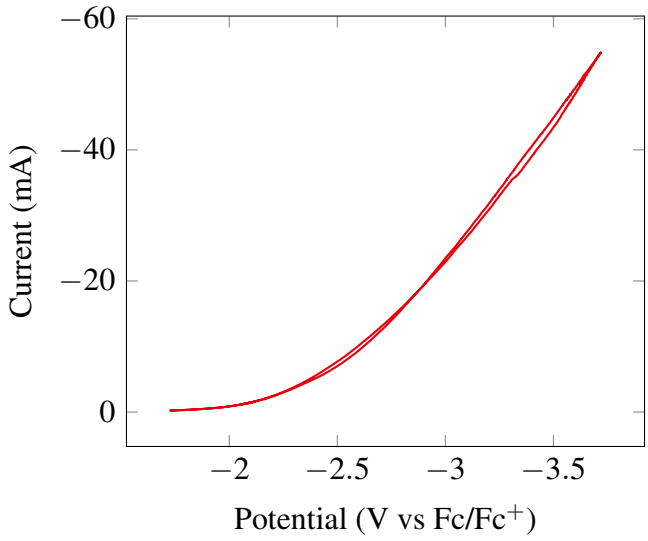

Figure 5.5: CO_2 reduction cyclic voltammogram on a Gold NMF at 30.21 bar of CO_2 headspace pressure at 50 mVs^{-}.

face area. The deposited foam was modified for the reactor by flattening a section of the foam in a vice. This created a sturdy surface to attach a gold clip that must be mounted inside the electrochemical cell. The electrochemical cell consisted of a modified Parr reactor to facilitate high-pressure electrochemistry. Cyclic voltammetry experiments were performed in tetrabutylammonium hexafluorophosphate-supported acetonitrile under 30.2 bar CO_2 head-space pressure with the NMF working a platinum rod counter electrode and a glass fritted silver reference electrode. The results of the cyclic voltammetry experiments are found in Fig. 5.5. We can see an onset potential of around 2 V vs. Fc/Fc^{+} reduction of CO_2 and high current density for a scan rate of 50 mVs^{-}. Further characterization can be done to determine the surface area of the NMF and allow us to more directly compare the performance of the catalyst to other catalyst for CO_2RR such as those outlined by Cossar *et al.*[20]. Additionally, the electrochemical methods outlined the work Cossar *et al.*[20] are electrochemical characterization of nickel foams. Potentially the double layer capacitance characterization could be used to determine the electrochemical surface area of the NMF.

5.4 Conclusion

Overall, the gold NMF looks like a quality candidate for electrochemical reduction of CO_2, and Ni foams are excellent substrates for developing high surface area electrodes. Unfortunately, the electrochemical characterization of this project is unfinished. Other more promising projects stole time from this work, and it was left without characterization of the catalyst's performance. If time permits, revisiting this work would result in a small publication that would include this catalyst's electrocatalytic performance and selectivity. In addition to the electrochemical characterization, further characterization of the pore size and the surface area of the electrode would be useful in some measurements of current density and other surface area-based performance metrics.

5.5 Supporting Information Figures

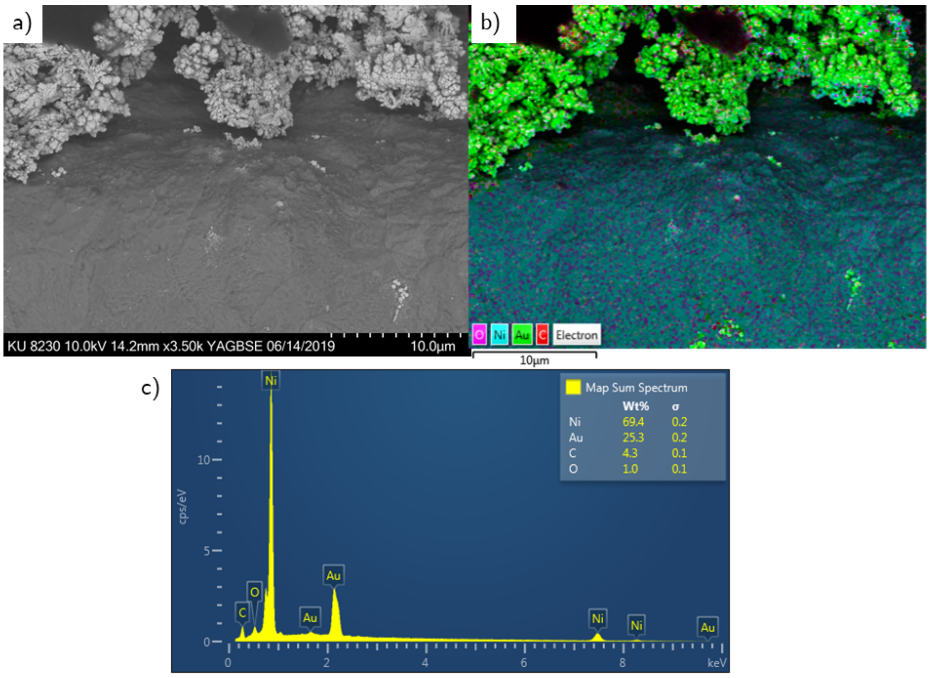

Figure 5.6: SEM image of a gap in the coverage of Au on a Ni foam (a) and the EDS elemental identification of the metals (b,c).

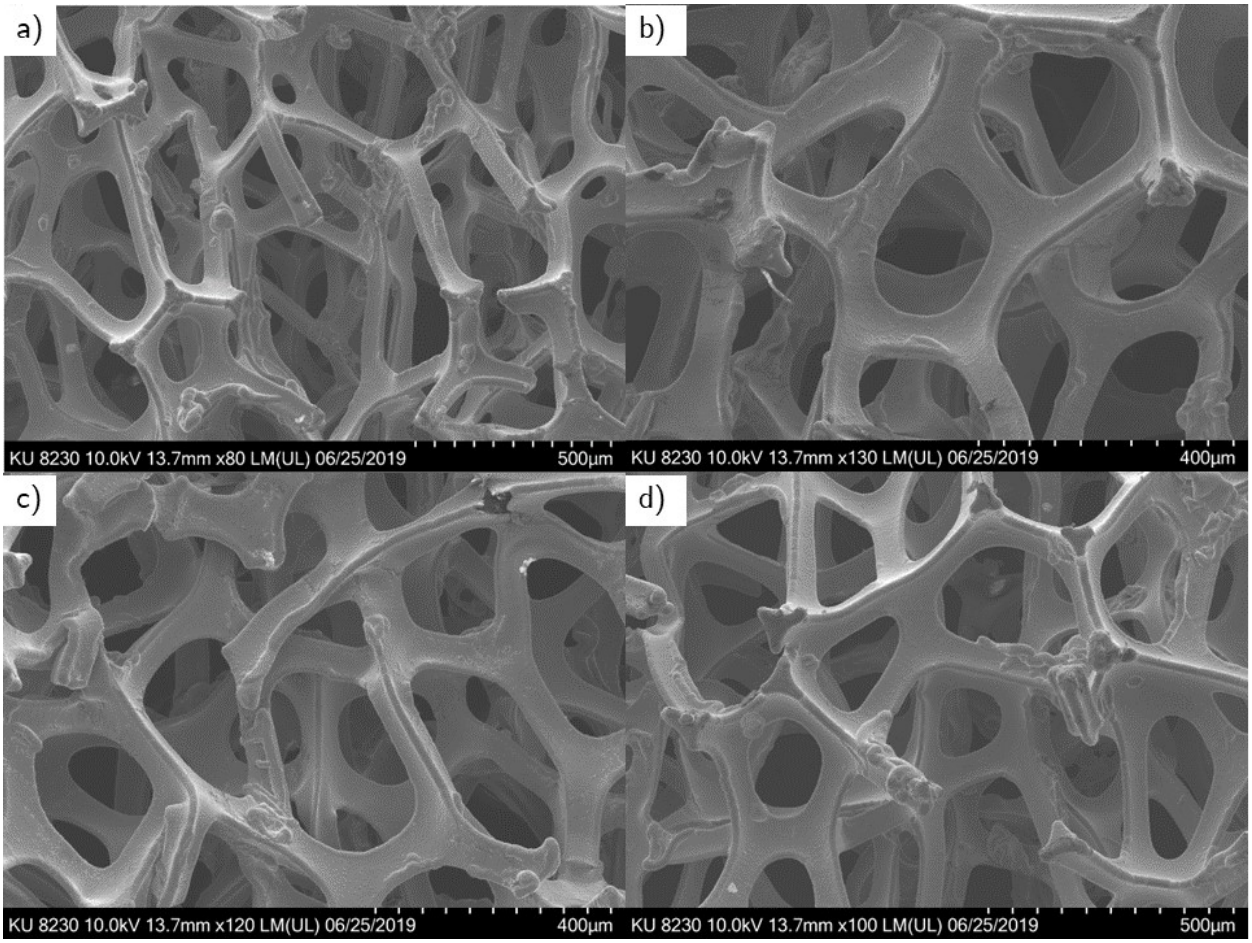

Figure 5.7: Scanning electron microscope (SEM) image of bare Ni Foam before etching (a) vs. etched in Aqua Regia for 30 s (b), 60 s (c), and 120 s (d).

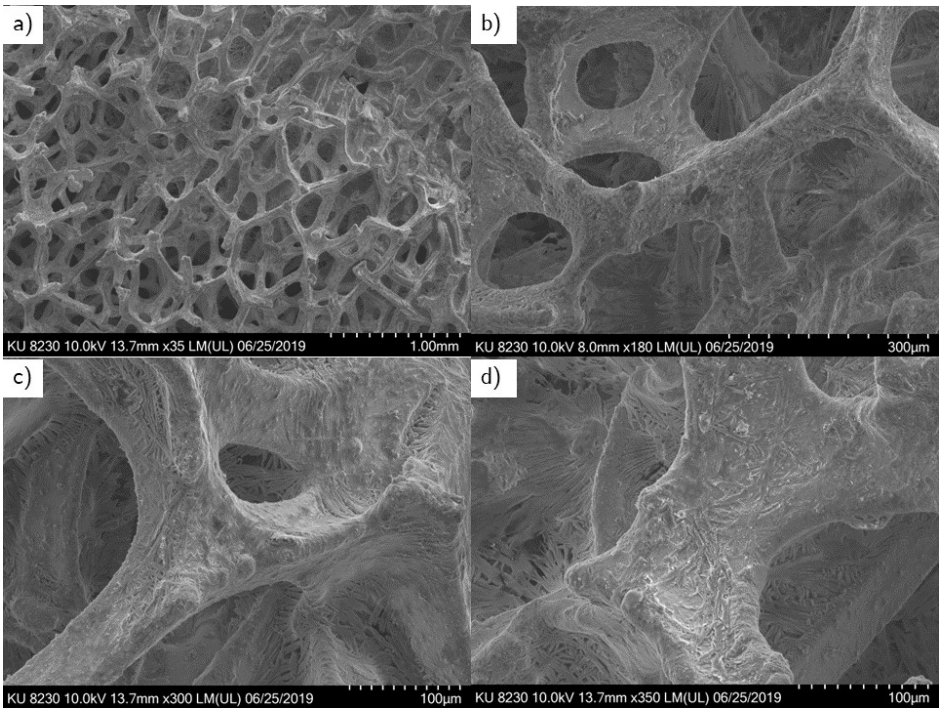

Figure 5.8: Scanning electron microscope (SEM) image of etched Ni foam after electrodeposition of Au at magnifications of 100x (b), 500x (c), and 20,000x (d).

.

References

[1] Bagger, A.; Ju, W.; Varela, A. S.; Strasser, P.; Rossmeisl, J. Electrochemical CO2 Reduction: A Classification Problem. *ChemPhysChem* **2017**, *18*, 3266–3273.

[2] Chen, Y.; Li, C. W.; Kanan, M. W. Aqueous CO_2 reduction at very low overpotential on oxide-derived au nanoparticles. *Journal of the American Chemical Society* **2012**, *134*, 19969–19972.

[3] Zhu, W. *et al.* Monodisperse Au Nanoparticles for Selective Electrocatalytic Reduction of CO_2 to CO. **2013**, *135*.

[4] Lucio, A. J.; Shaw, S. K. Pyridine and Pyridinium Electrochemistry on Polycrystalline Gold Electrodes and Implications for CO_2 Reduction. *Journal of Physical Chemistry C* **2015**, *119*, 12523–12530.

[5] Oberst, J. L.; Jhong, H. R. Kenis, P. J.; Gewirth, A. A. Insight into the electrochemical reduction of CO_2 on gold via surface-enhanced Raman spectroscopy and N-containing additives. *Journal of Solid State Electrochemistry* **2016**, *20*, 1149–1154.

[6] Zhang, W.; Hu, Y.; Ma, L.; Zhu, G.; Wang, Y.; Xue, X.; Chen, R.; Yang, S.; Jin, Z. Progress and Perspective of Electrocatalytic CO_2 Reduction for Renewable Carbonaceous Fuels and Chemicals. *Advanced Science* **2018**, *5*.

[7] Shaughnessy, C. I.; Sconyers, D. J.; Kerr, T. A.; Lee, H.-J.; Subramaniam, B.; Leonard, K. C.; Blakemore, J. D. Intensified Electrocatalytic CO_2 Conversion in Pressure-Tunable CO_2-Expanded Electrolytes. *ChemSusChem* **2019**, *12*, 3761–3768.

[8] Chen, Y.; Kanan, M. W. Tin oxide dependence of the CO_2 reduction efficiency on tin electrodes and enhanced activity for tin/tin oxide thin-film catalysts. *Journal of the American Chemical Society* **2012**, *134*, 1986–1989.

[9] Baruch, M. F.; Iii, J. E. P.; White, J. L.; Bocarsly, A. B.; Pander, J. E.; White, J. L.; Bocarsly, A. B. No Title. *ACS Catalysis* **2015**, *5*, 3148–3156.

[10] Zhang, S.; Kang, P.; Meyer, T. J. Nanostructured tin catalysts for selective electrochemical reduction of carbon dioxide to formate. *Journal of the American Chemical Society* **2014**, *136*, 1734–1737.

[11] Medina-Ramos, J.; Pupillo, R. C.; Keane, T. P.; Dimeglio, J. L.; Rosenthal, J. Efficient conversion of CO_2 to CO using tin and other inexpensive and easily prepared post-transition metal catalysts. *Journal of the American Chemical Society* **2015**, *137*, 5021–5027.

[12] Dimeglio, J. L.; Rosenthal, J. Selective conversion of CO_2 to CO with high efficiency using an inexpensive bismuth-based electrocatalyst. *Journal of the American Chemical Society* **2013**, *135*, 8798–8801.

[13] Yang, K. D.; Ko, W. R.; Lee, J. H.; Kim, S. J.; Lee, H.; Lee, M. H.; Nam, K. T. Morphology-Directed Selective Production of Ethylene or Ethane from CO_2 on a Cu Mesopore Electrode. *Angewandte Chemie International Edition* **2017**, *56*, 796–800.

[14] Lv, J. J.; Jouny, M.; Luc, W.; Zhu, W.; Zhu, J. J.; Jiao, F. A Highly Porous Copper Electrocatalyst for Carbon Dioxide Reduction. *Advanced Materials* **2018**, *30*, 1803111.

[15] Sen, S.; Liu, D.; Tayhas, G.; Palmore, R. Electrochemical Reduction of CO 2 at Copper Nanofoams. **2014**,

[16] Jones, J.-P.; Prakash, G. K. S.; Olah, G. A. Electrochemical CO_2 Reduction: Recent Advances and Current Trends. *Israel Journal of Chemistry* **2014**, *54*, 1451–1466.

[17] Jhong, H. R. M.; Ma, S.; Kenis, P. J. Electrochemical conversion of CO_2 to useful chemicals: Current status, remaining challenges, and future opportunities. *Current Opinion in Chemical Engineering* **2013**, *2*, 191–199.

[18] Du, R.; Jin, X.; Hübner, R.; Fan, X.; Hu, Y.; Eychmüller, A. 901945 (1 of 30) Engineering Self-Supported Noble Metal Foams Toward Electrocatalysis and Beyond. **2019**,

[19] Daiyan, R.; Ng, Y. H.; Lu, X.; Amal, R. Physical and Theoretical Chemistry.

[20] Cossar, E.; Houache, M. S.; Zhang, Z.; Baranova, E. A. Comparison of electrochemical active surface area methods for various nickel nanostructures. *Journal of Electroanalytical Chemistry* **2020**, *870*, 114246.

[21] Mistry, H.; Behafarid, F.; Reske, R.; Varela, A. S.; Strasser, P.; Cuenya, B. R. Tuning Catalytic Selectivity at the Mesoscale via Interparticle Interactions. *ACS Catalysis* **2016**, *6*, 1075–1080.

[22] Liu, W.; Herrmann, A. K.; Bigall, N. C.; Rodriguez, P.; Wen, D.; Oezaslan, M.; Schmidt, T. J.; Gaponik, N.; Eychmüller, A. Noble metal aerogels-synthesis, characterization, and application as electrocatalysts. *Accounts of Chemical Research* **2015**, *48*, 154–162.

[23] Hori, Y. *Electrochemical CO_2 Reduction on Metal Electrodes*; Springer New York, 2008; pp 89–189.

Chapter 6

Machine Learning for Catalysis Research

Abstract

The electrochemical reduction of CO_2 to form high carbon content compounds has long been a grand challenge in electrochemistry. Using carbon dioxide as a cheap and accessible feedstock alongside electrochemistry as a sustainable conversion technique offers the promise of sustainable hydrocarbon production. The chance to conquer this grand challenge and the current state of the global climate crisis has resulted in a truly monumental amount of research into using electrochemical methods to reduce CO_2 into valuable chemicals. This year, sixteen thousand papers have been published concerning the CO_2 reduction reaction. This immense body of work leaves scientists working in the area with the choice to either be buried in literature or fall behind in their knowledge of recent literature. The development of tools to overcome the vastness of recent literature is paramount to ensure that researchers are supplied with up-to-date information while still having time to conduct experiments. We have worked on the development of a machine-learning algorithm that uses natural language processing to extract relevant chemical information from text. This tool generates a database containing features such as reactants, products, and efficiencies that can summarize the literature information. Ideally, this tool would be used by researchers to filter out unwanted research articles providing them with papers that are the most relevant to their query. This optimization would significantly reduce the time required to catch up with current trends in literature.

6.1 Introduction

Machine learning (ML) is a field of study based on the design and development of software to make predictions, observe complex patterns, and in general, learn from the provided data.[1] As a tool, it has been used widely in medicine, materials science, and engineering as an automation tool for some processes.[2,3] Automating certain aspects of quality control and the speed at which ML can be done frees up a significant amount of resources for the industries that utilize them If similar ML tools were developed for the research space to read and annotate critical information, it would significantly reduce the time spent reviewing literature.

With the volume of work being produced regularly on the CO_2 reduction reaction (CO_2RR), it is a momentous undertaking for a researcher to stay up to date with the current literature.[4,5] Moreover, bringing new students and researchers up to a competent level of understanding in the state of the art can be even more challenging and require significant time investments.[6] Machine learning, specifically natural language processing (NLP), can alleviate some of the pain associated with traditional literature searches. In addition, developing NLP tools to read and extract relevant information from scholarly articles and organize the relevant information into a searchable database can increase the speed at which researchers can discover new information.

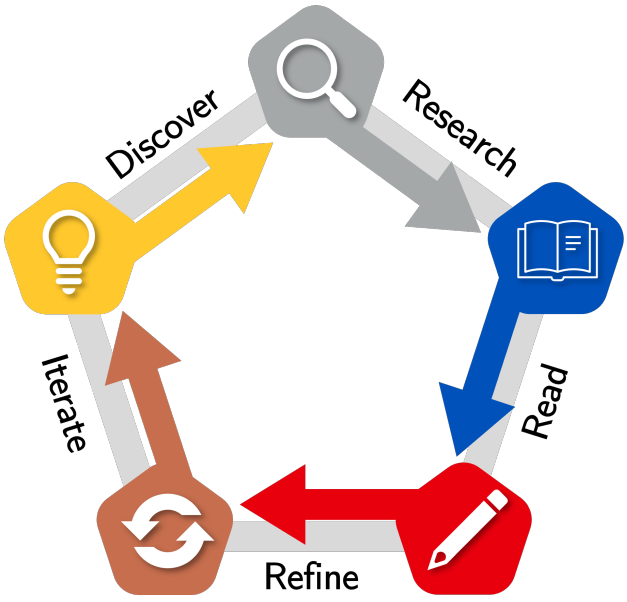

Figure 6.1: A graphical representation of a typical literature review cycle for research.

Traditionally the literature search process for scientific discovery proceeds down the pathway outlined in Fig. 6.1. Though there is nothing inherently wrong with this way of information discovery, the dense technical information in these papers can inhibit comprehension. In addition, if uninformed keywords are used, an inevitability for new researchers, the search results may not be

relevant. Finally, the time devoted to reading irrelevant papers can broaden a researcher's understanding; however, it is more likely to be a misappropriation of time. However, if ML was used to extract critical information from text, significant improvements over traditional literature searches could be made.

Experimental Parameters					Experimental Results	
Catalyst	Structure	Support	Electrolyte	Applied Potential	Major Product	Faradaic Efficiency
-	-	-	-	-	-	-
-	-	-	-	-	-	-
-	-	-	-	-	-	-

Table 6.1: Example database for the extraction of results from literature using natural language processing.

In electrochemistry, there are several parameters that experimentalists study as an intrinsic part of their research. As researchers, we are concerned with the products and reactants required for a reaction and the electrochemical cell construction.[6] For our ML tool's initial testing and development, the CO_2RR is used as a model reaction due to its popularity as a technique yielding a large dataset to train the model. This decision restricts the reactants to only include CO_2; however, CO_2RR is known for producing a wide range of products that will need to be identified by the algorithm.[7,8] Additionally, we are interested in the electrochemical construction of the cell. The electrochemical cell consists of electrodes, electrolytes, and supporting electrolytes. Researchers have been increasingly clever in developing a wide variety of electrode materials for the CO_2RR.[3] Therefore, for the model to be helpful, not only will the catalyst need to be extracted but also the structure and the support of the catalyst.[8,9] Furthermore, the supporting electrolyte and the electrolyte have often been referred to as co-catalysts in these systems. Therefore, it is necessary to extract the electrolyte composition from literature to replicate the experiments.

Additionally, we are also concerned with the performance of the catalyst. Several metrics are used to measure the performance of a catalyst, such as rate and selectivity; however, we will be looking at the faradaic efficiency and the selectivity of the catalyst. table 6.1 outlines the information the database would be able to extract and tabulate. From a user standpoint, the results would exist in a searchable database that can be sorted and filtered to study the reactions of interest. An

example query could be a copper catalyst that produce ethylene at faradaic efficiencies above 50%. This would return a literature survey that matches that criteria with the catalyst, structure, support, electrolyte, and potential applied. This set of literature search results would serve as an excellent initial literature survey for anyone looking to make ethylene on copper, massively cutting down on searching through online resources.

Unfortunately, the development process is not that simple. Many ML-based tools exist for other applications in the biomedical field and speech-to-text recognition; however, only recently have ML tools been developed for use in chemistry. The specific tool used to extract the information from the text is called natural language processing or NLP. NLP was developed at the intersection between artificial intelligence and linguistics in the 1950s; however, modern NLP borrows heavily from a diverse field of computer scientists, linguists, and statisticians.[10] We can use these NLP tools to tokenize, tag, and parse the textual information from a paper and output a entry to be included in the database. The process of tokenizing, tagging and parsing are outlined in Fig. 6.2 and this pipeline serves as the backbone for developing such a database.

As discussed previously, three main parts make up an NLP pipeline. First, tokenization is used to identify individual tokens (words or symbols) in a sentence. For our application, the tokens are words and line breaks such as returns or punctuation. Tagging or part of speech tagging (POS) is a step where the NLP model will tag parts of speech to each of the tags in a sentence and the useful features needed to populate the database table 6.1. These POS tags are critical in understanding the relationship between words in a sentence. Finally, the parsing or chunking of phrases is done. In this step, the model will identify phrases from the part of speech-tagged tokens. The model can then undergo Named Entity Recognition (NER). NER is a higher-level process where the words and phrases from the parser can be grouped and categorized as entities. The results from the NER will be what is processed to be included in the database.

Unfortunately, the utilization of NLP is often plagued by the vastness of natural language.[10] The unrestricted and ambiguous nature of how humans put together strings of words makes standardized text recognition exceedingly difficult. However, the formal language used in scientific

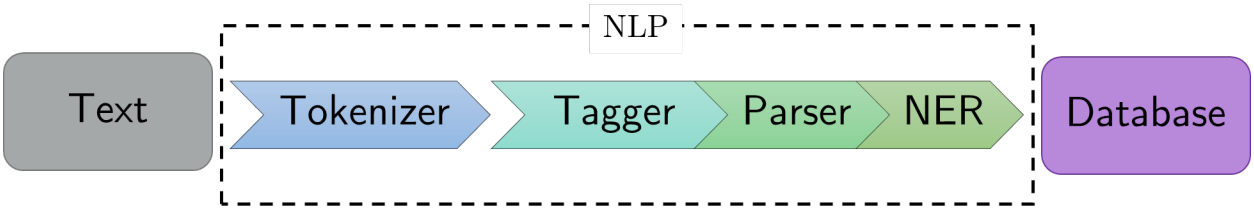

Figure 6.2: Natural language pipeline for taking textual information and outputting a database.

communication is better suited for NLP employment.[10] Additionally, the organization of chemical literature is fairly uniform. There are often sections of the text that contain information about the discussion in the section. The most useful information for researchers is often found in the abstract and the results sections. In addition to the ambiguity of non-standard language, other challenges are that few tools have been developed specifically to recognize chemical names and formulas. The NLP model has been trained to recognize the language of people that are not talking about chemicals or chemical structures. That means the model will have difficulty assigning the tokens to those tags due to its inadequate exposure to the chemical nomenclature. Fortunately, the Stanford Natural Language Processing group has trained a machine learning model on biological data that contains chemical names and formulas, giving an excellent starting point to build from. Outlining the reaction, parameters, and tools we will use to extract relevant chemical information from literature data sets up the groundwork required to approach this problem with a plan.

6.2 Results and Discussion

To understand the ML model's capability and get to know the specific changes, we will need to retrofit the existing model for our purposes, and a dataset needs to be assembled. This dataset needs to be representative of the CO_2RR literature; however, the search will be narrowed to heterogeneous electrocatalysis due to the volume of publications in this field. Further refinement of the literature was needed, and the digital nature of recent publications also led us to narrow the data of publications to those from the last 20 years. With those search parameters refined, the process underwent a similar approach to what is done in a traditional literature search. Online literature

search engines such as Google Scholar were used to accumulate papers that matched the search criteria. In total, 500 articles focused on CO_2RR were collected. There must be as many papers as possible to train the model on a large enough dataset. Unfortunately, we are limited by practicality. The curation and organization of those papers alone would require far too many resources. This is especially true since extracting text and processing the dataset for use in ML are not considered yet.

After the papers were collected, the time-intensive process of annotating the dataset began. To train the model on the types of words we expect it to tokenize and parse, it had to be given a subset of the data called a training split. The training split comprised 80% of the total papers while reserving 20% for testing. Next, we began tagging all the information that could be recognized as input for the database. Special attention was paid to special use cases and the ability to know that units or symbols usually have a number in front of them. For example, voltage and faradaic efficiency are numbers accompanied by V or % symbols, making them easily identifiable. Each of these small insights would help us better understand the nuances of how scientists report their findings across an entire field of electrochemistry.

After manually tagging the entire dataset, the model needed to be programmed to recognize chemical names and catalysts. This was done by using regular expressions to make a dictionary of terms that encompass most of the parameters and outputs of the dataset. This allowed the ML model to assign the proper tag to the string.

Once the model had regular expressions to assign tags to words. The model could then be run through the NLP pipeline. The training set was randomized and fed into the NLP pipeline, where it was tokenized into individual words instead of long strings of text. Those tokens were tagged using dictionaries of common catalyst materials and structures and common products we added in addition to those provided by the Stanford model. The tagging step also tagged the part of speech for each component of the sentence. The parsing step took the tagged data and unpacked its sentence dependency using the part of speech tags. This step allowed the ML model to identify the sentence structure and the dependencies of each part of speech. For example, the structure of

electrocatalysts is often a string of adjectives used to describe it. To have the model output all the adjectives, they need to modify the same noun. Finally, using the POS parser, the NLP pipeline can do NER, where it groups phrases based on their tag and part of speech.

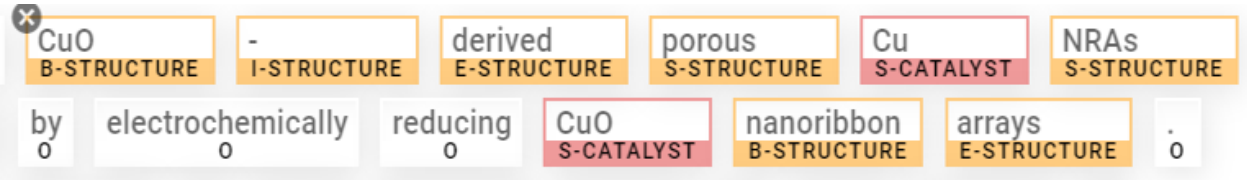

Figure 6.3: Example Named Entity Recognition parsing and tagging.

Fig. 6.3 shows an example of how the model can identify pertinent parts of literature. The model has been trained to recognize copper and copper oxide as potential catalysts in this sentence. In addition to the catalysts, it will also output CuO-derived, porous, and NRA's (nanorod arrays) as structural information about the copper catalyst. Furthermore, the NER portion of the model can group phrases associated with the catalysts. The grouping of the phrase is denoted in the tags as B, I, and E, plus the tag's name. Doing this shows the beginning (B), middle (I), and end (E) of the catalyst phrase. Unfortunately, it also recognized the precursor also as a catalyst and its structure. This is a common problem with NLP models, but it is solvable by optimizing the hyperparameters and using statistics to determine an importance of a specific string of words. Usually, a catalyst is mentioned in the abstract and multiple times in the body of the paper. Therefore, placing higher weight on phrases that recur in both places will have a higher chance of being the catalyst studied in the article.

After the model was trained and tested on the dataset, validation was done to determine the model's accuracy in tagging the relevant information. This particular iteration of the model had performed poorly due to inconsistencies in the tagging procedure. The vastness of the dataset required several individuals, each with varying levels of expertise in CO_2RR, to hand tag the information, resulting in inconsistent tags. Several passes through the tags were done to correct these errors to check each other's work and improve consistency. This effort overall improved the model; however, since there were so many tags, the testing set was re-evaluated by hand to ensure that the errors were from the model, not from human error. The addition of this validation step allowed

us to trust the results more, culminating in a database of annotated literature to be used for the development of ML for catalysis research.

6.3 Conclusion

This method for tagging and extracting the relevant data from a subject matter-specific paper was far more challenging than previously expected. Not only was it challenging to import and clean the text properly, but we had to develop separate tools for each respective journal we pulled papers from. Furthermore, tagging and checking the tags for human errors was arduous and time intensive. However, these efforts resulted in a model that learned how we talked about catalysts and was able to annotate a scholarly document to tag words that may be useful in developing a database. Unfortunately, this tool is not yet finished being developed. There is still work to be done to understand the tagged word's relevancy to extract the most useful information. We need to refine the model to add a statistical or word vectoring approach to determine the importance of specific phrases to the overall paper. Doing so will enable us to find the critical parts of the paper while leaving irrelevant information behind. One way this can be achieved is through different weights of hyperparameters. By making sections like the abstract and the results more heavily weighted in the word vector, the importance of catalyst terms found in those sections is much more likely to be the subject of the study. Furthermore, the most important parameters can be extracted and included in the database. Unfortunately, this step would also require insight from an expert in the field who read the paper and validate the results. Although there are still many steps in the long process of making such a versatile tool, we are hopeful that this technology can revolutionize how researchers conduct literature searches.

References

[1] Farris, B. R.; Niang-Trost, T.; Branicky, M. S.; Leonard, K. C. Evaluation of Machine Learning Models on Electrochemical CO2Reduction Using Human Curated Datasets. *ACS Sustainable Chemistry and Engineering* **2022**, *2022*, 10934–10944.

[2] Sun, Z.; Yin, H.; Liu, . K.; Cheng, S.; Gang, .; Li, K.; Kawi, S.; Zhao, H.; Jia, G.; Yin, Z. Machine learning accelerated calculation and design of electrocatalysts for CO2 reduction. *SmartMat* **2022**, *3*, 68–83.

[3] Goldsmith, B. R.; Esterhuizen, J.; Liu, J. X.; Bartel, C. J.; Sutton, C. Machine learning for heterogeneous catalyst design and discovery. *AIChE Journal* **2018**, *64*, 2311–2323.

[4] Malek, A.; Wang, Q.; Baumann, S.; Guillon, O.; Eikerling, M.; Malek, K. A Data-Driven Framework for the Accelerated Discovery of CO2 Reduction Electrocatalysts. *Frontiers in Energy Research* **2021**, *9*, 52.

[5] Chowdhary, K. R. Natural Language Processing. *Fundamentals of Artificial Intelligence* **2020**, 603–649.

[6] Zhang, N.; Yang, B.; Liu, K.; Li, H.; Chen, G.; Qiu, X.; Li, W.; Hu, J.; Fu, J.; Jiang, Y.; Liu, M.; Ye, J. Machine Learning in Screening High Performance Electrocatalysts for CO2 Reduction. *Small Methods* **2021**, *5*, 2100987.

[7] Hori, Y.; Koga, O.; Yamazaki, H.; Matsuo, T. Infrared spectroscopy of adsorbed CO and intermediate species in electrochemical reduction of CO_2 to hydrocarbons on a Cu electrode. *Electrochimica Acta* **1995**, *40*, 2617–2622.

[8] Guo, Y.; He, X.; Su, Y.; Dai, Y.; Xie, M.; Yang, S.; Chen, J.; Wang, K.; Zhou, D.; Wang, C. Machine-Learning-Guided Discovery and Optimization of Additives in Preparing Cu Catalysts for CO2Reduction. *Journal of the American Chemical Society* **2021**, *143*, 5755–5762.

[9] Chen, A.; Zhang, X.; Chen, L.; Yao, S.; Zhou, Z. A Machine Learning Model on Simple Features for CO2Reduction Electrocatalysts. *Journal of Physical Chemistry C* **2020**, *124*, 22471–22478.

[10] Nadkarni, P. M.; Ohno-Machado, L.; Chapman, W. W. Natural language processing: An introduction. *Journal of the American Medical Informatics Association* **2011**, *18*, 544–551.

Chapter 7

Hypothesis-Based Career Planning

Abstract

Every year 4 million students graduate with college degrees. Many of these students enter the workforce unaware of the breadth of career options available to them. Furthermore, students often hold inaccurate assumptions about various career paths, particularly for cross-disciplinary fields where job titles do not match the degrees, which can impede employment and add stress to an already stressful time. To help students more effectively navigate the transition from college to career, an educational curriculum called Hypothesis-Based Career Planning was developed and piloted at the University of Kansas for chemistry and chemical engineering graduate students. This curriculum aims to train students how to scientifically assess their assumptions and test hypotheses concerning potential career pathways, and provide strategies to bridge the communication gap between employers and themselves. Herein, we outline the tools and resources we have developed for the curriculum and how they can be paired with professional development skill-building to increase the likelihood of compatibility between students and their potential careers.

7.1 Introduction

Often college graduates leave their education under-prepared and under-educated about potential careers and the skills required to obtain their expected careers. The under-preparation has amounted to only a quarter of employers believing that college graduates are prepared for the workforce when they finish their education.[1]Unfortunately, college students are often unaware that they have not been prepared for the type of career they expect to obtain. Because they are unaware of the qualification needed for their potential roles, often students will accept positions that are below their level of education.[2] Fundamentally, this is due to the disjointed nature of the communication between professional environments and academics.

Currently, the responsibility of developing students to be career ready resides with career service professionals that are often employed through universities. Unfortunately, many students do not use these resources. Studies show that of the 69% of students that recognize the direct implications of career planning on finding a future occupation, only 15% actively participate in career planning exercises.[3,4] This effect is compounded since students also do not receive career planning advice from their academic advisors.[4] Missing out on these vital career resources leaves students without the necessary skills required in professional environments, leading to a long-standing problem faced by employers. For years employers have felt that recent graduates lack training in team building, critical thinking, team management, effective communication, and interpersonal skills.[1,5] To provide students with the best possible chance at securing the position they desire, institutional-level intervention in student career planning is critical.

Traditionally higher education emphasized the lecture format for educating students. Often these lectures are accompanied by assigned readings and tested by examination. Research has shown that this format of learning is largely ineffective, especially when it comes to a topic such as career planning.[6] Educational researchers have developed a host of more effective alternative teaching strategies, such as seminars, learning communities, collaborative assignments, and writing-intensive courses.[7] Applying these tools to career planning and education of career pathways can remove the apprehension of career planning and replace it with excitement

Students with advanced degrees in science and engineering find employment in a variety of careers. However, in recent years the production of graduate students has far outpaced the availability of typical careers for those students. As a result, students often accept post-doctoral positions to extend the time they can search for positions.[8] This pausing on the development of a career and lack of available positions has left a large body of highly skilled individuals dissatisfied with their occupations. Those looking for academic positions have recognized the decrease in prospective careers. Furthermore, those seeking other science-based careers feel unsupported and underprepared to pursue those careers. This leads to a high-stress environment for a well-trained and critical part of the scientific workforce. Advocates for advancing science have raised concerns about the general disregard for properly providing graduate students with the career planning required for their successful job placement. This high-stress environment can cause long-term damage to the production of highly educated scientists and engineers.

Two main gaps lie at the core of this issue. First, graduate students are unaware of the breadth of potential careers available to them. Secondly, these graduate students are undertrained in critical career planning, professional skills, or knowledge of area-specific skills to make a smooth transition into their intended careers. Additionally, in academia, the drive toward research-specific careers further compounds the inadequacies of career planning for graduate students. There is such an emphasis placed on discovery and the production of results that career planning and personal development could be seen as a distraction from the thesis or publication work. In today's ultra-competitive job market these students must be supported and empowered to make informed career decisions early in their training.

We have developed a framework for guiding students to self-discover viable career paths. Led by faculty, this curriculum gives structure to what has historically been an ad hoc process, giving students a way to systematically root out inaccurate assumptions about potential careers while also bridging the communication gap between professionals and academics. Overall, there are four stages to the curriculum, as outlined in Fig. 7.1. Initially, we educate the students on potential career paths and ask them to conduct research based on potential careers of interest to them. Then

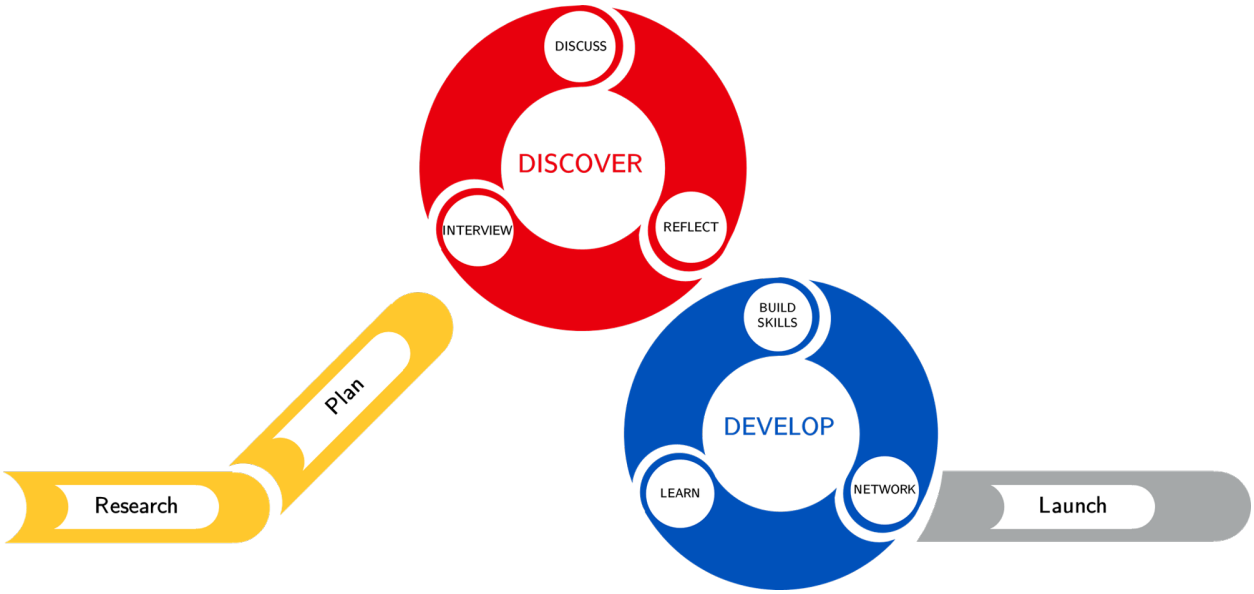

Figure 7.1: Overview of Hypothesis-Based Career Planning

we develop a plan with the students. In this step, students are generating hypotheses to test the careers they researched and are planning what professionals they would like to interview The students carefully select questions in this phase that will provide quantitative information to inform the hypotheses they need to test.

The next phase is the discovery phase where the students conduct short interviews with professionals of interest. After the interview, students are invited to discuss what they learned from the interviews with faculty and peers. Following the discussion, the students are asked to reflect on their discoveries and reassess their assumptions based on what they learned in the interviews. This process is iterative, and in each cycle, the students gain information about their future careers and potential jobs while also practicing to communicate with other professionals.

The final step in the process is the development stage. In this stage, students take the information gleaned from the discovery stage and apply it to their personal growth. This helps students seek out training for targeted skills—well before graduation—to prepare for careers of interest. From here students are also encouraged to network and stay connected to those contacts they made during the discovery phase. Building and maintaining a professional network allows the students to forge relationships that may help with job placement in the future. Ideally, this phase ends with

the successful launch of a student's career. However, this step does not end with the first job. Instead, we encourage students to continue to learn, build skills, and network to ensure that they are continuing to grow even as professionals.

7.2 Phase I: Research and Planning

To lay a proper foundation for students to understand their potential career paths, proper time and care must be put into the research phase. The time and effort that students contribute to this phase can help eliminate potential career pathways that are unlikely to match their interests. Furthermore, we formally introduce students to broad categories of careers to help them subdivide the immense amount of information available to search. These subdivisions for our audience of scientists and engineers consisted of four pathways: industrial, academic, governmental, and small business/entrepreneurship. These subdivisions encompass most careers that are available to the students and lay the framework for the first exercise, understanding assumptions.

Exercise 1: Addressing Assumptions We asked students to reflect on the career sectors that we grouped for them and come up with their assumptions solely based on the sector of the career. These assumptions ranged widely; however, a few assumptions were shared more often. The students agreed that governmental work was bureaucratic and structured, while in contrast, academic work was flexible but required other commitments like teaching and publishing. Additionally, industrial career assumptions tended to result in the assumption that there is no room for personal research interests. Finally, the small business/entrepreneurship was completely free to do as you wish; however, they assumed the venture was risky. These students were able to have a shared consensus on a few stereotypes related to potential careers and the purpose of bringing these assumptions out and onto paper is to address if they are factual.

This exercise serves as a primer for the students to think about what they know about a particular career path. From our experience, we see that the students we teach are most informed about academic careers because of their exposure as students to the inner workings of academia. However, often students are making career choices based on the assumptions they made in the previous

exercise. As the students begin to understand that they may not know what a professional in their discipline does, it opens up the discussion about the student's interests. Identifying their interests can be critical in comparing the offerings of different career pathways.

Exercise 2: Career Exploration and Development of Specific Assumptions Through this exercise the students were asked to use job search resources to research potential jobs of interest to them. Some guidance was given as to things to consider when doing these searches. For instance, a particular degree may have many different job titles so taking note of job titles and requirements can help illuminate the duties performed in that particular role. From these results, the students were then asked to develop specific assumptions based on the positions they researched.

This exercise is the backbone of the research phase. The establishment of the general assumptions and the realization that there are some aspects of their careers that they are unaware of help kick start the process that is career planning. The challenges for students in this exercise are complemented nicely with those from exercise 1. Students are not looking at the entirety of the available jobs for their degree and education level. Instead, they can narrow their focus to a specific range of careers and hopefully find real-world postings that outline potential duties that interest them. This strategy of reflection on job-search research through the lens of testable assumptions aims to improve concept retention. We emphasize that this is a process, and iteration on the cycle will only improve the outcome.

The next step in the planning phase is taking the assumptions the students made and developing hypotheses to test these assumptions. To train students how to develop a testable hypothesis, we explained in a traditional lecture format that hypotheses are statements that propose a possible explanation for some event or phenomenon. We use the if-then form to show the relationship between the result of a test and the implication of that result. A strong hypothesis should force us to think about the results we should expect from an experiment and should not just be a prediction. This distinction is particularly important when a hypothesis-driven approach is used in career planning otherwise the results are true or false and do not provide further insights. Furthermore, we want hypotheses to be quantifiable, relevant, specific, and testable (QRST). When we keep these attributes

in mind in hypothesis development for career planning we can get much more information from questions than yes or no information.

Exercise 3: Hypotheses Development Students were asked to develop QRST-style hypotheses for their assumptions by being as specific as possible based on several prompts. These prompts included if then examples for skills, culture/climate, time commitments, performance, and colleagues where we prompted students to analyze the many facets of a position that can affect the employee's outlook. These will serve as the testable hypotheses that we will be evaluating and reflecting on in the discovery phase.

To further support hypothesis development, we also discussed creating a value proposition, which is statement that expresses the worth of a product to the customer. In our case, the statement is to express the student's value to an employer. We introduced the students to the two main types of value propositions: pain-killers and gain-creators. The general idea is that pain-killing removes a negative feature from the company/employer while gain-creators supply something that adds to the existing company/employer. We had the students think about and reflect on what would an if/then statement look like if they were viewed as a pain-killer or gain-creator for an employer. This helped the student begin to think of themselves as an asset to an employer. This exercise also helps build communication skills, preparing students to more effectively communicate about themselves during job interviews.

7.3 Phase II: Discover

The discovery phase is fundamental in the development of the student's knowledge of actual job positions in their respective careers. In general, there are three major steps in the discovery phase: interview, discuss, and reflect. These three stages help students make the most of the interview as well as provide an iterative approach that helps them refine their assumptions and gives them opportunities to make new observations.

In the initial step of the discovery phase, students are asked to conduct interviews. To prepare the students for conducting interviews, we explained the components of an effective interview. We

started with perhaps two of the hardest tasks in a hypothesis-based approach to career planning, learning how to find and ask people for an interview. The students have information that they have collected in the research and planning phase that contains the information needed to find people employed in the careers they have an interest in. However, cold call interaction may not result in many accepted invitations for interviews. In general, the more interviews the students do in this phase the more informed they will be about all the potential career options for them. Thus, the goal for this phase is to conduct as many interviews as possible. We provided strategies to help increase the student's chances and many hinged on the establishment of commonality. A connection to someone can be as simple as sharing an alma mater with them or even a connection to another person. Furthermore, these connections could come from seeing someone at conferences to reading publications that are interesting. The basis of networking is being instilled within the students at this stage. It is paramount to their success at this stage that they do not get discouraged at a lack of response.

The strategies we used were general tips for communicating the interview properly. The students were instructed to ask for a minimum time commitment of 15 minutes, and they were given examples of good and bad practices for online correspondence. In general, we like the email to be short and to the point, and offers a low-pressure informational interview that can be used to find out more about what it is like to be a professional scientist. We also encouraged students to take time to develop their professional social media profiles, especially LinkedIn, to ensure discoverability and respectability online.

We then began preparing students for the interviews themselves. This consisted of general pacing and introductions, in addition to pre-planned questions and active listening feedback. A large emphasis was placed on the selection of questions to address the assumptions you made about the specific career you were interviewing. These questions should provide a route to insights that can be drawn from the position. If the hypothesis is asked directly, especially if it is one with a negative connotation, the interviewee may not provide a satisfactory answer. Otherwise, we made sure to express the importance of flowing conversationally from one topic to the next. By

doing this, the interview seems much less formal and can help everyone involved relax. Finally, we encouraged students to begin growing their network by connecting with them through professional social media and gauging interest in a longer format interview in the future.

After the interview, we invited the students to share what they had learned from their interviews. The central idea behind this is to have multiple inputs and points of view for the interpretation of the interviews. Additionally, if there was an overlap between students' interests, other students could potentially reach out to conduct a similar interview of their own. This stage also allowed the students to be held accountable. If they were not designating the time to conduct these interviews they could not contribute to the discussions.

The last stage of the discovery cycle is reflection. Students were asked to compile the information they learned from the interview and the discussion, and use the insights to iterate on their process. This instills the need to refine and learn about this process and provides a close to an uncompletable assignment. Their reflections may reveal new assumptions, new questions, and new pathways for investigation. The polishing and refining of this discovery phase will lead to deeper knowledge, better informing the next cycle.

7.4 Phase III: Develop

The final phase of hypotheses-based career planning is development. In this phase, a large emphasis is put on taking the information from the discovery phase and developing it into skills and building networks. Some of the questions we put particular interest in during the previous phase are questions regarding the skills employers are looking for in their prospective employees. Literature has shown that these are most often soft skills based on effective communication; however, in scientific communities, those skills can also be experimental techniques or software skills. This phase takes that information and focuses on building those skills so that the students are ready to meet the expectations of employers. In addition to building skills, this phase is also about the development of a professional network. Phase II laid the groundwork and stimulated the growth of the student's professional network, but in this phase, there is a larger emphasis on networking

for career goals, not just networking for answers. The final task in the Phase III loop is learning. It may seem like this entire process has been about learning. However, in this phase, the students are spending time learning about themselves and what skills they enjoy learning and building as well as what types of networking and communication they are most capable of. In this phase, we also ask students to be constantly pushing outside their comfort zone and understand that is where the most useful self-discovery can be found.

Since literature has reported that effective communication is often a weakness for new graduates, we emphasized the development of these skills in our students.[9] This was done through several exercises that focus on finding the most relevant information and then communicating it concisely and clearly to a non- (or less) technical audience. Being able to communicate your information without the need for any sub-context is an incredible challenge but gives the students experience in carefully choosing their words so that the message is as clear as possible. There are two main exercises that we employed to help our students grasp this concept. The first was half-life your message a communication transfer method developed by Aurbach *et al.*[10] and the second, a storytelling presentation style called PechaKucha.

Exercise 4: Half-Life your Message Half-life your message is a communication technique that was adapted from an improvisational prompt where the presenter iterates a single message over an ever decreasing amount of time.[10,11] Starting with 60 seconds the speaker describes a topic of interest. For our students, this topic was related to their research. That time then decreases to 30 seconds, then 15 seconds, and finally 8 seconds. Rapid iteration through the entire activity is desirable for two reasons. One, the pressure of presenting repeatedly limits the time for personal introspective and removes the embarrassment, judgment, and self-doubt an individual may experience in these types of exercises.[10] Additionally, delaying the next iteration can cause analysis of what should be said and inhibits the instinctual response from the presenter. After completing the exercise, students were asked to reflect on the outcome. It is important to remember that this is a message-discovery technique. The message that is conveyed may be vague or not necessarily correct but can serve as a starting point for further refinement. Aurbach *et al.*[10] propose that sev-

eral questions be asked as a follow-up to their experience: (1) Did you like your communicated message?, (2) Is your central message appropriate for the context of your communication?, (3) Did this exercise provide insight onto the critical information needed to support your central message?

This exercise was practiced a few times over the course of several months as a developmental tool for students to learn what the central idea is for their research at any given time. We understand that this type of communication can be challenging for an individual that has a lot of knowledge about a topic. Often, a presenter will incorrectly assume that the audience knows more information than they actually do. Thus, being able to limit the scope and develop a concise message for whatever type of communication being done is fundamental in effectively communicating. Additionally, this tool plays into the overall networking goals of the development phase so the students have a brief and targeted explanation of their research when meeting and networking with professionals. Additionally, this type of main idea searching can be used to discover a central topic and identify the critical information needed to support the topic when giving presentations.

Exercise 5: PechaKucha, Storytelling and Research PechaKucha is a storytelling technique where a presenter shows 20 slides for 20 seconds per slide where they can provide commentary. For our students, the ability to provide concise commentary about the purpose of their research while covering the breadth of the project, in a longer format than the half-life exercise, is crucial in networking. We employed the use of this storytelling technique to help the students plan and be deliberate about how they were to explain the breadth of their projects. Students assembled a 6-minute and 40-second presentation where the slides auto-advanced every 20 seconds. The students were given reference talks providing guidelines to follow; however, they were encouraged to personalize their presentations.

This exercise re-frames the traditional idea of a research talk. By relying heavily on pictures instead of text, the presenter captures the audience's attention with an engaging story. This type of presentation forces students to look at research presentations through the lens of storytelling, where an introduction is followed by rising action, a climax, and finally a resolution. The greatest challenge to our students was that they only had 20 seconds of commentary. Often, we saw students

present a picture of their results on each slide only to find that they did not have enough time to explain the important result that accompanied that figure. The strongest storytelling element came from the students who use the background image as supplemental or thematic information in their presentations. This prevented students from getting bogged down discussing details and allowed them to transition with the presentation, taking 5 minutes to briefly explain their research project.

This phase builds the skills necessary to stand out and network effectively in professional environments. The exercises we outlined in this phase are building blocks that help the students start to effectively communicate their message when developing a network of professionals. Ideally, this network of people is who our students will reach out to when they decide to enter the job market. These connections will be the launch pad and the skills learned and the fuel required for our students to launch their careers.

7.5 Conclusion

To summarize, hypothesis-based career planning is a curriculum that leverages the scientific method to help students find and prepare for a future job in the career best suited for them. It outlines clear and quantifiable assumptions and sets out to test those hypotheses in a way that furthers an individual's understanding of a career pathway. Each phase in the process iterates on itself and builds off the previous phases. In the research and planning phase, students learn about available career options of most interest to them. This stage clarifies their initial assumptions and forms a plan to test hypotheses. From this stage, the students begin to seek out professionals to answer their questions and begin to develop a better idea of what a career looks like. Additionally, self-reflection and peer discussion allow for new insights and hypotheses to be formed and further tested in a cycle that builds into a corpus of information. That information serves to direct skills that need to be developed and the relationships that need to be fostered in the development phase. Here, the students take the time to invest into skills and networking to develop into marketable professionals and establish contact with potential employers. Networking can provide students with more insight into skills to learn and refine until the students are ready to launch their careers. However, this is

not the termination point, learning and further developing their professional network and skills continue, ensuring a well-developed network is maintained over time, with the necessary skills to transition into future positions of interest.

References

[1] Associates, H. R. Falling Short? College Learning and Career Success. *NACTA Journal* **2016**, *60*, 1–6.

[2] Fox, K. F. Leveraging a Leadership Development Framework for Career Readiness. *New Directions for Student Leadership* **2018**, *2018*, 13–26.

[3] Despeaux, J. M.; Knotts, H. G.; Schiff, J. S. The Power of Partnerships: Exploring the Relationship between Campus Career Centers and Political Science Departments. *Journal of Political Science Education* **2014**, *10*, 37–47.

[4] Stebleton, M. J.; Kaler, L. S. Preparing College Students for the End of Work: The Role of Meaning. *Journal of College and Character* **2020**, *21*, 132–139.

[5] Mosca, J.; Curtis, K. New Approaches to Learning for Generation Z. *Journal of Business Diversity* **2019**, *19*.

[6] Afonso, A.; Ramírez, J. J.; Díaz-Puente, J. M. University-Industry Cooperation in the Education Domain to Foster Competitiveness and Employment. *Procedia - Social and Behavioral Sciences* **2012**, *46*, 3947–3953.

[7] Kuh, G. D.; O'Donnell, K.; Reed, S. Ensuring Quality and Taking High-Impact to Scale. **2013**, 1–50.

[8] Fuhrmann, C. N. Enhancing graduate and postdoctoral education to create a sustainable biomedical workforce. *Human Gene Therapy* **2016**, *27*, 871–879.

[9] National Academies of Sciences, E.; Medicine,, *et al.* Communicating science effectively: A research agenda. **2017**,

[10] Aurbach, E. L.; Prater, K. E.; Patterson, B.; Zikmund-Fisher, B. J. Half-Life Your Message: A Quick, Flexible Tool for Message Discovery. *Science Communication* **2018**, *40*, 669–677.

[11] Hall, W. *The playbook: Improv games for performers*; Fratelli Bologna, 2014.

Chapter 8

Conclusions and Future Work

This work has showcased the range and capability of CXEs for organic electrosynthesis. These electrolytes have provided access to chemistry that has not been available through traditional electrochemical techniques and facilitated selective carboxylation of acetophenone. Forming C-C bonds using high-pressure electrochemical techniques has improved the selectivity and overcome the mass transfer limitations associated with traditional electrochemical systems. Furthermore, we were able to study the relationship between CO_2 concentration and the kinetics of the reaction. These CO_2 concentration studies provide fundamental insights into the role of CO_2 availability in the carboxylation reaction. We discovered that the selectivity of the acetophenone carboxylation reaction is highly dependent on the concentration of CO_2 in the liquid phase. At CO_2 concentrations less than 0.1 M the reaction favored the production of 1-phenylethanol; however, increasing the concentration to 1.7 M and above led to the selective production of atrolactic acid. The formation of atrolactic acid at these modest CO_2 concentrations resulted in moderated rates and efficiencies toward the production of the carboxylated product. As the concentration increased the rate and selectivity of the reaction also increased until it reached a maximum at 28.8 bar CO_2 pressure. Higher CO_2 pressures resulted in a decrease in reaction performance over the 12-hour bulk electrolysis experiments.

These initial studies provide insights into how the CO_2 availability dramatically influences the selectivity of the reaction. For the first time, we were able to show concentration effects on the kinetics of the electrochemical carboxylation of acetophenone. These studies provided fundamental insight into the trade-off between CO_2 availability and electrochemical kinetics. The existence of an optimum CO_2 pressure demonstrates that the interaction between the chemical kinetics, which depend on CO_2 availability, and the electrochemical kinetics, which depend on the electron transfer rate, produce a complex environment for electrochemistry. In traditional electrochemical systems, this kinetic information is available through calculation. However, for irreversible ECE systems, the coupled chemical and electrochemical kinetic information is unavailable to us. To further investigate the kinetics of the electrochemical reduction the finite element analysis model was required to deconvolute the mass transfer and kinetics. This model was designed to better understand the

coupled chemical and electrochemical kinetics of acetophenone reduction and regress their values. The simulation of this system showed that the optimum behavior was due to changes in the properties of the electrolyte at high CO_2 concentrations. The changes in the microenvironment manifest as decreases in the rate of the electrochemical kinetics. As the solution became more like liquid CO_2, the ability to transfer charge became more difficult due to the dominating nature of the non-polar CO_2.

These insights further informed future experimentation. It is worth studying the ohmic resistance as a function of CO_2 pressure to ensure that the electrolyte is properly facilitating electrochemistry. It will be useful to look at how the decrease in the ionic strength of the electrolyte as a function of CO_2 pressure affects the electrochemical kinetics. This experiment is in progress and is using metallocenes to measure the kinetics as a function of both CO_2 pressure and electrolyte concentration. However, it is recommended to conduct experiments at constant ionic strength to ensure that any effects on electrochemical kinetics are directly related to changes in the solvent polarity.

Additionally, we studied a structure-property relationship for aromatic ketones and alkenes in acetophenone and styrene respectively. We found promising electrochemical behavior for each of the starting materials; however the solid formed after carboxylation was challenging to characterize. We hypothesized that this could be due to the magnesium salt of the product being stubbornly insoluble. Previous experiments have shown that magnesium salts of organic molecules can be difficult to dissolve resulting in similar struggles to characterization. The first step in re-evaluating this structure-property relationship is to revisit the sacrificial counter electrode. There are several suitable anodes for us to experiment with other than magnesium that give a variety of valencies such as zinc, tin, and aluminum. The carboxylic salt of these different counter ions could potentially be more easily protonated by the strong acid.

In addition to revisiting the sacrificial anode, we can further expand on the structure-property relationship for both styrene and acetophenone. The trifluoromethyl acetophenone exhibited an interesting effect on the voltammetry when compared to the acetophenone. The strongly electron-

withdrawing group of the trifluoromethyl shifted in the onset potential to less negative potentials providing evidence that substitutents can affect the potential of the reduction. However, the positive shift was not as great as expected offering the promising prospect of being able to study proton-donating groups without exceeding the stability of the electrolyte. The changes we would expect to see in the voltammetry is a more negative shift in the onset potential due to the enhanced stability of adding an electron-donating group. Unlike trifluoromethyl acetophenone, we would expect that the rate would be similar to what was seen in acetophenone since it depends on the first electron transfer rather than the rate of carboxylation.

Expanding the structure-property relationship study to proton-donating molecules like isobutylacetophenone could provide a direct electrochemical synthesis of ibuprofen. Developing electrochemical synthesis techniques for traditional chemical synthesis techniques can further enhance the sustainability of these processes. If an electrochemical route toward producing ibuprofen was found to produce ibuprofen at reasonable rates it could serve as the start of a paradigm shift in sustainable chemical production. Isobutyl acetophenone to ibuprofen electrochemically would remove the need for both Raney nickel and palladium catalysts as well as the use of carbon monoxide as a carbon source. This synthesis technique would traditionally provide both a reduction in the requirements necessary for the reaction and also utilize CO_2 as a carbon source raising the standard of sustainable chemical production.

With more time and the addition of new solvents for CORR, it would also be worth revisiting the noble metal foam electrode work. Preliminary data yielded promising results for its use as a catalyst; however proper characterization is necessary to characterize the performance. Bulk electrolysis experiments at various CO_2 headspace pressures must be conducted to generate CO. Then a sample of the headspace will be collected and analyzed through GC. This data would provide the pressure-dependent behavior of the catalyst, the product selectivity, and the production rate. Ideally, we would also develop an inline sensing technique to measure the production of gas phase products as a function of time rather than having to collect the gas and analyze it in a separate GC. Inline sensing would be useful in determining the accurate rate of formation for the gas phase

products without any losses to the environment. Additionally, using a mass flow controller for the inlet of the CO_2 would allow us to do a carbon balance on the system. To date, the efficiency of the reactor has remained at around 75%. It is worth looking into how carbon is utilized in these systems to show the carbon conversion efficiency as well as the Faradaic efficiency.

Overall, we have demonstrated that CXEs are an exciting electrolyte for both CO_2 reduction as well as CO_2 utilization through C-C bond formation. The pressure tunable concentrations of CO_2, reaction rates, and selectivity provide a unique environment for organic electrosynthesis. Further exploration of the formation of carboxylic acids and the potential to synthesize NSAIDs electrochemically could open the door to the utilization of electrochemistry as a replacement for traditional chemical synthesis techniques. CO_2 eXpanded Electrolytes provide a new and exciting environment to conduct electrochemistry and are on the cusp of CO_2 utilization and chemical synthesis making them a unique media capable of facilitating new and innovative chemistry.

Appendix A

Standard Operating Procedure and Troubleshooting Guide for High Pressure Electrochemical Reactors

A.1 Introduction

The purpose of this document is to outline the procedure to successfully set up and operate either the 20 mL or 50 mL Parr®style high pressure electrochemical reactors. In addition, this document will serve as a database of parts and equipment needed to replace and maintain the vessel.

A.2 Reactor Components

The reactor consists of three main parts. The first is the reactor cap shown in Fig. A.1. This reactor cap contains several ports that are used for stirring, electrochemical sensing, and pressure and temperature monitoring. The central port is where the Parr magnetic drive is located. The drive installed on the current iteration of the reactor s a general purpose drive with a 3/16" in shaft diameter for use in reactors 25 mL to 2 L.

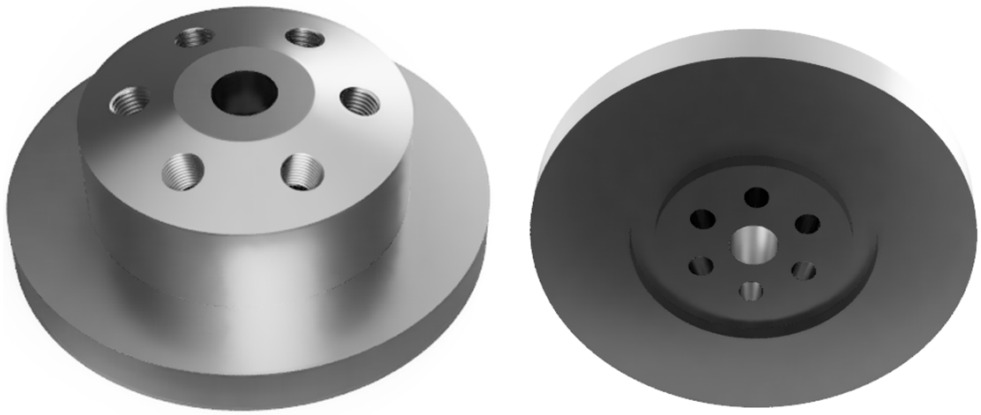

Figure A.1: Render of the Electrochemical Reactor Cap.

Of the ports on the exterior, one is dedicated as an inlet/outlet for the CO_2. If we follow the linkage for the inlet of CO_2 from the high pressure tank, the CO_2 must go through a three way

valve that is used to allow CO_2 into the system or, in its other position, to exit the system. Along that same linkage there is also a valve to control the flow of CO_2 into the reactor as well as a spring loaded pressure relief valve to ensure the system is not overpressurized.

Another port is dedicated to sensing equipment. There is a standard k-type thermocouple 1/16' in diameter connected through a linkage and a three way connector with an omega pressure transducer (PX309-100GI). Both the temperature and pressure data are monitored through a Labview VI.

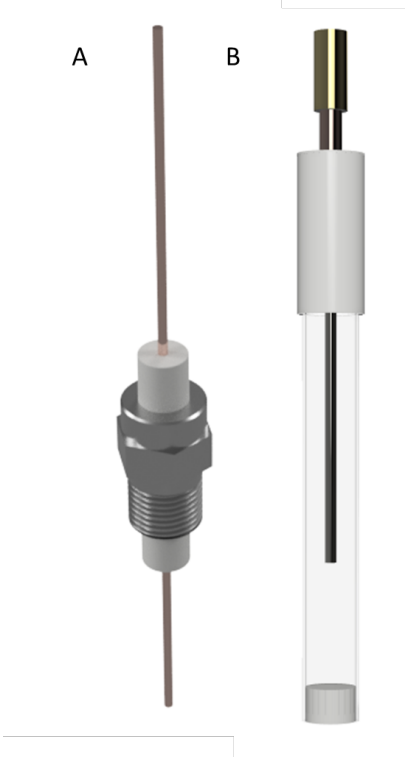

Figure A.2: Render of the Electrical Feedthroughs A and Render of reference electrode B.

Finally, the remaining four ports are where the electrodes will be present. Each of the remaining ports will have a CeramTec (2846-01-A) high pressure electrical feedthrough to connect the electrodes as seen in Fig. A.2, A. One of these feedthroughs is dedicated to the reference electrode. In our reactor the reference electrode has a different connection necessitating its specific assignment to a feedthrough. The reference electrode consists of a silver wire in a fritted glass chamber. The fritted chamber is custom made through a glass blower. The connection is made using a gold

pin and socket connector (VEAM CIR Series Connectors 27961-12) where the socket is soldered onto the feedthrough before installation. Otherwise the electrodes are fit over the 1 mm diameter copper feedthrough wires using gold crimp style clips (Digi-Key 66504-4) however I would recommend upgrading to a similar method to the reference to potentially increase reliability of the setup. To ensure that the electrodes are not grounded to the inside of the reactor cap, PTFE straws were placed in each opening as insulators.

The bottom of the reactorFig. A.3 and the clamps to hold it together are as purchased through Parr®. However, an additional glass liner was purchased and has been used (Parr-1431HC). A PTFE option is available if there is an environment that it would be required (Parr-1431HCH) The reactor rests in a double pass heat exchanger to regulate the temperature of the reactor. The temperature regulation is done by an isothermal water bath.

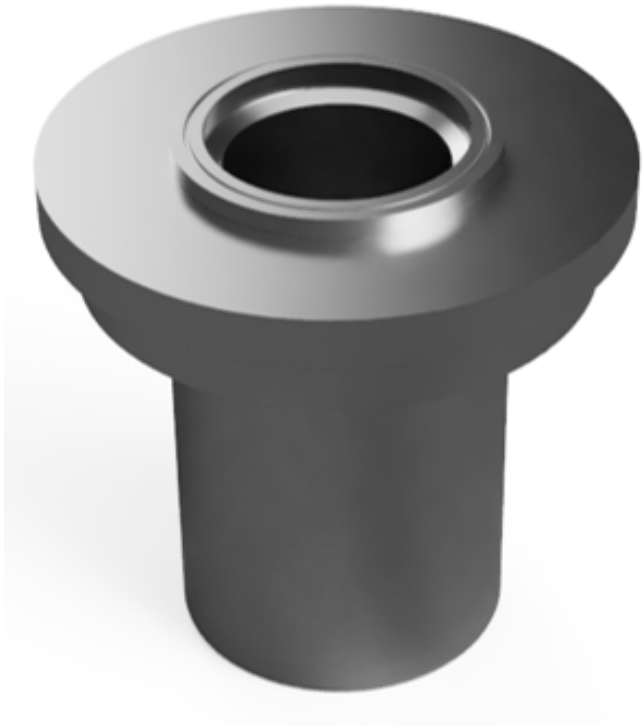

Figure A.3: Render of the base of the electrochemical cell.

A.3 Operating Procedure

1. Gather electrodes for testing. It is recommended if there is an unused placement for an electrode place another working electrode in its place to add redundancy.
2. Polish electrode surfaces using high grit sand paper.
3. Ensure gold clips are securely fastened to the lead of the electrode. If there is no gold clip attached remove one from the bag place the winged portion into the mouth of a pair of needle nose pliers. Then place the lead of the electrode into the winged potion and clamp down hard. Afterward, remove the crimped electrode from the pliers and re-crimp the newly flattened side of the electrode to ensure the clamp is tight.
4. Each of the electrodes aside from the reference electrode can be placed in on their feedthroughs at this time. The gold clip will slide over the copper wire of the feedthrough making a solid connection. Make sure the the wings of the clip do not open wide enough to make contact with the reactor cap.
5. (Optional) If it is desired to maintain rigorously dry conditions a glove bag will need to be used at this time. The glove bag needs to be purged for 30 minutes prior to experimentation so plan accordingly. Each component of the reactor should be placed in the glove bag including pipettes, electrodes, reactor cap and body,electrolyte solution, and clamps. Let the bag fill for 10 minutes and vent the bag. Repeat this twice to ensure the atmosphere is argon.
6. Fill the reference electrode with a small amount of the electrolyte solution and carefully place it into its position on the reactor cap.
7. Fill the electrochemical cell with the remainder of the pre-allocated amount of electrolyte. If the amount required is unknown consult the expansion curve associated with that solvent.
8. Ensure the electrodes are both clear of the stirrer and positioned away from the walls of the cap by first spinning the stir bar. If no electrodes make contact with the stir rod rotate the reactor cap upside down to get the best view of the electrode positions. From here ensure that they are evenly spaced away from the walls of the feedthrough holes. Also make sure

that each of the electrodes are positioned inside the ring containing the PTFE disk on the cap. This will ensure smooth insertion into the reactor body.

9. Brace your elbows on the laboratory bench and position the cap above the reactor body containing the electrolyte. Slowly lower the cap of the reactor onto the bottom of the reactor. I use the thermocouple as a guide to ensure the electrodes are not moving into another position on insertion. Once the cap is resting on the body of the reactor begin seating the top to the bottom. They should thud into place when seated.
10. Prepare the clamps to be placed onto the reactor by loosening each of the bolts on the top of the clamp. It should slide into place on the reactor. Begin tightening the bolts until snug in an alternating pattern and continue this pattern until bolts are snug but not over tightened.
11. Ensure the valve for the outlet of the CO_2 is closed to preserve the atmosphere.
12. Deflate and remove the reactor from the glove bag. The resulting reactor setup should look like Fig. A.4

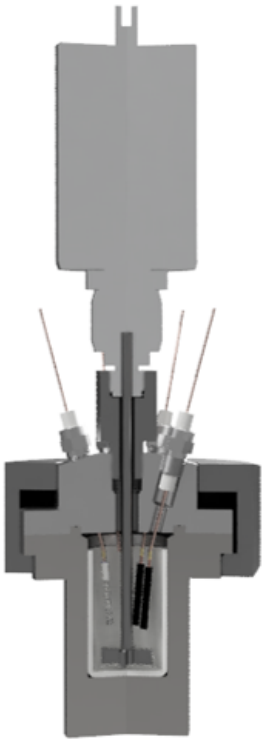

Figure A.4: Render of the base of the high pressure electrochemical reactor assembly.

13. Place the reactor into the isothermal jacket and connect thermocouple, pressure sensor and gas inlet conections.

14. Begin running the LabView document by either opening the Large Reactor.vi found on the desktop of the lab computer or if it is already open pressing the small white run arrow in the upper left corner of the VI.

15. Turn on the isothermal bath by pressing the enter button on the front of the machine twice . Wait for the machine to start up. The low water alarm is malfunctioning for the isothermal bath so after 30 seconds it will begin beep indicating low water. Manually override the alarm and continue the setup.

16. Lift the black tube on the stirrer motor and rotate the stirrer motor into position over the top of the reactor. Slide the Black cylinder over the stirrer.

17. Pressurize the reactor to the desired pressure slowly by turning the small valve on the inlet stream. Vent the reactor several times to ensure that the air in the lines is purged before experimentation.

18. Pressurize the reactor to the final pressure and flip the switch on the stirrer control box to enable stirring. If the stirring is too rapid or too slow adjust the dial; however, be cautious because it is very sensitive.

19. Attach the potientiostat leads to the reactor. Green is the working electrode and should have blue also connected, red is the counter electrode and should have orange also connected and finally white is attached to the reference electrode.

20. Wait for equilibrium pressure to be reached. The time to reach equilibrium depends on the pressure but the inlet stream needs to be shut off and the valve be tightened to test equilibrium. After cutting off the supply of CO_2 wait and watch for the pressure to drop. If it does not drop or is the pressure you anticipate then the reactor is ready for experimentation.

21. Electrochemistry is done using the Gamry software suite. The specific software for electrochemical experiments is the Gamry Framework. To ensure your data is saved correctly open

the path dropdown and under the data box input the location of the folder where you would like your data saved.

22. Turn off stirring and test for the Ferrocene/Ferrocenium redox couple by selecting the Cyclic voltametry experiment under the experiments drop down menu and scanning from 0 to 1 V. If the redox couple looks wrong see troubleshooting information.
23. Perform other experiments through the experiments tab such as EIS and chronoamperometry.
24. (optional) If gas phase analyis is required, a small length of wire rests below the reactor and is to be attached to the outlet of the reactor three way valve. Gather the large gas cylinder and pump down the contents of the cylinder to high vacuum.
25. (optional) Attach the gas cylinder to the outlet and vent the contents of the reactor into the cylinder. Keep stirring this entire time and wait until it reaches equilibrium again.
26. After gas sample is collected, vent the remaining contents of the reactor headspace slowly to avoid excessive bubbling of the electrolyte and wait until degassed.
27. Leaving the outlet valve open disconnect and remove the reactor from its isothermal jacket and place it on the bench.
28. Loosen the bolts and disassemble the reactor.
29. Clean each of the reactor components with acetone thoroughly.
30. Press the enter button on the isothermal bath to shut it down.
31. Press the red stop button on the labview to stop the run.

A.4 Troubleshooting

Problems setting up the reactor are very common. The efforts to make the process of learning how to successfully assemble the reactor are best learned through hands on experience. However, to accelerate the learning process I will go over the most common sources of improper reactor setup.

The first thing to ensure before continuing with any troubleshooting of the reactor is that each of the electrodes used are tested without the cap of the reactor. It is well known that the electrodes have a limited lifetime in this system and can easily cause problems. Additionally, make sure the potientiostat leads are not in contact with the exterior of the reactor.

The major source of time lost to improper setup is through not correctly compensating for the increase in reactor volume. In most cases the reactor is using a CO_2 eXpanded electrolyte or CXE. The liquid phase of the media will increase as a function of CO_2 pressure and at high CO_2 pressures the increase can be very sensitive to small changes in pressure. If the volume is too high, the resulting voltammetry experiment will look like it is shorting out at certain points in the Ferrocene CV. To low and there will be no current. To ensure this does not happen, be sure to measure an appropriate reactor volume. This is done by taking an alcohol marker and drawing a line on the middle of one or several of the electrodes. The middle volume will serve as the operating volume of the reactor. Then add acetone until the mark is erased by the acetone. The volume you added is now the new target for the total volume of the expanded liquid. Choosing the middle gives a larger margin of error.

Another major source of setup error is in the gold clips and general attachment of the electrodes to the feedthroughs. The first step is to make sure the electrode leading wire does not freely rotate or is easily removable from the gold clip. If the electrode is, tighten or replace the gold clip. Additionally, when the electrodes are positioned in the reactor there are two wings of the clips that will spread out. If these wings come in contact with the side of the reactor cap it will effect the voltammetry. The resulting voltammetry experiment will look resistive. The usually vertical onset potential leading up to the peak current for ferrocene will have a more shallow slope and the limiting potential will increase linearly. Recently, we have incorporated an engineering barrier in the form of PTFE straws to help mitigate this problem. However, this can be avoided by completely turning the cap upside down during assembly and ensuring the electrodes are not touching the sides.

If you are absolutely sure the clips are not touching the side and yet the ferrocene voltammetry is bad, the electrical feedthroughs can be problematic. The act of pushing in clips takes a fair

amount of force. This force can cause the copper feedthrough to bend and make contact with the reactor cap. Usually this can be seen using a flashlight to examine the openings. In the case that the copper is touching the sides, using a pare of needle-nose pliers gently pull the feedthrough straight. This will straighten the wire and resolve the grounding issues.

There are rare occasions wen the feedthroughs have corroded or have snapped due to the wear and tear of the reactor. In those situations, be sure to have a few extra on hand. They are very easily replaceable but take a considerable amount of time to be delivered. Additionally, stainless steel should never be bolted into stainless steel without first using PTFE tape. This ensures that if overtightened or stripped the feedthrough can still be removed. Voltammetry of these experiments are much harder to quantify but usually manifest in wildly inconsistent data. Be sure to examine the condition of the feedthroughs regularly to make sure they remain in good working condition. The major sign that a feedthrough is approaching the end of its lifetime is the wire will become more prone to bending near the ceramic plug. Eventually, the wire will snap from this location.

Hopefully this guide will improve the success of students operating the reactor. I implore students to edit and iterate this document to ensure it remains up to date with the most important information.